8-8-2016 12:00 AM

Inhibition Of MT1-MMP Proteolytic Function And ERK1/2 Signalling Influences Breast Cancer Cell Migration And Invasion Through Changes In MMP-2 And MMP-9 Expression

Caitlin L. Evered, *The University of Western Ontario*

Supervisor: Dr. Sashko Damjanovski, *The University of Western Ontario*

A thesis submitted in partial fulfillment of the requirements for the Master of Science degree in Biology

Abstract

Membrane-type 1 matrix metalloproteinase (MT1-MMP) is a multifunctional protease that invokes changes extracellularly via cleavages of ECM substrates, and intracellularly through induction of cell signalling cascades, both to influence cell behaviour and motility. The effects of MT1-MMP activation, MMP catalytic activity, and ERK1/2 signalling were examined by chemically or genetically altering each parameter. Regardless of treatment, expression of the two gelatinases, *MMP-2* and *-9*, were always altered in an inverse relationship. This work proposes a pathway through active MT1-MMP initiation of ERK1/2 phosphorylation and subsequent targeting the NF-κB transcription factor, to ultimately influence *MMP-9* expression. Modulation of MT1-MMP activation, activity, or downstream signalling, all resulted in decreased invasive potential in MDA-MB-231 breast cancer cells. In a chicken embryo tumour model, only untreated MDA-MB-231 cells caused tumour vascularization and complete wound closure. Furthermore, these results suggest that cells lacking active MT1-MMP, phospho-ERK1/2, or adequate MMP-9, have considerably reduced invasive potential.

Keywords

Extracellular matrix, matrix metalloproteinases, MT1-MMP, MMP-2, MMP-9, phospho-ERK1/2, cell invasion, 3D cell culture

Acknowledgments

First and foremost, thank you to my supervisor, Dr. Sashko Damjanovski for accepting me into your laboratory as an undergraduate student and further allowing me to grow as a graduate student. Thank you for your endless academic feedback, life advice, and support of my future endeavors. My experiences over the last three years in your laboratory have instilled skills that I will carry with me far outside of my time at Western.

Thank you to my advisors Dr. Thomas Drysdale and Dr. Alex Timoshenko for their feedback and guidance throughout my academic accomplishments over the past two years. Additionally, thank you to Dr. Rob Cumming, Dr. Greg Kelly, and Dr. Hon Leong, for their generosity in providing the use of equipment and resources essential to the completion of this project. To the past and present members of the Dr. Cumming, Dr. Kelly, and Dr. Timoshenko labs, thank you for your collegiality, scientific opinions, and willingness to offer help when help is needed. It has been a pleasure being in this department with you all.

I would also like to acknowledge those in the Damjanovski lab, Mario Cepeda, Jessica Willson, Jacob Pelling, and Carlie Muir, for making this academically challenging experience feel easier through your friendship. Jake, thank you for being my other half, my second opinion, my biggest critic, but also my most supportive friend throughout this process. To say my time in graduate school without you would have turned out the same is impossible.

Most importantly, Mario Cepeda, thank you for recognizing my potential early on and continuing to challenge me to push my limits. Your mentorship and friendship over the past two years have been a true testament to my achievements. From your passion for science and indispensible work ethic, I have no doubt that you will go on to continue to exceed expectations and achieve great success in both your academic endeavors and personal life goals. I wish you nothing but the best.

Table of Contents

List of Tables

List of Figures

List of Abbreviations

2D	Two-dimensional
3D	Three-dimensional
α1-PDX	Alpha1-antitrypsin Portland
ANOVA	Analysis of variance
AP-1	Activator protein 1
ARP2/3	Actin related proteins 2 and 3
BCA	Bicinchoninic acid
BM	Basement membrane
BSA	Bovine serum albumin
CAM	chorioallantoic membrane
CBD	Collagen binding domain
cDNA	Complimentary deoxyribonucleic acid
CD44	Cluster designation 44
CHO	Chinese hamster ovary
CM	Conditioned media
DAPI	4',6-diamidino-2-phenylindole
DMEM	Dulbecco's Modified Eagle Medium
DMSO	Dimethyl sulfoxide
ECM	Extracellular matrix
EDTA	Ethylenediaminetetraacetic acid
EGF	Epidermal growth factor
ER	Estrogen receptor
ERK	Extracellular regulated kinase
FBS	Fetal bovine serum

FGF	Fibroblast growth factor
GAPDH	Glyceraldehyde 3-phosphate dehydrogenase
HER2	Human epidermal growth factor receptor 2
IF-1β	Interleukin 1 beta
JNK	c-Jun N-terminal kinase
KRE	Keratinocyte differentiation-factor responsive element
MAPK	Mitogen-activated protein kinase
MAPKK	Mitogen-activated protein kinase kinase
MAPKKK	Mitogen-activated protein kinase kinase kinase
MCF-7	Michigan Cancer Foundation -7
MDA-MB-231	MD Anderson Metastatic Breast 231
MEK	MAPK/ERK kinase
MLC	Myosin light chain
MLCK	Myosin light chain kinase
MMP	Matrix metalloproteinase
MMPI	Matrix metalloproteinase inhibitor
mRNA	Messenger ribonucleic acid
MT-MMP	Membrane-type matrix metalloproteinase
NF-κB	Nuclear factor κB
PBS	Phosphate-buffered saline
Phospho-ERK1/2	Phosphorylated extracellular regulated kinase 1 and 2
PR	Progesterone receptor
qPCR	Quantitative (real-time) polymerase chain reaction
Raf	Rapidly accelerated fibrosarcoma
RCE	Retinoblastoma control element
SDS-PAGE	Sodium dodecyl sulfate polyacrylamide gel electrophoresis

SEM	Standard error of the mean
TBST	Tris buffered saline with Tween
TGF-β	Transforming growth factor beta
TIE	TGF-β inhibitory element
TIMP	Tissue inhibitor of metalloproteinases
TNF-α	Tumour necrosis factor alpha
VEGF	Vascular endothelial growth factor
WASP	Wiskott-Aldrich syndrome protein
WNT	Wingless-related integration site
ZsGreen	Zoanthus species green

Chapter 1

1 Introduction

1.1 The Extracellular Matrix

The Extracellular Matrix (ECM) is a three-dimensional, cross-linked structure of secreted macromolecules present within all tissues and is essential for life as it regulates eukaryotic cell development, function, and homeostasis (Lu et al.,2011; Rozario and DeSimone, 2010). The ECM aids in the support, repair, and regeneration of differentiated tissues and organs, whereby integrity is maintained through regulation of structural proteins, embedded cytokines, growth factors, growth factor receptors, as well as maintenance of hydration and pH of the all-encompassing cell-surrounding environment (Naba et al., 2012; Sanes, 2003; Torricelli et al., 2013). The functional importance of the ECM is illustrated by the wide range of tissue defects or, in severe cases, embryonic lethality caused by mutations in genes that encode essential ECM components (Bateman et al., 2009; Järveläinen, 2009).

In mammals, the ECM is composed of approximately 300 different protein types, known as the core matrisome, including proteins such as collagen, proteoglycans, and glycoproteins (Järveläinen, 2009; Schaefer and Schaefer, 2010). There are two main types of ECM that are distinct due their location and composition within tissues: the interstitial connective tissue matrix, which surrounds cells and provides structural scaffolding for tissues; and the basement membrane, which is a specialized form of ECM that separates the epithelium from the underlying stroma. More specifically, the basement membrane is comprised predominately of type IV collagen (Martin and Timpl, 1987) and functions to provide support for epithelial, endothelial, muscle and fat cells (Paulsson, 1992; Kalluri, 2003), acts as a mechanical barrier to cells and other macromolecules, and serves as sites for cell-ECM adhesions and interactions (Mouw et al., 2014).

ECM proteins can also function as ligands for various cell surface receptors present on the embedded cells, stimulating diverse cell-signalling pathways, which regulate cell adhesion, migration, proliferation, apoptosis, survival, or differentiation (Egeblad and

Werb, 2002). Furthermore, the ECM sequesters and locally releases growth factors, such as epidermal growth factor (EGF), fibroblast growth factor (FGF) and other signalling molecules, such as WNTs and transforming growth factor-β (TGF-β), which additively influence cell behaviour (Lu et al., 2011). Cells are capable of rebuilding and remodeling the ECM through synthesis, degradation, reassembly, and chemical modification of ECM components. The principle molecules responsible for degrading and remodeling the ECM are Matrix Metalloproteinases (MMPs) and their endogenous inhibitors, Tissue Inhibitors of Metalloproteinases (TIMPs) (Lambert et al., 2004). The actions of MMPs and TIMPs within the ECM are complex and need to be tightly regulated to maintain tissue homeostasis and to respond to developmental cues, as well as physiological stresses, such as injury, wound repair, and disease (Järveläinen, 2009; Hynes, and Naba, 2012; Frantz et al., 2010). Collectively, the composition and status of the ECM surrounding, supporting, and interacting with cells within a given tissue can vary tremendously, whether it is from one tissue to another (muscle versus skin versus bone), within a given tissue (atria versus ventricle), or from one physiological state to another (embryonic development versus adult maintenance versus cancer metastasis) (Zhen and Cao, 2014).

1.2 Key ECM Remodelers and Inhibitors: Matrix Metalloproteinases and Tissue Inhibitor of Metalloproteinases

MMPs comprise a family of zinc-dependent endopeptidases, which function to selectively cleave all components of the ECM, resulting in substrate degradation and subsequent remodeling. To date, 24 MMPs have been identified in vertebrates and are classified into one of five groups based on their structure and ECM substrate specificity: collagenases (e.g. MMP-1, -8, -13), gelatinases (MMP-2 and MMP-9), membrane-type (MT1-MMP – MT6-MMP), stromelysins (e.g. MMP-3, -10, -11) and matrilysins (e.g. MMP-7 and MMP-26) (Bourboulia, and Stetler-Stevenson, 2010). As the list of known MMP substrates increases in number and complexity, a more simplistic categorization of MMPs has formed, which describes their structure and cellular localization: Membrane-Type MMPs (MT-MMPs), which are anchored at the cell surface, and secreted MMPs, which are soluble in the ECM (Egeblad and Werb, 2002)

Most MMPs share a common domain structure, consisting of an N-terminal pro-peptide domain, the catalytic domain, and the hemopexin-like domain. Synthesized as inactive zymogens, the MMP pro-peptide domain contains a conserved cysteine residue that interacts with the catalytic domain to prevent substrate binding. Activation of MMPs occurs upon removal of the pro-domain. Membrane-Type MMPs are activated intracellularly in the trans-Golgi by a protein-convertase-dependent mechanism, principally by furin, and are anchored at the cell membrane in an active form (Sternlicht and Werb, 2001). Secreted MMPs are secreted as pro-enzymes and are activated extracellullarly by other, already active, proteinases. After activation, within the catalytic domain of MMP's lies the active site, a conserved histidine motif (HEXXHXXGXXH) in which the three histidine residues are essential for zinc chelation and subsequent catalytic activity (Stöcker and Bode, 1995). The hemopexin-like domain (located at the C-terminal end of secreted MMPs) is comprised of a four bladed β-propeller structure, which dictates substrate specificity and mediates protein-protein interactions (Visse and Nagase, 2003). Moreover, Membrane-Type MMPs contain an N-terminal pro-domain, catalytic domain, and a hemopexin-like domain, but with the addition of a transmembrane domain for anchorage into the cell membrane and the C-terminal cytoplasmic tail essential for localization and recycling to the membrane surface. Collectively, the catalytic domain and hemopexin-like domain in all MMP family members, allow these proteins to function proteolytically, to achieve ECM degradation and remodeling, and non- proteolytically, by binding of extracellular or cell surface proteins to initiate down stream signalling pathways (Strongin, 2010).

MMPs were initially discovered in tadpole metamorphosis during tail resorption, where collagen triple helix degradation was detected, marking the earliest observation of MMP mediated ECM remodeling (Gross and Lapiere, 1962). Since this discovery, MMPs have been documented to degrade all constituents of the ECM, promoting both cell migration and influencing cell behaviour through growth factor availability. Additionally, more recent evidence has demonstrated that MMPs are also capable of cleaving chemokines, growth factor receptors, and cell adhesion molecules (Egeblad and Werb, 2002). Therefore, not only can MMPs influence cell behavior by regulating the integrity and composition of the ECM with which a cell interacts, but also by regulating the levels of

available growth factors and their receptors through cleavage of ECM and non-ECM proteins.

In order to maintain tissue integrity, the correct MMPs must be present at the correct time, in the correct location, and in the appropriate form (inhibited or active). Control of MMP-dependent cleavages of the ECM is critical in order to maintain proper organismal development and maintenance of normal adult tissues. Retaining proper MMP activity in tissues is achieved through regulation of MMP gene expression, pro-enzyme activation, and the level of their enzymatic activity through catalytic inhibition by their endogenous inhibitors, Tissue Inhibitors of Metalloproteinases (TIMPs) (Visse and Nagase, 2003). Currently, there are 4 defined mammalian TIMPs (TIMP 1-4), all of which are small-secreted proteins consisting of structurally and functionally distinct N- and C-terminal domains. TIMP N-terminal domains are responsible for direct inhibition of MMP activity by binding, and therefore blocking, the MMP catalytic site (Nagase et al., 2006). TIMP C-terminal domains interact with the hemopexin domains of select MMPs to aid in MMP activation (Stetler-Stevenson, 2008), as well as carry out various MMP-independent functions, such as binding to a variety cell surface receptors to induce downstream signalling cascades (Stetler-Stevenson and Seo, 2005).

1.3 MT1-MMP Structure, Activation, and Function in Development and Disease

Unlike secreted MMPs, which are activated extracellullarly and may diffuse freely throughout the ECM, Membrane-Type MMPs (MT-MMPs) are activated intracellularly and embedded in the plasma membrane; thus, the activities of MT-MMPs are limited to the surface of the cells that produced them (Seiki, 2003). Of the six MT-MMPs, MT1-MMP (also known as MMP-14) was the first identified and most well characterized. MT1-MMP plays an integral role in ECM remodeling, as it possesses both proteolytic and non-proteolytic functions. Proteolytically, MT1-MMP is directly involved in pericellular cleavage of collagen types I, II, and III, laminins-1 and -5, fibronectin, vitronectin, fibrin and aggrecan. Additionally, MT1-MMP is responsible for cleavage of other cell surface proteins (CD44, cadherins, or integrins), and activation of other secreted pro-MMPs most notably pro-MMP-2 and pro-MMP-9 (Toth et al., 2003). Non-

proteolytically, MT1-MMP interacts with other ECM molecules to stimulate intracellular signalling cascades, such as the Mitogen-Activated Protein Kinase (MAPK) pathway, resulting in changes in cell behaviour and function (Pahwa et al., 2014). Collectively, MT1-MMP is a key regulator of cellular invasion in development and disease.

MT1-MMP is classified as a type I transmembrane protein, and is synthesized as an inactive zymogen, containing a single transmembrane domain important for membrane integration and a short cytosolic C-terminal domain essential for regulating cellular localization and turnover (Strongin, 2010). The pro-domain of MT1-MMP contains a furin cleavage motif; therefore furin is a crucial component in the activation pathway that results in active MT1-MMP present on the cell surface. Furin is a specialized serine endoproteinase belonging to the protein convertase family. Furin cleaves the multibasic motifs R-X-R/K/X-R to transform many pro-proteins into biologically active proteins and peptides (Seidah et al., 2008). In humans, furin is ubiquitously expressed, where it is primarily localized in the trans-Golgi network and secondarily found in vesicles cycling to the cell surface. The importance of furin in proper cell function is illustrated by its developmental lethality in furin knockout mice (Scamuffa et al., 2006). Furin and other protein convertases are self-activated and, as a result, they initiate proteolytic cascades through their wide variety of targets including, MT1-MMP, TGF-β, stromolysin-3 (MMP-11), growth factors, and adhesion molecules, all of which are essential in the processes of cellular transformation, acquisition of the tumourogenic phenotype, and metastases formation (Strongin, 2010). The cytosolic C-terminal tail of MT1-MMP is important in regulation of cell migration and invasion as the tail of MT1-MMP facilitates MT1-MMP localization to invadapodia— cell membrane protrusions that serve as focal sites of ECM degradation (Poincloux et al., 2009). Additionally, the tail of MT1-MMP has been linked to internalization and turnover of the enzyme with respect to its presence on the membrane surface, highlighting the importance of this domain in regulating MT1-MMP function (Uekita et al., 2001).

As well as cleaving known ECM substrates, MT1-MMP is involved in the activation of pro-MMP-2, which further potentiates the migratory and invasive potential of MT1-MMP expressing cells through amplified ECM degradation (Itoh et al., 2001). In brief,

during the activation of pro-MMP-2, one MT1-MMP protein acts as a cell surface receptor for a TIMP-2, as the inhibitory N-terminus of TIMP-2 binds MT1-MMP at its active site. The C-terminal domain of the same TIMP-2 molecule then binds the hemopexin-like domain of pro-MMP-2, which can orient the latter into close proximity to the active site of a second, adjacent active MT1-MMP. After formation of the MT1-MMP/TIMP-2/pro-MMP-2 complex, MT1-MMP is in the correct orientation to cleave the pro-peptide domain of pro-MMP-2 and release the activated MMP-2 into the ECM (Itoh et al., 2001; Lehti et al., 2000). Additionally, the MT1-MMP/TIMP-2/MMP-2 complex has been shown to activate secreted pro-MMP-9, demonstrating the dependence of proper protein associations for subsequent MMP activation events (Toth et al., 2003). In conjunction with the activation of pro-MMP-2 and pro-MMP-9, MT1-MMP and TIMP-2 can also form an additional complex via the hemopexin domain of MT1-MMP to initiate the intracellular cascade of the MAPK pathway leading to the downstream phosphorylation of Extracellular Signal-Regulated Kinase (ERK1/2) (Sounni et al., 2010). Among the cell signalling pathways involved in cancer, the MAPK pathway is one of the most prominent, as it regulates diverse cellular functions including cell proliferation, survival, angiogenesis, and migration (Fujioka et al., 2006).

All of the activities MT1-MMP elicits and initiates in the extracellular matrix have functions during, and thus impact, development and disease. MT1-MMP is essential for proper organismal cellular function during embryogenesis, as knockout of MT1-MMP is developmentally lethal in mice. MT1-MMP deficient mice die shortly after birth exhibiting craniofacial dysmorphism, arthritis, osteopenia, dwarfism, and fibrosis of soft tissues. Of all the 24 known MMP family members, MT1-MMP knockout is the only phenotype that is developmentally lethal (Holmbeck et al., 1999), demonstrating the importance of proper MT1-MMP function during embryogenesis. Its importance in disease is exemplified in pathological conditions, such as cancer, as MT1-MMP promotes cell migration and invasion as well as potentiation of ECM remodeling through activation of other pro-MMPs. *MT1-MMP* exhibits increased expression in a wide variety of cancer types, classifying MT1-MMP as a pro-invasive and pro-tumourogenic protein. The causes of increased *MT1-MMP* expression in cancer cell types is attributed to

transcriptional changes during tumour formation, as there have been no documented mutations in the *MT1-MMP* gene in cancerous cells (Pahwa et al., 2014).

1.4 Ras-Raf-MEK-ERK Mitogen-Activated Protein Kinase Cascade

Mammalian cells possess four well-characterized MAPKs. The cascades resulting in the activation of these MAPK's are comprised of three protein kinases that act as a signalling relay: a MAPK kinase kinase (MAPKKK), which activates a MAPK kinase (MAPKK), resulting in the final activation of a MAPK (e.g. ERK1/2, JNK, p38, or ERK5) that generally impacts transcription (Roberts, and Der, 2007). In general, the ERK1/2 pathway is activated by growth factor-stimulated cell surface receptors, whereas the JNK, p38, and ERK5 pathways are activated by stress and growth factors (Mebratu and Tesfaigzi, 2009)

The MAPK pathway of Ras-Raf-MEK1/2-ERK1/2 is of particular interest as ERK1/2 signalling promotes cell proliferation, cell survival, and cell motility. In this pathway Raf is the MAPKKK, MEK1/2 the MAPKK and ERK1/2 the MAPK. Unsurprisingly, this pathway is abnormally activated in many cancer types, highlighting the important role of ERK1/2 signalling in regulation of proper cell function. During development, ERK1 (44 kDA) and ERK2 (42 kDa) knockout studies have revealed non-compensatory roles between these two proteins, as absence of one is not replaced by the action of the other. ERK2 is essential for development as ERK2 knockout mice showed defects in placental development resulting in embryonic death, while ERK1 knockout mice were viable, fertile, and normal in size (Mebratu and Tesfaigzi, 2009).

In brief, the Ras-Raf-MEK1/2-ERK1/2 pathway is tightly controlled by a series of protein phosphorylation events. Ras directly interacts with Raf, whereby activation of MEK1/2 by Raf protein family members leads to the phosphorylation of threonine and tyrosine residues within TEY (Thr-Glu-Tyr) recognition sites of ERK1 and ERK2. Phosphorylated ERK1/2 can then either be retained within the cytosol or translocated to the nucleus, where phospho-ERK1/2 influences gene expression through phosphorylation of serine, threonine, or proline residues of downstream transcription factors (Roberts and

Der, 2007). Collectively, active phosphorylated ERK1/2 regulates the expression of over 160 proteins including growth factors, cytokines, cell surface receptors, and MMPs, which in turn influence the composition and conditions of the ECM (Meloche and Pouysségur, 2007).

1.5 The Gelatinases: MMP-2 and MMP-9

The gelatinases, MMP-2 (gelatinase A) and MMP-9 (gelatinase B), differ from other MMP family members as they have a collagen-binding domain (CBD) embedded within their catalytic domain. The CBD is composed of fibronectin type II repeats and is involved in the binding of collagenous substrates, elastin, and fatty acids (Klein, and Bischoff, 2011). MMP-2 and MMP-9 are considered potent ECM remodelers as they both share the target substrate collagen IV, an abundant component of physiologically important basement membranes.

MMP-2 is synthesized in a 72 kDa pro- form and upon removal of the pro-domain by active MT1-MMP, the 63 kDa active form of MMP-2 cleaves a wide variety of substrates found within the extracellular milieu (Khasigov et al., 2003). MMP-2 has substrate specificity for ECM and non-ECM components such as collagens (I, IV, V, VII, and X), gelatin, elastin, fibronectin, laminins, galectin-3, aggrecan, as well as various cell surface receptors, growth factors, and chemokines (Järveläinen, 2009). Moreover, active MMP-2 has the ability to activate pro-MMP-9 to further increase ECM degradation. As a potent ECM remodeler with large substrate specificity, altered expression and activity of MMP-2 has been linked with poor prognosis in multiple cancer types including colorectal, melanoma, breast, lung, and prostate. For example, in colorectal cancer many metastatic cases involving increased MMP-2 activity have been correlated with increased expression in surrounding healthy tissues, in addition to metastatic lesions (Mook et al., 2004).

MMP-9 is produced as an inactive 92 kDa pro-MMP-9 and degrades both ECM and non-ECM substrates in an 82 kDa active form (Khasigov et al., 2003). MMP-9 possess substrate specificity for collagens III, IV and V, gelatin, elastin, vitronectin, and entactin, as well as TNF-α and IL-1β (Järveläinen, 2009). In cancer, MMP-9 contributes to angiogenesis of the pre-existing metastatic niche by recruiting macrophages and

hematopoietic stem cells (Kaplan et al., 2005; Hiratsuka et al., 2006). In some cases metastatic potential of tumors is associated with increased MMP-9 protein levels, and down-regulation of MMP-9 depresses metastasis (Björklund and Koivunen, 2005). *MMP-9* expression is increased through the oncogenic properties of the Ras/Raf pathway to activate MEK1/2 and phospho-ERK1/2 (Gum et al., 1997). Phosphorylation of ERK1/2 leads to upregulation of MMP-9 transcription factors AP-1 and NF-κB (Fig. 1), which can increase transcription of pro-MMP-9 (Lee et al., 2013), ultimately resulting in further degradation of the ECM.

Until recently, the data obtained from most studies suggested that gelatinases played a dominant role in basement membrane invasive events because of their ability to degrade collagen IV. However, recent studies in cancer cells engineered to express active MMP-2 and MMP-9 (Hotary et al., 2006) and fibroblasts isolated from MMP- $2^{-/-}$ and MMP-$9^{-/-}$ mice (Sabeh et al., 2009) strongly suggest that gelatinases do more than promote basement membrane invasion. Recent evidence shows that gelatinases play major, but indirect roles in cell signalling by controlling the bioavailability and bioactivity of molecules that target specific receptors regulating cell growth, migration, inflammation, and angiogenesis. For example, cleavage of laminin-5 by MMP-2 results in the exposure of an epitope that enhances endothelial cell migration (Giannelli et al., 2016), while MMP-9 can release ECM-sequestered factors VEGF, TGF-β and FGF-2, which stimulate proliferation and migration of endothelial cells (Bergers et al., 2000; Yu and Stamenkovic, 2000).

In cancer, there is a loss of tissue organization resulting from aberrant behaviour of ECM remodeling proteins. Tumours are characteristically stiffer than the surrounding normal tissue resulting from increased ECM deposition and remodeling by MMPs (Butcher et al., 2009) , which in turn release more chemokines and growth factors embedded within the ECM (De Wever et al., 2008). The release of growth factors, such as VEGF by MMP-9, enhances vascular permeability and promotes new vessel growth to potentiate tumour growth and survival via angiogenesis and cell invasion to ultimately support

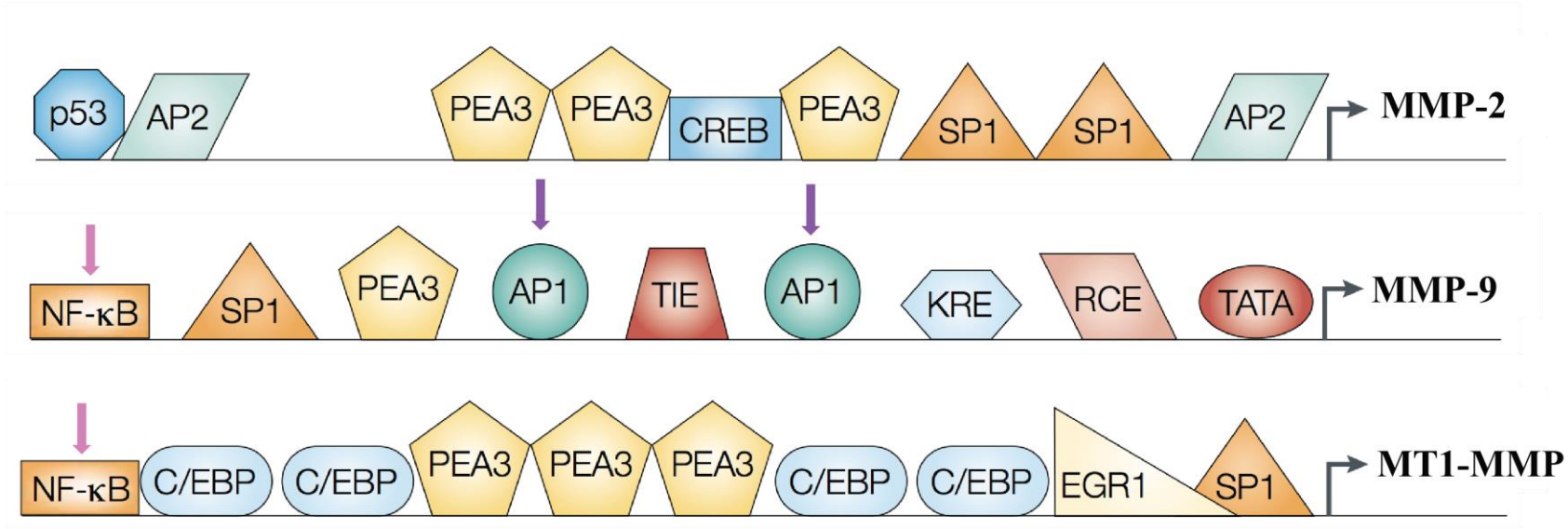
p53
AP2
PEA3
PEA3
CREB
PEA3
SP1
SP1
AP2
MMP-2
NF-κB
SP1
PEA3
AP1
TIE
AP1
KRE
RCE
TATA
MMP-9
NF-κB
C/EBP
C/EBP
PEA3
PEA3
PEA3
C/EBP
C/EBP
EGR1
SP1
MT1-MMP

Figure 1. Only *MMP-9* contains binding sites for transcription factors AP-1 and NF-κB within its promoter region.

Shown are the known cis up-stream regulatory elements in the promoter regions of three human MMP genes: *MMP-2*, *MMP-9*, and *MT1-MMP* (*MMP-14*). The promoters are shown in the 5'-3' direction, with the transcriptional start site indicated by a bent arrow. Transcription-factor-binding sites include: the activator proteins (AP)-1 (purple arrows) and -2 site, the CCAAT/enhancer-binding protein (C/EBP) site, the cyclic AMP response-element binding protein (CREB) site, the early growth response-1 (EGR1) site, the keratinocyte differentiation-factor responsive element (KRE), the nuclear factor of κB (NF-κB) site (pink arrows), the polyomavirus enhancer-A binding-protein-3 (PEA3) site, retinoblastoma control element (RCE), TGF-β inhibitory element (TIE), and the TATA-box (TATA). The functional activity of the indicated binding sites has been verified by either using cell-transfection studies with MMP promoter constructs or functional analysis in transgenic mice models. Only the promoter region for *MMP-9* contains both an AP-1 and NF-κB binding site, while the promoter region for *MT1-MMP* contains NF-κB, and the promoter region for *MMP-2* contains neither. Adapted from Christopher Mark Overall and Carlos López-Otín (2002).

metastasis (Butcher et al., 2009; Erler and Weaver, 2009; Paszek et al., 2005).

1.6 Proteolytic and Non-Proteolytic Functions of MT1-MMP in Promoting Cell Motility

Cell migration and invasion extensively contribute to the development and metastasis of cancers. The process of cell migration has been well characterized, and is initiated by the binding of chemoattractants or other pro-migratory ligands to cell surface receptors. Binding of ligands induces cell-signalling cascades, which influences gene transcription and cytoskeletal dynamics. At the leading edge of the cell during migration, actin is polymerized and stabilized by localized activity of multiple actin binding proteins including WASP and ARP2/3. Actin polymerization drives membrane extensions from the cell surface, called filipodia or lamellipodia, which contact and bind to the ECM using specific integrins to form focal adhesions. Actin and myosin contract to drive the cell body forward along ECM substrates, while the trailing edge of cells detaches from the ECM (Friedl and Wolf, 2003).

In order to move through ECM barriers, a migrating cell must also be capable of ECM degradation. It is well documented that MT1-MMP localizes to the leading edge of cells, where it is presumed to promote matrix cleavage directly and indirectly at the cell-ECM interphase (Mori et al., 2002). Direct cleavage of laminin-5 by MT1-MMP in numerous cell types has been shown to promote cell migration. Additionally, CD44 and MT1-MMP co-localize within lamellipodia of migrating cells, whereby cleavage and subsequent shedding of CD44 initiated by MT1-MMP, promotes cell migration (Itoh, et al., 2006; Koshikawa et al., 2000, Ueda et al., 2003). In invasive cells, specific degradative cellular structures form that are rich in MT1-MMP. While structurally similar to filipodia and lamellipodia in migration, these structures are called podosomes in physiological cells and invadapodia if formed in cancer cells (Alblazi and Siar, 2015). The formation of invadapodia occurs on the basal side of a cell, whereby membrane protrusions are formed by actin polymerization, followed by shuttling of MT1-MMP to the distal ends (Artym, 2006). This formation relies on hundreds of individual proteins that regulate the initiation and regulation of actin dynamics, vesicular transport, and cellular adhesion (Alblazi and Siar, 2015). While the fundamental organization of invadapodia can still form in the

absence of MT1-MMP, the resulting structures are non-functional and do not degrade ECM substrates (Buccione et al., 2009; Itoh et al., 2006).

It is hypothesized that soluble pro-MMPs such as the gelatinases, are transported in vesicles destined for cell surface protrusions such as invadapodia (Itoh et al., 2006). In addition to direct ECM proteolysis, localized MT1-MMP activates pro-MMP-2, by which active MMP-2 can activate pro-MMP-9, to further potentiate ECM degradation (Khasigov et al., 2003). Cell protrusion localized MT1-MMP can also non-proteolytically initiate the MAPK pathway at the distal ends. Phosphorylated ERK1/2 is involved in both migration and invasion through phosphorylation and activation of cytoskeletal proteins. For example, phospho-ERK1/2 positively regulates the filamentous F-actin regulatory protein, cortactin. Cortactin plays an important role in tumour cell movement and invasion, as cortactin stabilizes ARP2/3 mediated actin networks (Kelley et al., 2011). Additionally, phospho-ERK1/2 activates the cells' motility machinery by enhancing myosin light-chain kinase (MLCK) activity leading to increased myosin light chain (MLC) phosphorylation, allowing for myosin to bind actin filaments and resultantly contract to allow for cell movement (Reddy et al., 2003).

Collectively, MT1-MMP localized during migration and invasion to cell specific motility structures, orchestrates both proteolytic and non-proteolytic cell functions necessary to promote both ECM degradation and movement along ECM substrates.

1.7 Development of Synthetic MMP Inhibitors as Cancer Therapeutics

Within distinct cancer types, diverse MMP family members are upregulated resulting in abnormal ECM remodeling, making MMPs an ideal target for therapeutic treatments. Many different MMP inhibitors (MMPIs) have been designed to target MMPs in cancer and although these compounds differ in their inhibitory potencies towards MMPs, none of them are selective for individual MMPs (including the gelatinases). The first generation of MMPIs were peptidomimetics (such as batimastat and marimastat) that mimicked the structure of collagen. They acted as competitive inhibitors and chelated the zinc ion present at the MMP's active site. To improve specificity, non-peptidomimetics

were synthesized on the basis of the MMP active site's three-dimensional conformation. Other MMPIs included tetracycline derivatives that inhibited both the MMPs' enzymatic activity and their synthesis (by blocking gene transcription) (Cathcart et al., 2015).

To date, all clinical trials of these MMPIs in advanced cancer patients have failed. There are several possible reasons for the failure of MMPIs in the clinic such as dose limiting toxicity to surrounding healthy cells, interference with non-targeted cell signalling pathways, and structural similarity among the MMPs' catalytic domains. Moreover, the role of MMPs in cancer progression is not restricted to ECM-degrading activity, as various MMPs are also involved in, and influenced by, different signalling pathways that additionally impact tumour cell behaviour (López-Otín and Matrisian, 2007). All clinical trials regarding MMPs have converged upon the same problems, difficulty in designing MMPIs or cell signalling pathway targets with high selectivity. This project investigates the broad cellular function consequences of using non-selective inhibitors.

1.8 Hypothesis and Objectives

The presence and activation of both gelatinases (MMP-2 and MMP-9) within the ECM is heavily influenced by the abundance of active MT1-MMP present on the cell surface, while intracellular signalling pathways, such as the MAPK pathway, influence MMP-2 and MMP-9 transcription factor activity and govern the availability of secreted gelatinase MMPs. In order to achieve proper cell function, the amount of active MT1-MMP, phosphorylated ERK1/2, and *MMP-2* and *-9* expression must be tightly regulated, as imbalance can result in aberrant ECM remodeling allowing for increased cell migration and invasion among other irregular cell functions.

I hypothesized that the levels of phosphorylated ERK1/2 will be directly proportional to the levels of active MT1- MMP, and be correlated with increased gelatinase (*MMP-2* and *-9*) MMP mRNA levels and increased invasive potential of breast cancer cells.

Using MCF-7 (MT1-MMP and phospho-ERK1/2 deficient), MCF-7 MT1-MMP C2 (predominately active MT1-MMP, high phospho-ERK1/2), MDA-MB-231 (High active

MT1-MMP, constitutive phospho-ERK1/2, high gelatinase MMP expression), and 231-PDX (high pro and active MT1-MMP, high phosphoERK1/2) breast cancer cell lines (Table 1 and 2), this study was conducted to examine how altering ERK1/2 phosphorylation, MMP catalytic activity, and MT1-MMP activation, affects *MMP-2* and *MMP-9* expression and subsequent breast cancer cell migration and invasion.

The above breast cancer cell lines were treated with U0126, a MEK1/2 kinase inhibitor, BB-94, a pan-MMP catalytic site inhibitor, and Furin Inhibitor I targeting MT1-MMP activation. Each treatment was used to observe how changes to the MT1-MMP, phospho-ERK1/2, gelatinase relationship influenced: 1) MT1-MMP and phospho-ERK1/2 protein levels, 2) changes in *MT1-MMP*, *MMP-2*, *MMP-9*, *TIMP-2* mRNA levels, 3) transcription factor availability, 4) cell migratory and invasive potential, 5) cellular 3D morphology, and 6) ability of breast cancer cells to form vascularized tumours within chicken embryos. My Master's research has taken an approach of selective removal of key players involved in breast cancer cell invasion in order to better understand each parts necessity in promoting this phenotype.

Table 1. A comparison of the relative levels of MT1-MMP and phospho-ERK1/2 protein, gelatinase expression, and invasive potential of MCF-7, MCF-7 MT1-MMP C2, MDA-MB-231, and 231-PDX breast cancer cells.

	MT1-MMP protein	**MMP-2 expression**	**MMP-9 expression**	**Phospho-ERK1/2**	**Invasive Potential**
MCF-7	+	+	+	+	+ (Cepeda et al., 2016)
MCF-7 MT1-MMP C2	+++++++++	+++	+++++	+++++	++ (Cepeda et al., 2016)
MDA-MB-231	++++	++++++	+++++++	+++++++	++++++
231-PDX	++++++	++++	+++++++++	++++++++	+++++

Table 2. Origin, classification, and key characteristics of MCF-7 and MDA-MB-231 breast cancer cell lines.

MCF-7 cells are less invasive compared to MDA-MB-231 cells. The presence or absence of ER (estrogen receptor), PR (progesterone receptor), or HER2 (human epidermal growth factor receptor 2) receptors is indicative of how well cells respond to endocrine signals and chemotherapy treatment. Ki67 is a marker for cell proliferation; during interphase Ki67 is exclusively present within the nucleus. Ki67 protein is present during all active phases of the cell cycle (G_1, S, G_2, and mitosis), but is absent from resting cells (G_0). Adapted from Holliday and Speirs 2011.

	Tumour Source	**Pathology**	**Organism**	**Classification**	**Immunoprofile**	**Other Characteristics**
MCF-7	Metastasis; pleural effusion	Adenocarcinoma	Human	Luminal A	ER^+, $PR^{+/-}$, $HER2^-$	Ki67 low, endocrine responsive, often chemotherapy responsive, invasive potential (+)
MDA-MB-231	Metastasis; pleural effusion	Adenocarcinoma	Human	Claudin-low/ triple negative	ER^-, PR^-, $HER2^-$	Ki67 high, low E-cadherin, claudin-3, claudin -4, and claudin 7, intermediate response to chemotherapy, invasive potential (++++++)

Chapter 2

2 Material and Methods

2.1 Cell Culture Conditions

Human adenocarcinoma breast cancer cell lines MCF-7 (ATCC® HTB-22™) and MDA-MB-231 (ATCC® HTB-26™) were generously donated by Dr. Lynne-Marie Postovit, University of Alberta.

Three MCF-7 breast cancer cell lines that overexpress *MT1-MMP* were generated by PhD candidate Mario Cepeda, Western University. MCF-7 MT1-MMP C1, expressed ~2,500 fold increase in *MT1-MMP* mRNA compared to MCF-7 parental cells, MCF-7 MT1-MMP C2 showed a ~1,100 fold increase, and MCF-7 MT1-MMP C3 had the lowest with an ~11 fold increase. These lines will be called MCF-7 C1, C2 and C3. Additionally, three MDA-MB-231 breast cancer cell lines were generated by Mario Cepeda that overexpress *MT1-MMP*. MDA-MB-231 MT1-MMP C1, expressed ~10 fold increase in *MT1-MMP* mRNA compared to MDA-MB-231 parental cells, MDA-MB-231 MT1-MMP C2 showed a ~7 fold increase, and MDA-MB-231 MT1-MMP C3 had a ~2 fold increase. These lines will be referred to as MDA-MB-231 C1, C2, and C3. For relative comparison, MDA-MB-231 cells express ~175 fold more *MT1-MMP* mRNA compared to MCF-7 cells. Each stable cell line was characterized according to their levels of pro- and active MT1-MMP, expression of other ECM remodeling proteins, as well as their cellular movements in 2D and 3D space (Cepeda et al., 2016).

Cells were cultured in Dulbecco's Modified Eagles (DMEM)/F-12 medium (Thermo Fisher) supplemented with 10% fetal bovine serum (FBS), 100 IU/mL penicillin, 100 μg/mL streptomycin, in a humidified incubator at 37°C and 5% CO_2. Cells were maintained under 80% confluency and passaged accordingly using 0.25% Trypsin-EDTA (Thermo Fisher).

2.2 Generation of 231-PDX Stable Cell Line

Additionally, to observe changes in cell behaviour following alteration to MT1-MMP activation, cellular expression of *α1-PDX* was used to block furin dependent processing of protein precursors. The Alpha1-Antitrypsin Portland, *α1-PDX* cDNA, contained within the mammalian expression pRc/CMV vector (Thermo Fisher), was obtained by generous donation from Dr. Gary Thomas, University of Pittsburgh (Pittsburgh, PA).

MDA-MB-231 breast cancer cells were seeded at a density of $5x10^5$ cells/mL in a 35 mm cell culture dish (Corning) and incubated for 24 hours. Following incubation, cells were transfected with α1-PDX pRc/CMV vector, which contains a neomycin selection marker, using OPTI-MEM (Gibco) reduced serum medium and Lipofectamine 2000 (Thermo Fisher) according to the manufacturer's instructions. Following transfection, cells were split 1:1000 and incubated in DMEM/FBS medium containing 1 mg/mL neomycin analog G418 (VWR). Individual colonies were selected after four weeks of incubation in selection medium and expanded to assay for alpha1-Antitrypsin Portland (*α1-PDX*) expression by qPCR and changes in MT1-MMP protein forms (pro- and active) via western blot analysis.

2.3 Generation of MDA-MB-231 and 231-PDX ZsGreen Stable Cell Lines

To identify MDA-MB-231 and 231-PDX cells injected into wounded vasculature of avian embryo CAM, ZsGreen fluorescent stable cell lines were generated. MDA-MB-231 breast cancer cells and 231-PDX stable cells were subjected to viral transfection with cDNA encoding ZsGreen, a cytoplasmic-localized fluorescent protein, to generate the respective stably expressing ZsGreen lines ZsMDA-MB-231 and Zs231-PDX. This procedure was generously performed by personnel in the laboratory of Dr. Hon Leong, Lawson Health Research. In brief, cells were treated with a lentivirus containing ZsGreen in polybrene, a reagent that aids in viral transfection. One-day post transfection cells were treated with selection agent, puromycin (2 μL/mL), which was replenished for three days. Successful stable transfection was determined using fluorescence microscopy. These cell lines were used exclusively in the avian embryo

Table 3. Select chemical inhibitors used to treat MCF-7 and MDA-MB-231 cells, targeting ERK1/2 phosphorylation, MMP catalytic activity and MT1-MMP activation.

	Treatment		
	U0126	**BB-94**	**Furin Inhibitor I**
Action	• Targets MEK1 and MEK2 directly by inhibiting catalytic activity of active MEK1/2 • Prevents phosphorylation of ERK1 and ERK 2 • Inhibition is noncompetitive with respect to ERK and ATP substrates (DeSilva et al., 1998)	• Broad spectrum MMP inhibitor • Competitive inhibition • Substrate analog binds to the zinc ion in MMP catalytic site (Low et al., 1996)	• Competitive inhibitor of pro-protein convertase (furin) • Binds catalytic site of furin, blocking activity (Coppola et al., 2008)

Table 4. Primer sequences used for qPCR.

	Forward	**Reverse**
MT1-MMP	5'-GCAGAAGTTTTACGGCTTGCA-3'	5'- TCGAACATTGGCCTTGATCTC-3'
MMP-2	5'- AGCTCCCGGAAAAGATTGATG-3'	5'-CAGGGTGCTGGCTGAGTAGAT-3'
MMP-9	5'-CCTGGAGACCTGAGAACCAATC-3'	5'-GATTTCGACTCTCCACGCATCT-3'
TIMP-2	5'-'CGACATTTATGGCAACCCTATC-3'	5'-GCCGTGTAGATAAACTCTATATCC-3'
α1-PDX	5'-TGAAATCCTGGAGGGCCTGA-3'	5'-AACCAGCCAGACAGCCAGCT-3'
GAPDH	5'-ACCCACTCCTCCACCTTTGA-3'	5'-CTGTTGCTGTAGCCAAATTCGT-3'

tumour assay.

2.4 Chemical Inhibitors

The following inhibitors were used: BB-94 (Batimastat; Santa Cruz Biotechnology), U0126 (Santa Cruz Biotechnology), and Furin Inhibitor I (Millipore; Table 3). Dosages of respective inhibitors were determined using cell viability assays performed in the Damjanovski laboratory, and are as follows: U0126 10 μM, BB-94 10 μM, and Furin Inhibitor I 5 μM, 10 μM, 20 μM.

2.5 RNA Extraction and Quantitative real-time PCR

Cells were seeded at a density of $1x10^6$ cells/mL in 35 mm cell culture plates (Corning) in 2 mL of DMEM/FBS medium and were treated with U0126 (10 μM), BB-94 (10 μM), Furin inhibitor I (5, 10, 20 μM), or DMSO (0.1%) for 24 hours, lysed, RNA was collected using the RNeasy Kit (Qiagen). cDNA was synthesized from 1 μg of RNA using qScript cDNA supermix (Quanta). The relative mRNA levels of *MT1-MMP, MMP-2, MMP-9,* alpha1-Antitrypsin Portland *(α1-PDX),* and *TIMP-2* (Table 4) were assayed by qPCR using SensiFAST SYBR No-ROX Kit (FroggaBio) and the CFX Connect™ Real-Time PCR Detection System (Bio-Rad). mRNA levels were quantified by the ΔΔCT method and displayed as fold change relative to MCF-7 or MDA-MB-231 breast cancer cells under normal culture conditions. The level of glyceraldehyde 3-phosphate dehydrogenase *(GAPDH)* mRNA was used as the internal control.

2.6 Antibodies

For immunoblot analysis, the following primary antibodies were used: Human MT1-MMP (1:1000, AB6004, Millipore), Phospho-ERK1/2 (phospho-ERK1/2) (1:2000, D13.14.4E), Total ERK1/2 (1:2000, 137F5) (Cell Signalling Technology), and β-Actin (1:1000, C4). Goat anti-mouse IgG (H+L) (Bio-Rad) and goat anti-rabbit IgG (H+L) (Thermo Fisher) HRP conjugates were used as secondary antibodies (1:10000).

2.7 Protein Collection and Immunoblotting

Cells were seeded at a density of $1x10^6$ cells/mL in 35 mm culture plates (Corning) in 2

mL of DMEM/FBS medium and treated with U0126 (10 μM), BB94 (10 μM), Furin inhibitor I (5, 10, 20 μM), or DMSO (0.1%) for 24 hours. Post-incubation cells were washed with PBS (pH=7.2) and disrupted using lysis buffer (150 mM NaCl, 1% NP-40, 0.5% NaDC, 0.1% SDS, 50 mM Tris pH 8.0) supplemented with protease/phosphotase inhibitor (Thermo Scientific). Cell lysates were incubated on ice for 20 minutes and homogenized by sonication (Misonix Ultrasonic Liquid Processors XL-2000 Series). Total protein concentration was determined by Pierce BCA Protein Assay Kit (Thermo Fisher) performed as per manufacturer's instructions and absorbance was measured at 595 nm by the Microplate Reader Model 3550-UV (BioRad). Protein aliquots (15 μg) were analyzed by immunoblotting with MT1-MMP, β-actin, phospho-ERK1/2 or total ERK1/2 primary antibodies, followed by incubation with the appropriate secondary HRP-conjugated antibody and detected using SuperSignal West Pico chemiluminescent substrate (Thermo Fisher). Blots were blocked using either 0.5% BSA or 5% BSA in TBST, as directed by the primary antibody manufacturer, and probed using the appropriate primary antibodies. Incubation with primary antibodies occurred overnight at 4°C, and secondary antibodies for one hour at room temperature. Images were captured using the Molecular Imager® ChemiDoc™ XRS System (BioRad) and blots were analyzed using QuantityOne 1-D analysis software.

2.8 Generation of MMP-2 Conditioned Medium for Cell Culture Treatment

MMP-2 conditioned medium was provided by PhD candidate, Mario Cepeda, Western University, and used to verify the efficiency of BB-94 in preventing substrate cleavage activity of MMPs as determined by gelatin zymography analysis In brief, conditioned medium (CM) containing high levels of MMP-2 protein was created by transfecting MCF-7 breast cancer cells with a cDNA construct coding for pro-MMP-2 protein. Following a 24-hour incubation period, pro-MMP-2 transfected MCF-7 cells were washed with phosphate buffered saline (PBS) and incubated in DMEM/F12 medium void of FBS for 24 hours. This serum-free medium conditioned with the soluble pro-MMP-2 transfection product was then collected, aliquoted, and stored at -80°C for later use.

2.9 Gelatin Zymography and Reverse Gelatin Zymography

Gelatin zymography was performed as previously described (Toth et al., 2001) to compare the levels of secreted pro- and activated MMP-2 and MMP-9 in the medium of MCF-7, MCF-7 MT1-MMP C2, and MDA-MB-231 cells following treatment with DMSO (0.1%), U0126 (10 μM), or BB-94 (10 μM). Briefly, 15 μL of medium collected from treated cells were loaded to a 10% polyacrylamide-0.1% gelatin gel and subjected to electrophoresis. After electrophoresis, the gels were incubated in renaturing buffer (25% v/v Triton X-100 in dH2O) to ensure MMP functional ability, and then incubated in developing buffer (0.5 M Tris–HCl, pH 7.8, 2 M NaCl, 0.05 M CaCl2, and 0.2% Brij 35) at 37°C for 48 hours to allow the MMPs to cleave the gelatin embedded within the polyacrylamide gel. After the incubation period, the gel was stained with a 0.5% Coomassie blue, 5% methanol, 10% acetic acid solution. The gel was then progressively destained with a 20% methanol, 10% acetic acid solution until bands that represent cleaved gelatin were clearly visible. Images were taken using the Molecular Imager® ChemiDoc™ XRS System (BioRad).

Reverse zymography, which measured TIMP activity, was performed by adding MMP conditioned medium to the 10% polyacrylamine-0.1% gelatin gel lacking denaturing detergents. Conditioned medium was obtained by incubating HS578t breast cancer cells in serum-free medium for 24 hours, as these cells naturally express high levels of MMP-2 (Takahashi et al., 1999). Samples subjected to gelatin zymography were additionally subjected to reverse gelatin zymography. Protein loading, renaturing, and staining processed are identical to gelatin zymography analysis, however in reverse zymography when the gel is destained it will remain clear, while dark blue banding represents TIMP proteins bound to MMPs embedded in the polyacrylamide gel.

2.10 Firefly Luciferase Transcriptional Activity Assay

Transcriptional activity of AP-1 and NF-κB, MT1-MMP and MMP-9 specific transcription factors, was examined in MCF-7, MCF-7 MT1-MMP C2, MDA-MB 231, and 231-PDX cells following respective inhibitor treatment. In brief, cells were seeded at a density of 3.0 $x10^4$ cells/well in a 96-well culture plate (Corning) and incubated for 24

hours. Following incubation, cells were transfected with Lipofectamine 2000 (Thermo Fisher) according to the manufacturer's instructions and OPTI-MEM (Gibco) reduced serum medium, in combination with 0.2 μg of mammalian 3xAP1pGL3 (Plasmid # 40342) (Transcription factor: AP-1) or p1242 3xKB-L (Plasmid #26699) (Transcription factor: NF-κB) luciferase plasmids (Addgene). 24 hours post transfection, MCF-7, MCF-7 MT1-MMP C2, and MDA-MB-231 cells were subjected to treatment with DMSO (0.1%), U0126 (10 μM), or BB-94 (10 μM). 12 hours later cells were lysed and treated with Firefly Luciferase Glow Assay reagents (Thermo Fisher) according to the manufacturer's instructions. Luminescence was detected using Modulus™ II Microplate Multimode Reader and the GloMax®- Multi Detection System with Instinct® Software.

2.11 Scratch Wound Closure Migration Assay

To examine the effects of respective inhibitor treatment on cell migratory potential, MDA-MB-231 breast cancer cells were seeded at a density of $2.5x10^5$ cells/mL in a 35 mm cell culture dish (Corning) in 2 mL of DMEM/FBS medium and allowed to form a monolayer for 24 hours. Following incubation, medium was aspirated and the monolayer was disrupted using a 1000 μL pipette tip to create a wound down the length of the culture dish. The remaining adhered cells were washed three times with PBS (pH 7.2) to remove cell debris and then incubated with fresh DMEM 10% FBS, 1% pen/strep medium containing treatment of DMSO (0.1%), U0126 (10 μM), BB-94 (10 μM), or Furin Inhibitor I (20 μM). 2 hours post wound generation, using the Zeiss Observer.A1 AX10 microscope, 10 images were captured down the length of the scratch that represent the 'initial' size of the wound for each respective sample. The same area of the wound was imaged at 6, 12, and 24 hours following wound healing to examine the ability to migrate into the wound space. Scratch closure was quantified by measuring the width of the scratch each day and normalizing it to the initial size of the scratch. Scratch closure is presented as a mean percentage of the initial scratch size ± SEM.

2.12 Transwell Cell Motility Assays

The migratory and invasive potential of MDA-MB-231 cells was measured using 24-well 8 μm pore transwell inserts (Corning). 2.0×10^4 cells were seeded on the upper chamber

of the transwell in serum-free medium treated with DMSO (0.1%), U0126 (10 μM), or BB-94 (10 μM). Treated cells were allowed to migrate (24 hours) or invade (48 hours) towards the bottom chamber which was placed in DMEM/F-12 medium supplemented with 10% FBS and 1% pen/strep, serving as the chemoattractant. Migration assays were performed with uncoated transwell inserts, whereas invasion assays were performed with inserts coated with 20% Matrigel, a basement membrane analog. 20% Matrigel was generated by diluting Matrigel (BD Biosciences) in DMEM/F-12 serum-free medium. Cells that migrated to the lower chamber of the transwell insert were fixed, stained, and quantified as per Marshall, 2011. To quantify cell migration, cells were fixed in 100% methanol, and non- motile cells remaining in the upper surface of the transwell removed with a damp cotton swab. Cells on the bottom of transwells were stained using a 0.5% solution of crystal violet in distilled water. These stained transwells were then individually destained in 33% acetic acid, and the absorbance of this solution at 490 nm was quantified using the Microplate Reader Model 3550-UV (BioRad) as a correlative measurement of cell number. Invasion transwells, were fixed with 100% methanol and cells that did not invade through the transwell insert and residual Matrigel were removed from the upper membrane surface with a damp cotton swab. Invading cells were then stained with a 0.5% crystal violet solution and residual stain was removed using a cotton swab. Invasion transwells were imaged using the Leica DM16000 B microscope with Hamamatsu camera controller (C10600) at 20X magnification. 15 images were taken per transwell and were blindly quantified using ImageJ software (U.S. National Institutes of Health, Bethesda, Maryland, USA).

2.13 Three Dimensional (3D) Cell Culture

MDA-MB-231 and 231-PDX cells were embedded in 50% Matrigel matrix (BD Biosciences) and processed for fluorescent staining to assess changes in invasive morphological features as described by Cvetković, et al., 2014. 35 mm Glass-bottom cell culture dishes (MatTek) were prepared by coating the glass with 50% Matrigel (BD Bioscience) in serum-free medium, allowing the matrix to solidify, and seeding $2.5x10^4$ cells in 50% Matrigel in serum-free medium above this layer to result in cells completely suspended in matrix. DMEM/F-12 serum-free medium combined to generate 50%

Matrigel and DMEM/F-12 medium supplemented with 10% FBS and 1% pen/strep were treated with DMSO (0.1%), U0126 (10 μM), or BB-94 (10 μM).

Fluorescent staining procedure was done as described in Cvetković, et al., (2014) using Alexa Fluor 633 phalloidin (1:100) and DAPI (1 ug/mL) staining. Cell colony morphology was monitored for five days using bright-field microscopy (Leica DM16000 B microscope with Leica DFC425 camera) at 10X magnification, and representative 50 μm z-stack images (2 μm interval) taken at random locations across the matrix were captured using Leica MMAF software (Metamorph®). After five days, cells within the matrix were fixed using 20% acetone, 80% methanol and prepared for fluorescent staining using Alexa Fluor 633 phalloidin (Thermo Fisher, 1:100), and DAPI (1 μL/mL, BioShop Canada) to examine F-actin and nuclei, respectively. Prepared samples were imaged using a Nikon A1R+ confocal microscope and NIS Elements software (Nikon), capturing Z-stacks of approximately 100 μm.

To analyze and score morphology of cell colonies, images representing a field of view at 20x magnification, were blindly analyzed using ImageJ software (U. S. National Institutes of Health, Bethesda, Maryland, USA). Protrusions were defined as thin extensions that emanated from a round cell colony. The number of protrusions on all cell colonies in an image was counted, with longer protrusions counted as multiples of the average protrusion length seen in that image to adjust for the heterogeneity in size observed. Disseminations were identified as small, round cells immediately adjacent to a larger colony. The score, representing the total number of protrusions or total number of disseminations for each treatment, was divided by the total number of colonies to arrive at the final measurement of protrusions or disseminations per colony.

2.14 Avian Embryo Tumour Vascularization Assay

The vascularization of artificial Matrigel tumours of ZsGreen tagged MDA-MB-231 cells (ZsMDA-MB-231) treated with DMSO (0.1%), U0126 (10 μM), or BB-94 (10 μM), and ZsGreen tagged 231-PDX cells (Zs231-PDX) in Matrigel (BD Bioscience) was assessed in avian embryos following the technique developed by Dr. Hon Leong, Lawson Health Sciences, Western University. Avian embryos, materials, equipment, and facilities were

generously provided by Dr. Hon Leong, Lawson Health Research Institute, London Ontario. Chick embryos were incubated in culture boats for nine days at 37°C in a humidified chamber. A superficial wound was introduced to the vasculature of the chorioallantoic membrane (CAM) of embryos and an artificial tumour composed of 10 μL of Matrigel (BD Bioscience) containing ~500 000 cells was injected into the wound. Embryos were incubated for a further eight days, during which appropriate inhibitor treatments were applied every 48 hours directly on top of the tumour using a 10 μL pipette within the wounded CAM vasculature. Tumours were then examined using fluorescent stereomicroscopy to assess if vasculature had developed at the tumour site. Vascularization was determined to have occurred if the wound site showed capillaries associated with a tumour, which had successfully grown beneath the CAM layer. This was accomplished by comparing observed vasculature using bright field microscopy to areas of contrast observed under fluorescent conditions. Vascularization was quantified as a binary measurement, indicated by the presence or absence of tumour-localized vasculature in individual embryos. Degree of wound closure was also used as a measure of tumor invasion, whereby wound closure was characterized as the presence of the tumor completely under the CAM and regression of initially wounded vasculature.

2.15 Densitometry Analysis

Quantitative densitometric analysis of immunoblots was performed using QuantityOne software (Bio-Rad). Band intensity was obtained for the MT1-MMP, β-Actin, phospho-ERK and total ERK1/2 signal of each sample from three independent biological experiments. MT1-MMP pro- and active protein is presented as a ratio between each respective band intensity and β-Actin signal. ERK1/2 activation is presented as a ratio between phospho-ERK1/2 and total ERK1/2 band intensity normalized to MCF-7 or MDA-MB-231 cells under control conditions.

2.16 Statistical Analysis

Statistical analysis and graphing was performed using GraphPad Prism version 6.0 (GraphPad software, La Jolla, CA, USA). Data is presented as mean ± SEM, where all experiments were comprised of at least 3 biological replicates. One-way and Two-way

ANOVA followed by Tukey's, Dunnett's, or Sadik's post-hoc tests or students t-test were used and are indicated respectively in each figure legend. Different levels of statistical significance are denoted by a different number of asterisks and are as follows: ****, $p \leq 0.0001$, ***, $p \leq 0.001$, **, $p \leq 0.01$, *, $p \leq 0.05$, ns, $p < 0.05$.

Chapter 3

3 Results

3.1 MEK1/2 inhibitor altered *MMP-2* and *MMP-9* mRNA levels in MCF-7 MT1-MMP C2 and MDA-MB-231 cells

Overexpression of *MT1-MMP* in MCF-7 cells (MCF-7 MT1-MMP C1, C2, and C3) resulted in higher levels of phosphorylated ERK1/2 compared to MCF-7 parental cells. MCF-7 C2 cells notably contained the highest levels of phospho-ERK1/2 and were thus chosen for further investigation. In addition to showing the highest phospho-ERK1/2 levels, these MCF-7 C2 cells were the only cell line exhibiting MT1-MMP protein predominately in its active form (Cepeda et al., 2016), and also had the highest expression of *MMP-2* and *MMP-9*. When each MCF-7 cell line was treated with the MEK1/2 inhibitor, U0126, ERK1/2 phosphorylation was consistently decreased in each cell line (Fig. 2a). In addition, treatment of MCF-7 C2 cells with the MEK1/2 inhibitor resulted in a prominent inverse relationship between *MMP-2* and *MMP-9* mRNA levels, with a significant ($p \leq 0.01$) ~1.6 fold increase in *MMP-2* and a significant ($p \leq 0.01$) ~7.5 fold decrease in *MMP-9*, respectively (Fig. 2b). These results indicated that inhibiting ERK1/2 phosphorylation in cells with predominately active MT1-MMP protein, expression of *MMP-9* was impacted more greatly than expression of *MMP-2*.

While MCF-7 C2 cells provide a model demonstrating the impact of artificially elevated levels of active MT1-MMP protein on phospho-ERK1/2, and *MMP-2* and *-9* expression, MDA-MB-231 breast cancer cells naturally posses high basal levels of active MT1-MMP, phospho-ERK1/2, and increased *MMP-2*/*-9* expression (Cepeda et al., 2016), and are thus a target for comparison. To determine if the relationship between phospho-ERK1/2 and *MMP-2* and *-9* mRNA levels is conserved between breast cancer cells MDA-MB-231 cells were treated with the MEK1/2 inhibitor. Treatment of MDA-MB-231 cells with 10 μM of U0126 (Fig. 3a) resulted in a significant ($p \leq 0.0001$) decrease in ERK1/2 phosphorylation (~10.9 fold difference), but negligible changes were observed in the levels of pro- and active forms of MT1-MMP ($p > 0.05$) (Fig. 3b). Nonetheless, *MT1-*

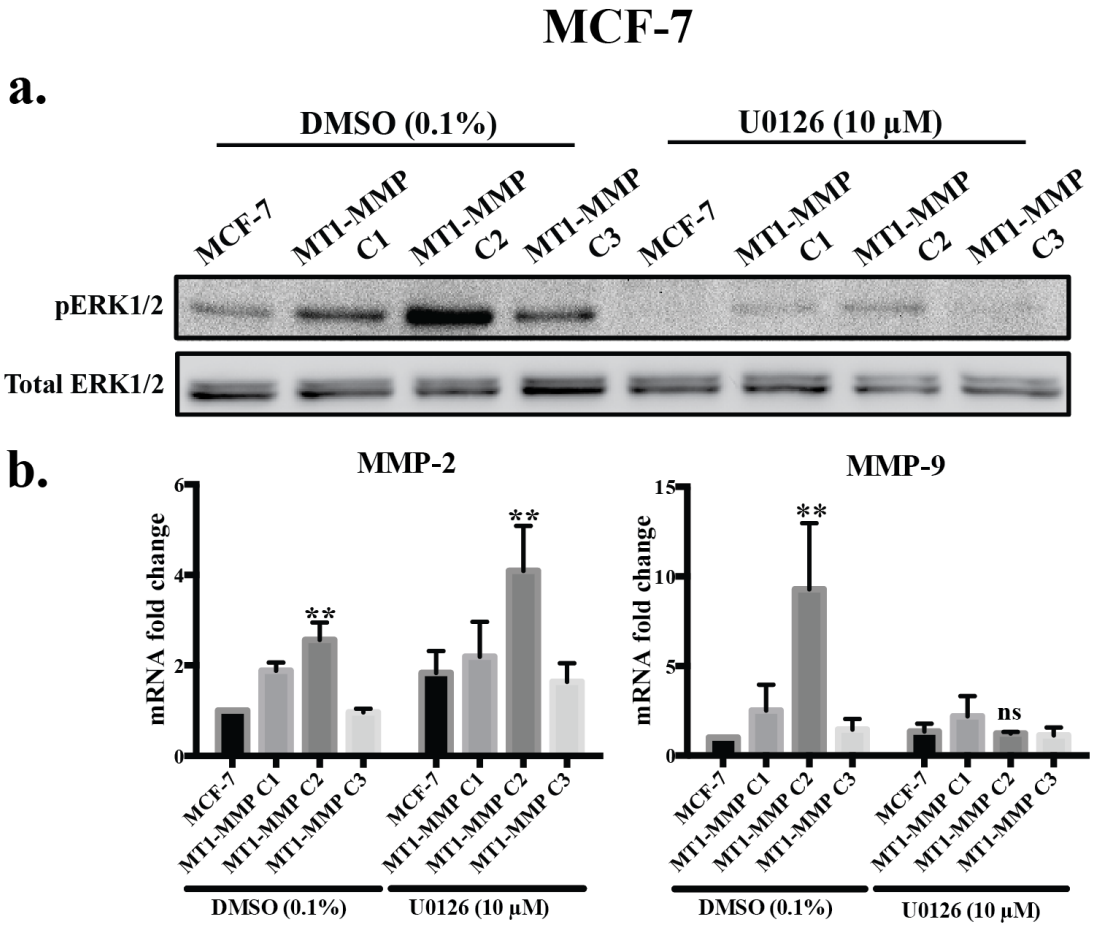
MCF-7
a.
DMSO (0.1%)
U0126 (10 µM)
MCF-7
MT1-MMP C1
MT1-MMP C2
MT1-MMP C3
pERK1/2
Total ERK1/2
b.
MMP-2
MMP-9
mRNA fold change
**
ns
MCF-7
MT1-MMP C1
MT1-MMP C2
MT1-MMP C3
DMSO (0.1%)
U0126 (10 µM)

Figure 2. Phosphorylated ERK1/2 mediates an inverse relationship between *MMP-2* and *MMP-9* gene expression in MCF-7 breast cancer cells.

(a) Western blot analysis showing levels of phosphorylated ERK1/2 protein in MCF-7 breast cancer cells and three clonally selected MCF-7 cell lines that stably express different levels of *MT1-MMP,* treated with MEK1/2 inhibitor (U0126 10 μM) or vehicle control (DMSO 0.1%). Total ERK1/2 was used as a loading control. MCF-7 MT1-MMP C2 cells exhibited the highest levels of phospho-ERK1/2, however all cell lines demonstrated a decrease in phosphorylated ERK1/2 protein following treatment with U0126. **(b)** qPCR analysis of *MMP-2* and *MMP-9* mRNA in MCF-7 breast cancer cells and three clonally selected MCF-7 cell lines that stably express different levels of *MT1-MMP* subjected to U0126 (10 μM) or DMSO (0.1%). Fold change was quantified using the ΔΔCT method and shown as mean ± SEM. One-way ANOVA followed by Tukey's post-hoc test; **, $p \leq 0.01$, ns, $p > 0.05$. MCF-7 C2 cells showed an inverse relationship between *MMP-2* and *MMP-9* mRNA levels, which significantly increased and decreased respectively, following treatment with U0126.

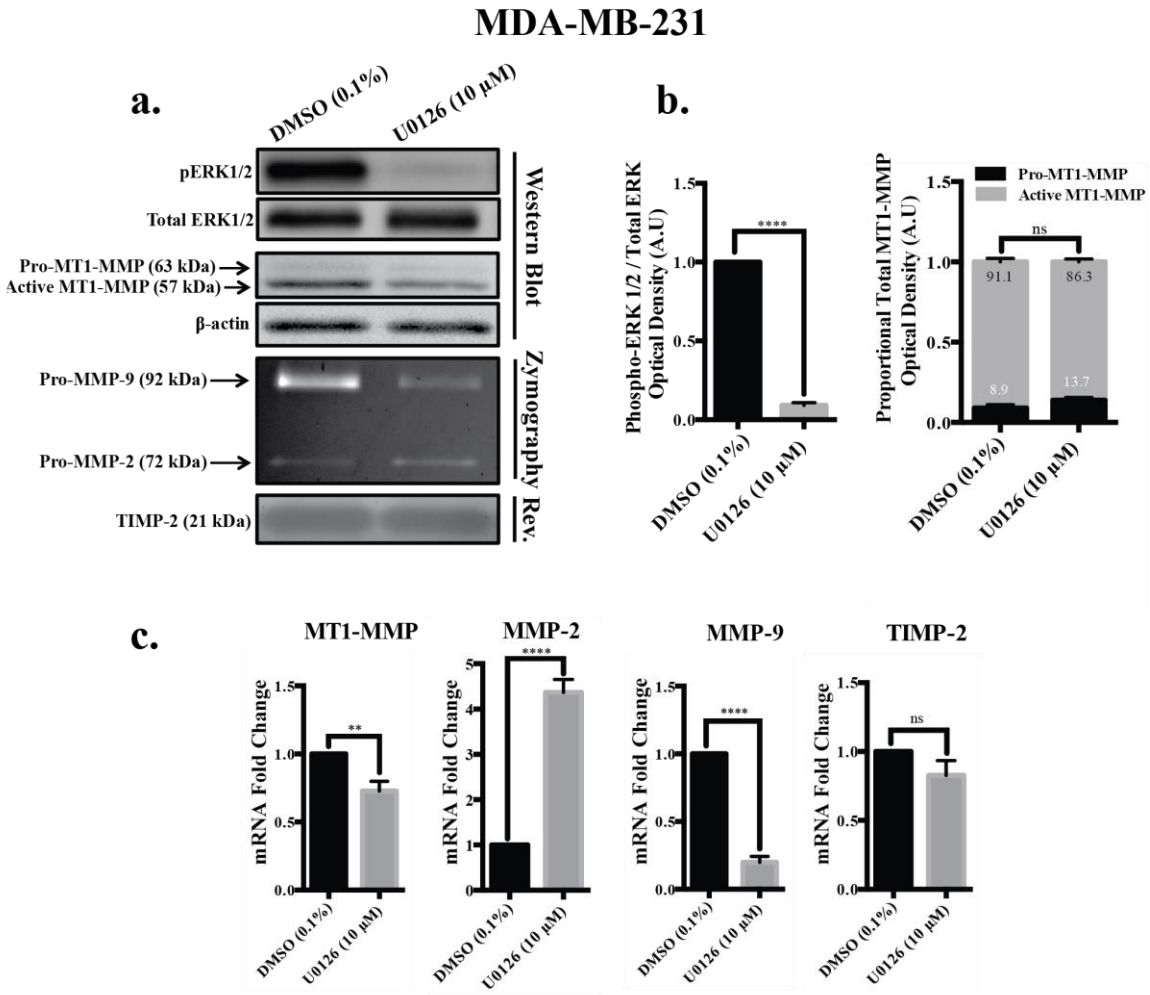
MDA-MB-231
a.
DMSO (0.1%)
U0126 (10 μM)
pERK1/2
Total ERK1/2
Pro-MT1-MMP (63 kDa)
Active MT1-MMP (57 kDa)
β-actin
Western Blot
Pro-MMP-9 (92 kDa)
Pro-MMP-2 (72 kDa)
Zymography Rev.
TIMP-2 (21 kDa)
b.
Phospho-ERK 1/2 / Total ERK Optical Density (A.U)
****
DMSO (0.1%)
U0126 (10 μM)
Proportional Total MT1-MMP Optical Density (A.U)
Pro-MT1-MMP
Active MT1-MMP
ns
91.1
86.3
8.9
13.7
c.
MT1-MMP
MMP-2
MMP-9
TIMP-2
mRNA Fold Change
**
****
****
ns

Figure 3. Phosphorylated ERK1/2 mediates an inverse relationship between *MMP-2* and *MMP-9* gene expression in MDA-MB-231 breast cancer cells.

(a) Western blot (top 4 panels), gelatin zymography (middle panels), and reverse gelatin zymography analysis (bottom panel) of MDA-MB-231 breast cancer cells subjected to MEK1/2 inhibitor (U0126 10 μM) or vehicle control (DMSO 0.1%) presenting ERK1/2 phosphorylation, pro- and active MT1- MMP, pro-and active MMP-2 and -9, and TIMP-2 protein levels, respectively. For western blot analysis, total ERK1/2 and β-actin served as loading controls. **(b)** Densitometry quantification of phospho-ERK1/2 protein measured in western blots, Student's t-test; ****, $p \leq 0.0001$, where U0126 was effective at decreasing ERK1/2 phosphorylation, however MT1-MMP pro- and active protein levels were unchanged, analyzed by two-way ANOVA followed by Tukey's post hoc test; ns, $p > 0.05$. **(c)** qPCR analysis of MT1-MMP, MMP-2, MMP-9 , and TIMP-2 mRNA isolated from MDA-MB-231 breast cancer cells treated with U0126 (10 μM) or DMSO (0.1%). Fold change was quantified using the ΔΔCT method and shown as mean ± SEM, as analyzed by Student's t-test; ****, $p \leq 0.0001$, **, $p \leq 0.01$, ns, $p > 0.05$. Following treatment with U0126, MDA-MB-231 cells showed a significant increase in MMP-2 mRNA levels and a significant decrease in MMP-9 mRNA levels, and therefore indicated that this MMP expression relationship was conserved between the MCF-7 MT1-MMP C2 and MDA-MB-231 breast cancer cell lines.

MMP mRNA levels were significantly ($p \leq 0.01$) decreased ~1.4 fold. Furthermore, treatment of MDA-MB-231 cells with U0126 (10 μM) resulted in a significant ($p \leq 0.0001$) ~4.4 fold increase in *MMP-2* mRNA levels, but a significant ($p \leq 0.0001$) ~5 fold decrease in *MMP-9* mRNA levels, with no change ($p > 0.05$) in *TIMP-2* mRNA (Fig. 3c), all of which are consistent with gelatin zymography analysis of these proteins (Fig. 3a). The consistency of the inverse relationship of increased *MMP-2* mRNA and decreased *MMP-9* mRNA following inhibition of ERK1/2 phosphorylation not only suggests how these gelatinases are regulated, but also that their regulation is conserved between breast cancer cell lines used.

3.2 Inhibition of MT1-MMP catalytic site increased total MT1-MMP protein levels and altered subsequent *MMP-2* and *MMP-9* mRNA levels in MCF-7 and MDA-MB-231 breast cancer cells

Gelatin zymography analysis of low MT1-MMP protein MCF-7 parental cells and high, predominately active MT1-MMP, MCF-7 C2 cells treated with the pan-MMP catalytic site inhibitor BB-94 showed the effect of MMP inhibition on pro-MMP-2 activation. Using gelatin zymography, MCF-7 C2 cells treated with pro-MMP-2 conditioned medium demonstrated a transition of pro-MMP-2 through its intermediate to active form (Fig. 4a, lane 3). Additionally, MCF-7 C2 cells treated with BB-94 lack active MMP-2 (Fig. 4a, lane 4) and confirmed the efficiency of the BB-94 chemical inhibitor in preventing MMP catalytic site activity. BB-94 treatment to inhibit MT1-MMP catalytic activity was used along with MEK1/2 inhibitor, U0126, to further examine the regulation of MT1-MMP protein forms.

Treatment of parental MCF-7 and MCF-7 C2 cells with DMSO (0.1%), U0126 (10 μM), and BB-94 (10 μM) changed the total amount of MT1-MMP protein present within MCF-7 C2 cells, with most prominent changes in the active form, as shown by western blot (Fig. 4b). Specifically, inhibition of ERK1/2 phosphorylation caused a significant ($p \leq 0.0001$) decrease in active MT1-MMP thus reducing the total amount of MT1-MMP

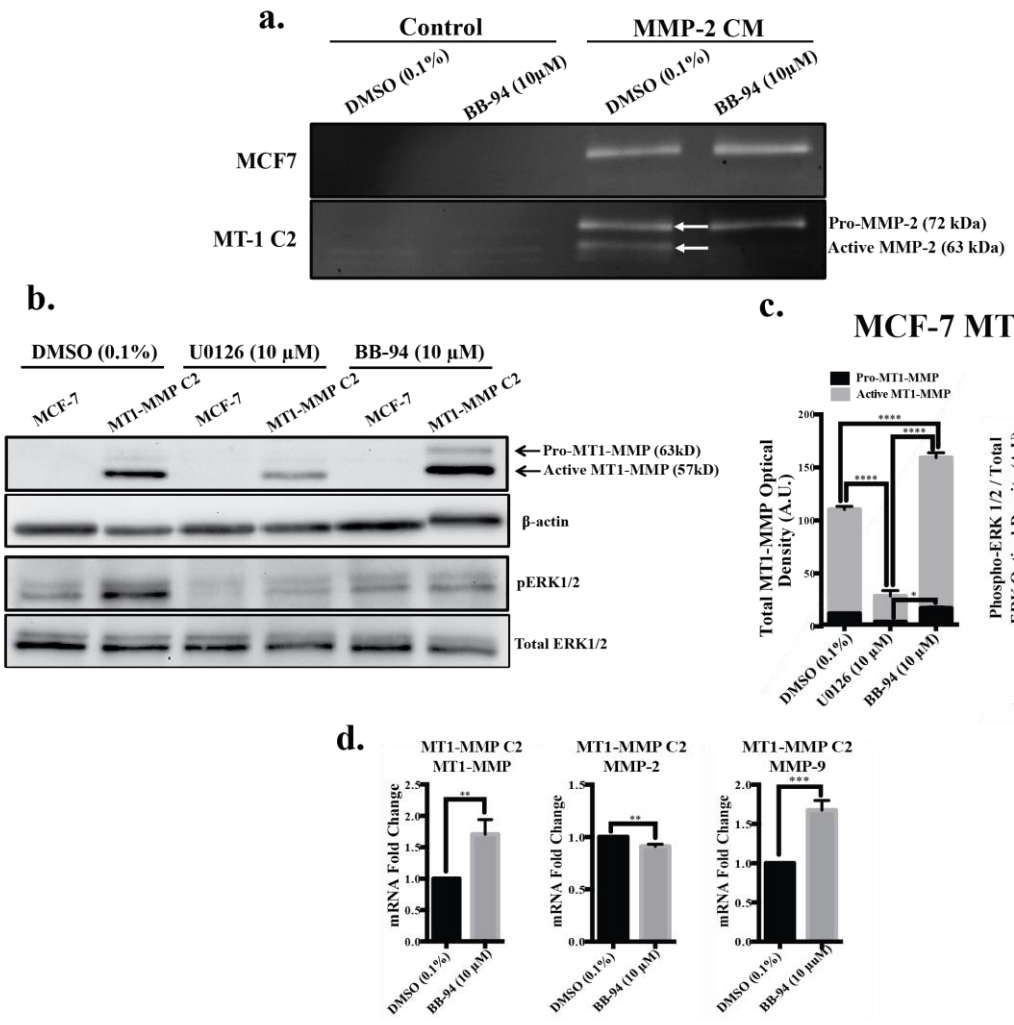
a.
Control
MMP-2 CM
DMSO (0.1%)
BB-94 (10μM)
DMSO (0.1%)
BB-94 (10μM)
MCF7
MT-1 C2
Pro-MMP-2 (72 kDa)
Active MMP-2 (63 kDa)
b.
DMSO (0.1%)
U0126 (10 μM)
BB-94 (10 μM)
MCF-7
MT1-MMP C2
MCF-7
MT1-MMP C2
MCF-7
MT1-MMP C2
Pro-MT1-MMP (63kD)
Active MT1-MMP (57kD)
β-actin
pERK1/2
Total ERK1/2
c.
MCF-7 MT1-MMP C2
Pro-MT1-MMP
Active MT1-MMP
Total MT1-MMP Optical Density (A.U.)
DMSO (0.1%)
U0126 (10 μM)
BB-94 (10 μM)
Phospho-ERK 1/2 / Total ERK Optical Density (A.U)
DMSO (0.1%)
U-0126 (10uM)
BB-94 (10uM)
d.
MT1-MMP C2
MT1-MMP
mRNA Fold Change
DMSO (0.1%)
BB-94 (10 μM)
MT1-MMP C2
MMP-2
mRNA Fold Change
DMSO (0.1%)
BB-94 (10 μM)
MT1-MMP C2
MMP-9
mRNA Fold Change
DMSO (0.1%)
BB-94 (10 μM)

Figure 4. Inhibition of ERK1/2 phosphorylation and MT1-MMP catalytic site changes MT1-MMP pro- and active protein forms and associated *MMP-2* and *MMP-9* mRNA levels in MCF-7 MT1-MMP C2 cells.

(a) Gelatin zymography analysis of MCF-7 and MCF-7 MT1-MMP C2 cells treated with pan-MMP catalytic site inhibitor BB-94 (10 μM) or vehicle control (DMSO 0.1%) and incubated for 12 hours with serum-free medium (control) or serum-free medium supplemented with conditioned medium (CM) containing pro-MMP-2. Only MCF-7 C2 cells treated 0.1% DMSO and supplemented with CM containing pro-MMP-2 showed a transition of pro-MMP-2 through its intermediate and active forms, whereas application of BB-94 prevented pro-MMP-2 activation, and demonstrated the effectiveness of BB-94 in inhibiting MMP catalytic activity. **(b)** Western blot analysis of MCF-7 and MCF-7 C2 cells showing pro- and active MT1-MMP protein levels and ERK1/2 phosphorylation following treatment with DMSO (0.1%), U0126 (10 μM), or BB-94 (10 μM). β-actin and total ERK1/2 respectively serve as loading controls. **(c)** Densitometry quantification of western blotted MT1-MMP protein isoforms in MCF-7 C2 cells, Two-way ANOVA followed by Tukey's post hoc test; ****, $p \leq 0.0001$,*, $p \leq 0.05$ and phospho-ERK1/2 protein, Student's t-test; ***, $p \leq 0.001$, **, $p \leq 0.01$. U0126 treated MCF-7 C2 cells exhibited less total MT1-MMP, therefore both decreased pro- and active forms, while MCF-7 C2 cells treated with BB-94 showed more total MT1-MMP, comprising of increased pro- and active forms. **(d)** qPCR analysis of *MT1-MMP*, *MMP-2*, and *MMP-9* mRNA from MCF-7 C2 cells treated with BB-94 (10 μM) or DMSO (0.1%). Fold change was quantified using the ΔΔCT method and shown as mean ± SEM. Student's t-test; ***, $p \leq 0.001$,**, $p \leq 0.01$. An inverse, yet opposite relationship to that of U0126 treatment, between *MMP-2* and *MMP-9* mRNA levels following BB-94 treatment was observed, comprising of significantly decreased *MMP-2* mRNA and significantly increased *MMP-9* mRNA.

protein compared to MCF-7 parental cells by ~75%. Inhibition of MT1-MMP catalytic activity significantly ($p \leq 0.0001$) increased both active MT1-MMP and overall total MT1-MMP protein levels by ~69%. In addition, treatment of MCF-7 C2 cells with U0126 significantly ($p \leq 0.0001$) reduced ERK1/2 phosphorylation, while treatment with BB-94 significantly ($p \leq 0.05$) increased ERK1/2 phosphorylation (Fig. 4b lane 4, and c). As shown by qPCR, treatment of MCF-7 C2 cells with BB-94 significantly increased *MT1-MMP* ~1.8 fold ($p \leq 0.01$) and *MMP-9* mRNA levels ~1.6 fold ($p \leq 0.001$), but significantly decreased *MMP-2* mRNA ~0.1 fold ($p \leq 0.01$) (Fig. 4d). BB-94 treatment altered MMP mRNA levels in an inverse manner (decreased *MMP-2*, increased MMP-9) when compared to that of U0126 treatment (increased MMP-2, and decreased MMP-9).

In order to determine if this alteration of *MMP-2* and *MMP-9* mRNA levels upon BB-94 treatment was breast cancer cell specific, MDA-MB-231 cells were also treated with 10 μM of BB-94. MDA-MB-231 cells appeared more resistant to treatment, as MT1-MMP protein levels and ERK1/2 phosphorylation were not significantly ($p > 0.05$) changed (Fig. 5a and b). However, these BB-94 treated cells did exhibit changes in *MT1-MMP* and *MMP-9* mRNA levels which were significantly increased ~1.8 fold ($p \leq 0.01$) and ~1.5 fold ($p \leq 0.05$) respectively. Additionally *MMP-2* mRNA levels were significantly decreased ~0.7 fold ($p \leq 0.01$) (Fig. 5c). There is a consistent inverse relationship between the mRNA levels of the gelatinases when treated with BB-94. This inverse relationship, decreased *MMP-2* and increased *MMP-9* mRNA levels, following inhibition of MMP catalytic activity is conserved among breast cancer cell lines, and may provide insight as to how these gelatinases are regulated.

3.3 Inhibiting pro-MT1-MMP activation changed *MMP-2* and *MMP-9* mRNA levels and resulted in altered migratory and invasive potential in MCF-7 and MDA-MB-231 breast cancer cells

To determine the effects of reduced MT1-MMP active protein levels in influencing phosphorylation of ERK1/2, MCF-7 C2 cells which contain predominately active MT1-MMP, were treated with increasing concentrations of protein convertase Furin inhibitor. (Fig. 6a). 24-hour treatment of MCF-7 C2 cells with 20 μM of Furin inhibitor I was

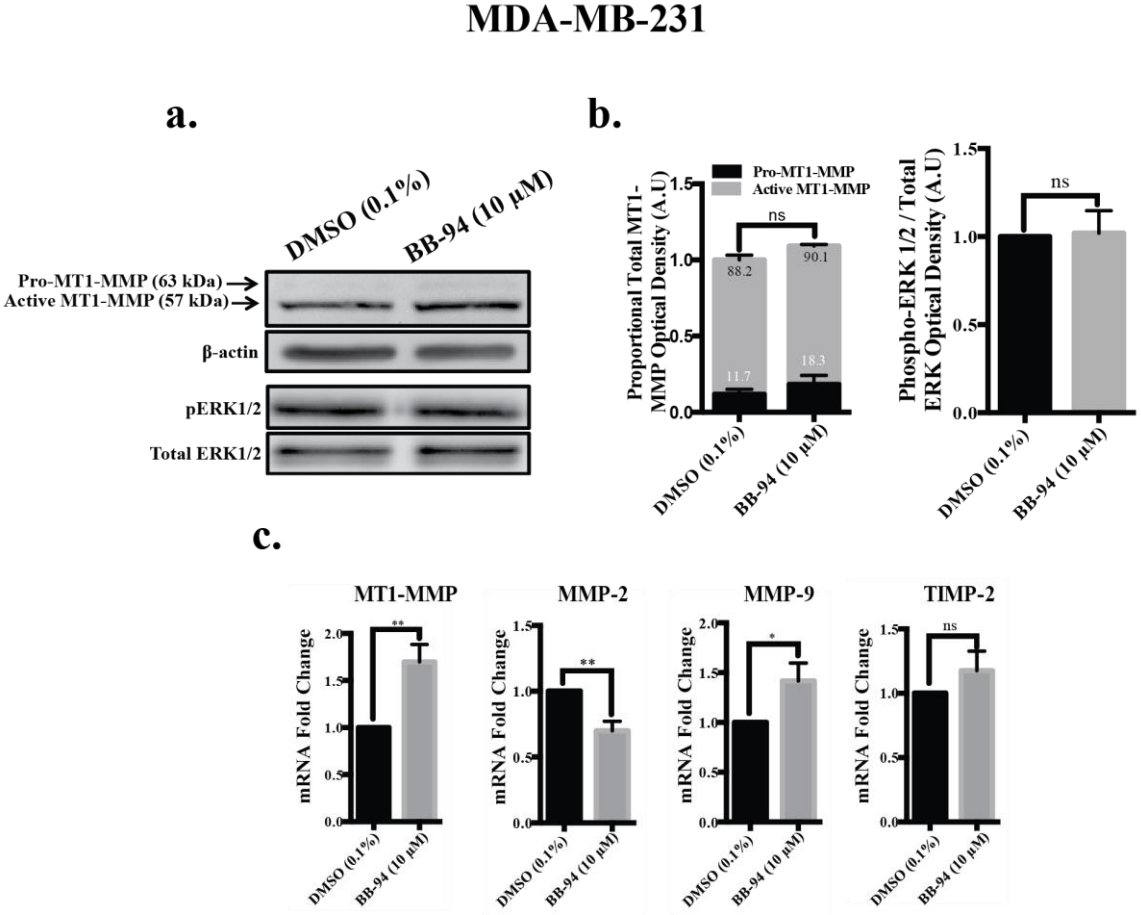
MDA-MB-231
a.
DMSO (0.1%)
BB-94 (10 µM)
Pro-MT1-MMP (63 kDa)
Active MT1-MMP (57 kDa)
β-actin
pERK1/2
Total ERK1/2
b.
Pro-MT1-MMP
Active MT1-MMP
Proportional Total MT1-MMP Optical Density (A.U)
ns
88.2
90.1
11.7
18.3
DMSO (0.1%)
BB-94 (10 µM)
Phospho-ERK 1/2 / Total ERK Optical Density (A.U)
ns
c.
MT1-MMP
MMP-2
MMP-9
TIMP-2
mRNA Fold Change
**
**
*
ns

Figure 5. Inhibition of the MT1-MMP catalytic site does not changes MT1-MMP pro- and active protein forms, but does change *MT1-MMP, MMP-2*, and *MMP-9* mRNA levels in MDA-MB-231 breast cancer cells.

(a) Western blot analysis showing pro- and active MT1-MMP protein and ERK1/2 phosphorylation following treatment of MDA-MB-231 breast cancer cells with pan-MMP catalytic site inhibitor BB-94 (10 μM) or vehicle control (DMSO 0.1%). β-actin and total ERK1/2 respectively serve as loading controls. **(b)** Densitometry quantification of western blotted MT1-MMP protein isoforms, Two-way ANOVA followed by Tukey's post hoc test; ns, $p > 0.05$ and phospho-ERK1/2 protein, Student's t-test; ns, $p > 0.05$. **(c)** qPCR analysis of *MT1-MMP*, *MMP-2*, *MMP-9* , and *TIMP-2* mRNA from MDA-MB-231 cells treated with BB-94 (10 μM) or DMSO (0.1%). Fold change was quantified using the ΔΔCT method and shown as mean ± SEM and analyzed by Student's t-test; **, $p \leq 0.01$, *, $p \leq 0.5$, ns, $p > 0.05$. An inverse, yet opposite relationship to that of U0126 treatment, between *MMP-2* and *MMP-9* mRNA following BB-94 treatment was observed, comprising of significantly decreased *MMP-2* mRNA levels and significantly increased *MMP-9* mRNA levels. This observed relationship, decreased *MMP-2* and increased *MMP-9* mRNA levels, was conserved between MCF-7 MT1-MMP C2 and MDA-MB-231 breast cancer cell lines.

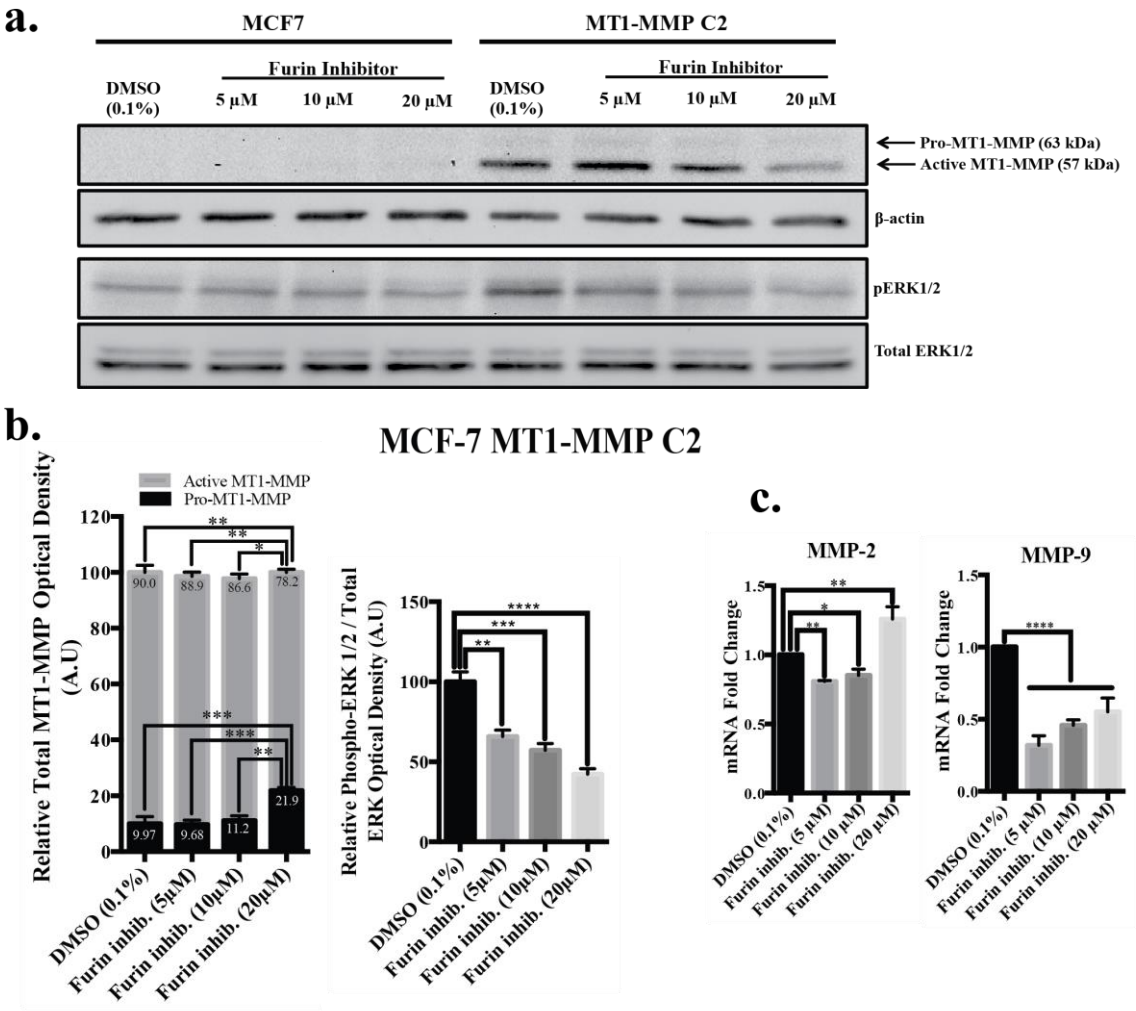
a.
MCF7
MT1-MMP C2
Furin Inhibitor
DMSO (0.1%)
5 µM
10 µM
20 µM
Pro-MT1-MMP (63 kDa)
Active MT1-MMP (57 kDa)
β-actin
pERK1/2
Total ERK1/2
b.
MCF-7 MT1-MMP C2
Active MT1-MMP
Pro-MT1-MMP
Relative Total MT1-MMP Optical Density (A.U)
90.0
88.9
86.6
78.2
9.97
9.68
11.2
21.9
DMSO (0.1%)
Furin inhib. (5µM)
Furin inhib. (10µM)
Furin inhib. (20µM)
Relative Phospho-ERK 1/2 / Total ERK Optical Density (A.U)
c.
MMP-2
MMP-9
mRNA Fold Change

Figure 6. Inhibition of MT1-MMP activation reduces active MT1-MMP levels and ERK1/2 phosphorylation with subsequent changes *MMP-2* and *MMP-9* mRNA levels in MCF-7 MT1-MMP C2 cells.

(a) Western blot analysis showing pro- and active MT1-MMP and phospho-ERK1/2 protein levels following treatment of MCF-7 and MCF-7 MT1-MMP C2 cells with MT1-MMP activation inhibitor, Furin Inhibitor I, at increasing concentrations (5, 10, 20 μM) or vehicle control (DMSO 0.1%). β-actin, and total ERK1/2 served as loading controls respectively. **(b)** Densitometry quantification of western blot analysis of MT1-MMP protein isoforms in MCF-7 C2 cells showed decreased levels of active MT1-MMP with increasing concentration of Furin Inhibitor I, as analyzed by two-way ANOVA followed by Sidak's post hoc test; ***, $p \leq 0.001$, **, $p \leq 0.01$,*, $p \leq 0.05$. Densitometry quantification of western blotted phospho-ERK1/2 protein showing decreased ERK1/2 phosphorylation with increasing concentration of Furin Inhibitor I, as analyzed by one-way ANOVA followed by Tukey's post hoc test; ****, $p \leq 0.0001$, ***, $p \leq 0.001$,**, $p \leq 0.01$. **(c)** qPCR analysis of *MMP-2* and *MMP-9* mRNA in MCF-7 C2 cells subjected to increasing concentrations (5, 10, 20 μM) of Furin inhibitor I or DMSO (0.1%) exhibiting significantly increased *MMP-2* mRNA levels and significantly decreased *MMP-9* mRNA levels. Fold change was quantified using the ΔΔCT method and shown as mean ± SEM. One-way ANOVA followed by Dunnett's post-hoc test; ****, $p \leq 0.0001$,**, $p \leq 0.01$, *, $p \leq 0.05$.

determined to be the most effective in altering the forms of MT1-MMP (Fig. 6a, lane 8). This treatment caused an 11.9% significant ($p \leq 0.001$) increase in pro-MT1-MMP protein levels, and 11.8% significant ($p \leq 0.01$) decrease in active MT1-MMP protein levels. 20 μM of Furin inhibitor I also significantly ($p \leq 0.0001$) reduced ERK1/2 phosphorylation by 50% (Fig. 6b). Furthermore, this treatment resulted in ~0.8 fold significant ($p \leq 0.01$) increase in *MMP-2* and ~1.8 fold significant ($p \leq 0.0001$) decrease in *MMP-9* mRNA levels (Fig. 6c).

Because 20 μM of Furin Inhibitor I successfully reduced active MT1-MMP and phospho-ERK1/2 levels, and induced changes in gelatinase expression in MCF-7 C2 cells, MDA-MB-231 cells were treated with the same concentration in order to determine if the furin inhibitor was capable of eliciting the same effect in cells which naturally contain higher levels of active MT1-MMP protein. Treatment of MDA-MB-231 cells with this inhibitor did not significantly ($p > 0.05$) change MT1-MMP protein forms, and did not effect ERK1/2 phosphorylation (Fig. 7a and b). However, this inhibitor changed *MT1-MMP* mRNA levels, as treated MDA-MB-231 cells displayed a significant ($p \leq 0.05$) decrease in *MT1-MMP* (~0.22 fold) and *MMP-9* (~0.2 fold) mRNA levels and a significant ($p \leq 0.05$) increase in *MMP-2* mRNA (~0.9 fold) (Fig. 7c. The changes in *MMP-2* and *MMP-9* mRNA levels in MDA-MB-231 cells following treatment with Furin inhibitor I were consistent with the changes observed in the MCF-7 C2 cells.

As the use of chemical inhibitors is transient, to elucidate the effect of a more consistent alteration of furin function, MDA-MB-231 stable cell lines were generated expressing the alpha1-Antitrypsin Portland gene, *α1-PDX* (Fig. 8a). The alpha1-Antitrypsin Portland gene contains an R-X-X-R conserved sequence, which similarly to Furin Inhibitor I, targets the activation site of furin (Thomas, 2002) inhibiting its protein convertase activity. These 231-PDX stable cells contained overall higher levels of total MT1-MMP protein, and while they contained significantly ($p \leq 0.01$) increased (~6 fold) levels of pro-MT1-MMP, they also contained significantly ($p \leq 0.001$) increased (~3 fold) levels of active MT1-MMP (Fig. 8b and c). 231-PDX cells also had significantly ($p \leq 0.05$) more phosphorylated ERK1/2 (Fig. 8b and c) and significantly increased mRNA levels of

MT1-MMP (~3.1 fold) ($p \leq 0.001$), and *MMP-9* (~7.2 fold) ($p \leq 0.01$), and a significantly decreased MMP-2 (~2.2 fold) ($p \leq 0.0001$) mRNA levels (Fig. 8d).

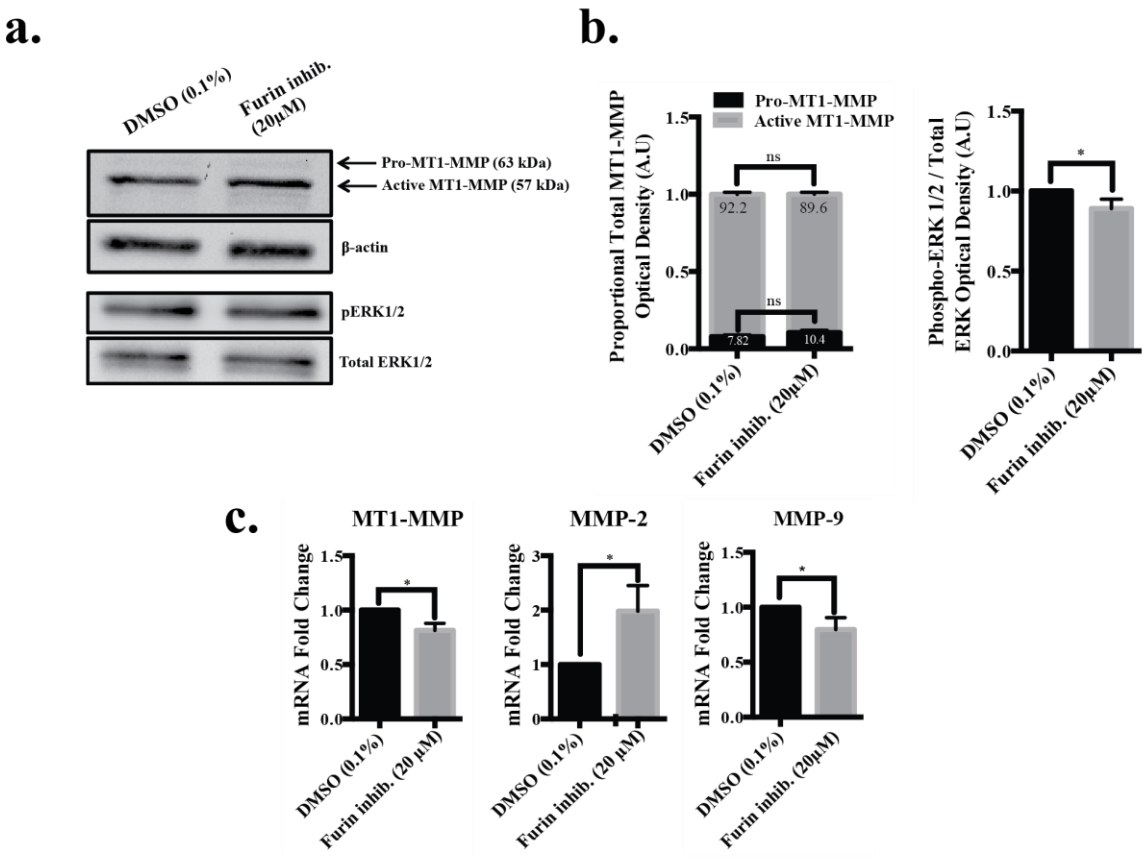
MDA-MB-231
a.
b.
c.
DMSO (0.1%)
Furin inhib. (20μM)
Pro-MT1-MMP (63 kDa)
Active MT1-MMP (57 kDa)
β-actin
pERK1/2
Total ERK1/2
Pro-MT1-MMP
Active MT1-MMP
Proportional Total MT1-MMP Optical Density (A.U)
ns
92.2
89.6
7.82
10.4
Phospho-ERK 1/2 / Total ERK Optical Density (A.U)
MT1-MMP
MMP-2
MMP-9
mRNA Fold Change
Furin inhib. (20 μM)

Figure 7. Chemical inhibition of MT1-MMP activation does not change active MT1-MMP levels, but does change *MT1-MMP*, *MMP-2* and *MMP-9* mRNA levels in MDA-MB-231 breast cancer cells.

(a) Western blot analysis showing pro- and active MT1-MMP and phospho-ERK1/2 protein levels following treatment of MDA-MB-231 breast cancer cells with MT1-MMP activation inhibitor Furin Inhibitor I (20 μM) or vehicle control (DMSO 0.1%). β-actin and total ERK1/2 respectively serve as loading controls. **(b)** Densitometry quantification of western blots for MT1-MMP protein isoforms in MDA-MB-231 cells treated with 20 μM of Furin Inhibitor I, analyzed by two-way ANOVA followed by Tukey's post hoc test; ns, $p > 0.05$ and for phospho-ERK1/2 protein exhibiting significantly decreased phospho-ERK1/2, Student's t-test; *, $p \leq 0.05$. **(c)** qPCR analysis of *MT1-MMP*, *MMP-2*, and *MMP-9* mRNA in MDA-MB-231 cells treated with either DMSO (0.1%) or Furin inhibitor I (20 μM). Fold change was quantified using the ΔΔCT method and shown as mean ± SEM. MDA-MB-231 cells treated with Furin Inhibitor I show significantly increased *MMP-2* mRNA levels and significantly decreased *MMP-9* mRNA levels, Student's t-test; *, $p \leq 0.05$. The inverse change in gelatinase mRNA levels upon treated with Furin inhibitor I is a conserved relationship between MCF-7 MT1-MMP C2 and MDA-MB-231 breast cancer cell lines.

Alpha1-Antitrypsin Portland

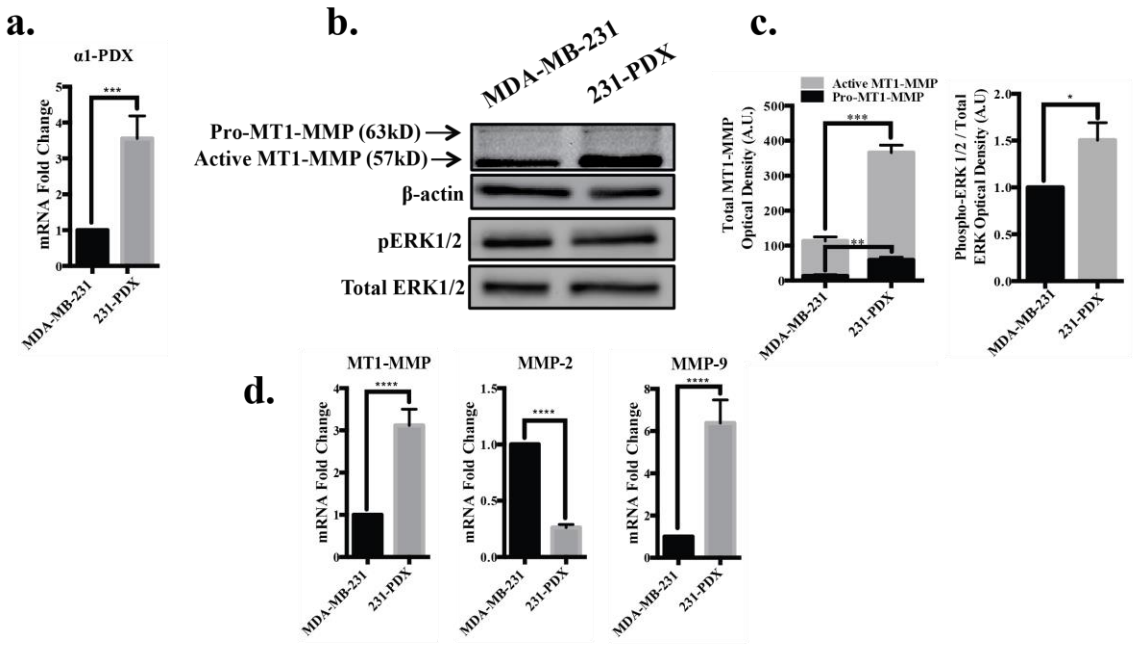

Figure 8. Overexpression of *α1-PDX* in MDA-MB-231 breast cancer cells alters MT1-MMP activation causing changes in MT1-MMP protein forms, ERK1/2 phosphorylation, and *MMP* expression.

(a) qPCR analysis of alpha1-Antitrypsin Portland *(α1-PDX)* mRNA a protein which binds and inhibits the protein convertase activity of furin confirms its overexpression, in generated MDA-MB-231 cells stably expressing alpha1-Antitrypsin Portland (231-PDX cells). Fold change was quantified using the ΔΔCT method and shown as mean ± SEM, Student's T-test; ***, $p \leq 0.001$. **(b)** Western blot analysis showed pro- and active MT1-MMP protein and ERK1/2 phosphorylation in MDA-MB-231 breast cancer cells and 231-PDX cells. β-actin and total ERK1/2 served as loading controls. **(c)** Densitometry quantification of MT1-MMP pro- and active protein forms in MDA-MB-231 and 231-PDX cells, exhibited significantly more pro- MT1-MMP in 231-PDX cells, (Two-way ANOVA followed by Sidak's post hoc test; ***, $p \leq 0.001$, **, $p \leq 0.01$) and phospho-ERK1/2 protein levels, showing significantly increased ERK1/2 phosphorylation (Student's t-test; *, $p \leq 0.01$). **(c)** qPCR analysis *MT1-MMP*, *MMP-2*, and *MMP-9* mRNA in MDA-MB-231 and 231-PDX cells. Fold change was quantified using the ΔΔCT method and shown as mean ± SEM. 231-PDX cells exhibited significantly decreased *MMP-2* mRNA levels and significantly increased *MMP-9* mRNA according to Student's T-test ; ****, $p \leq 0.0001$, ***, $p \leq 0.001$.

3.4 Low levels of pro-MT1-MMP and high levels of active MT1-MMP in stable *MT1-MMP* overexpression MDA-MB-231 cell lines resulted in increased *MMP-9* mRNA levels

Three MDA-MB-231 cell lines stably overexpressing *MT1-MMP* were generated to determine if the levels of pro- and active MT1-MMP protein influenced the transcription of other MMPs. Similar to the MCF-7 cell lines described previously, these cell lines were MDA-MB-231 MT1-MMP C1 which had high levels of both pro- and active MT1-MMP, MDA-MB-231 MT1-MMP C2 which had low pro and predominantly active levels of MT1-MMP, and MDA-MB-231 MT1-MMP C3 which had low pro and slightly more active MT1-MMP protein compared to MDA-MB-231 parental cells as shown by western blot (Fig 9a). For simplicity, these cell lines will be referred to as MDA-MB-231 C1, C2 and C3, respectively. Both MDA-MB-231 C2 and C3 cell lines exhibited high *MMP-9* mRNA levels coupled with lower *MMP-2* mRNA levels, while MDA-MB-231 C1 cells displayed the opposite of low *MMP-9* mRNA levels in conjunction with high *MMP-2* mRNA levels. MDA-MB-231 C1 cells had ~9 fold significantly ($p \leq 0.0001$) increased *MMP-2* mRNA levels and ~13-fold significantly ($p \leq 0.0001$) decreased *MMP-9* mRNA levels (Fig. 9b), which were confirmed at the protein level using gelatin zymography analysis (Fig. 9c). When the MDA-MB-231 MT1-MMP overexpression stable cell lines were treated for 12 hours in serum-free medium conditioned with pro-MMP-2, gelatin zymography analysis showed that all three cell lines have the ability of activate pro-MMP-2 (Fig. 9c), however MDA-MB-231 C1 cells activated the most pro-MMP-2. Genetically altering MDA-MB-231 cells to overexpress different levels of *MT1-MMP*, subsequently changed the levels of pro- and active MT1-MMP protein forms present in each cell line. This in turn influenced *MMP-2* and *MMP-9* mRNA levels in consistently opposite directions.

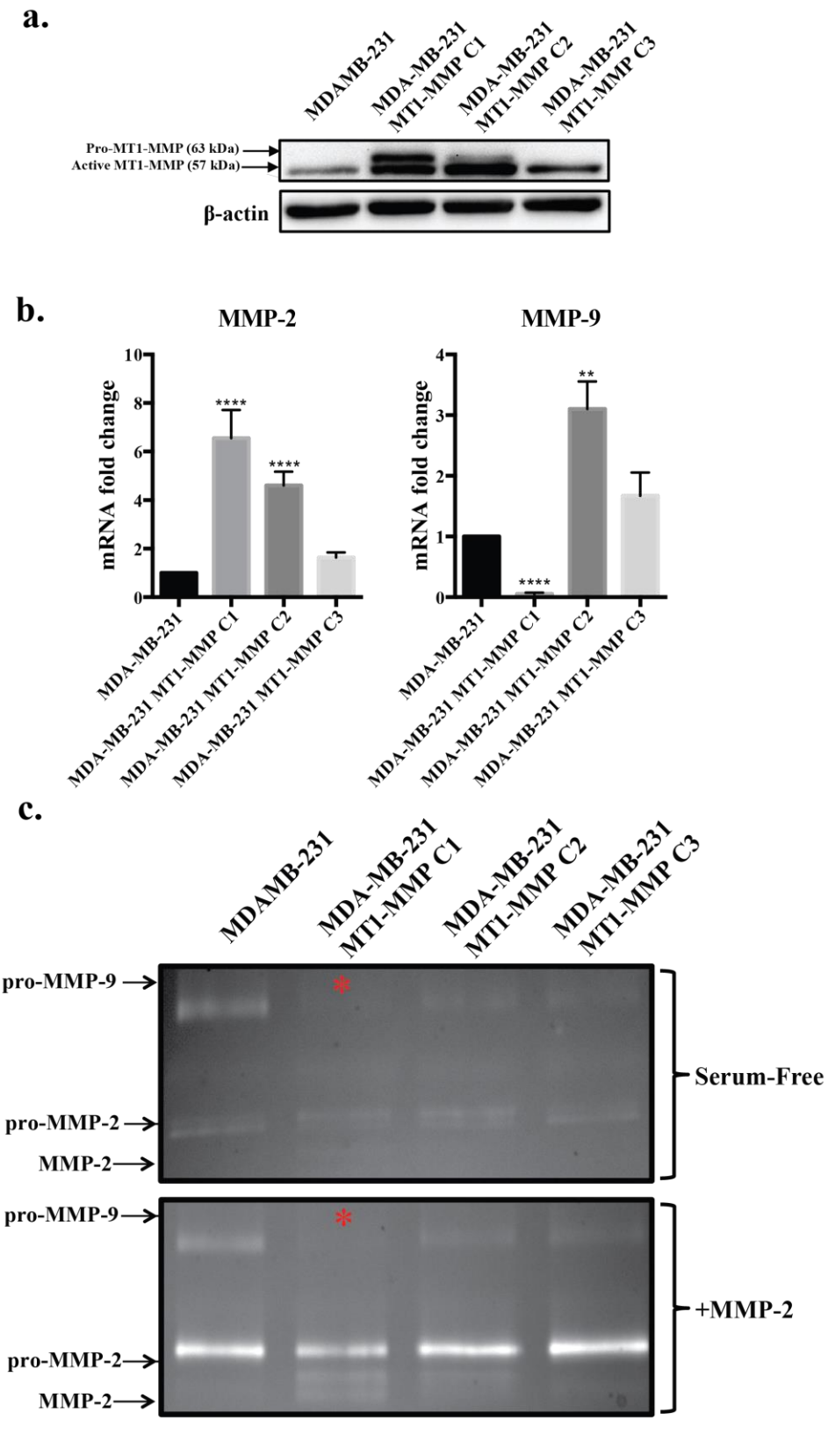
a.
MDAMB-231
MDA-MB-231 MT1-MMP C1
MDA-MB-231 MT1-MMP C2
MDA-MB-231 MT1-MMP C3
Pro-MT1-MMP (63 kDa)
Active MT1-MMP (57 kDa)
β-actin
b.
MMP-2
MMP-9
mRNA fold change
****
**
MDA-MB-231
MDA-MB-231 MT1-MMP C1
MDA-MB-231 MT1-MMP C2
MDA-MB-231 MT1-MMP C3
c.
MDAMB-231
MDA-MB-231 MT1-MMP C1
MDA-MB-231 MT1-MMP C2
MDA-MB-231 MT1-MMP C3
pro-MMP-9
pro-MMP-2
MMP-2
Serum-Free
+MMP-2

Figure 9. *MT1-MMP* over-expression in MDA-MB-231 breast cancer cells alters pro- and active MT1-MMP protein forms and subsequently results in distinct inverse relationships between *MMP-2* and *MMP-9* gene expression.

(a) Western blot analysis showing pro- and active MT1-MMP protein in MDA-MB-231 breast cancer cells and three clonally selected MDA-MB-231 cell lines that stably express different levels of *MT1-MMP*, which result in altered levels of pro- and active MT1-MMP protein forms. β-actin was used as a loading control. **(b)** qPCR analysis of *MMP-2* and *MMP-9* mRNA from isolated from MDA-MB-231 cells and three MDA-MB-231 *MT1-MMP* over expression stable cell lines. Fold change was quantified using the ΔΔCT method and shown as mean ± SEM. One-way ANOVA followed by Tukey's post-hoc test; ****, $p \leq 0.0001$, **, $p \leq 0.01$. MDA-MB-231 C1 cells displayed the inverse expression relationship between *MMP-2* and *MMP-9* a significant increase and a significant decrease in mRNA levels respectively. **(c)** Gelatin zymography analysis of MDA-MB-231 parental and MDA-MB-231 MT1-MMP over expression stable cell protein extracts incubated for 12 hours with serum-free medium (control) or serum-free medium supplemented with conditioned medium containing pro-MMP-2. Red asterisks highlights low levels of pro-MMP-9 protein present in the MDA-MB-231 MT1-MMP C1 stable cell line corroborating the low *MMP-9* mRNA levels observed by qPCR.

3.5 MEK1/2 inhibitor decreased NF-κB transcription while AP-1 transcription was unaffected in MCF-7 MT1-MMP and MDA-MB-231 breast cancer cells

To further investigate possible mechanisms for the observed changes in *MMP-2* and *MMP-9* mRNA levels and alterations to cell invasive potential, a luciferase gene reporter assay was conducted to assess the transcriptional activity of AP-1 and NF-kB transcription factors. Plasmids encoding luciferase under the regulation of either AP-1 or NF-kB promoters were transiently transfected into MCF-7, MCF-7 C2, MDA-MB-231, and 231-PDX, which were incubated for 24 hours, then subjected to DMSO (0.1%), U0126 (10 μM), or BB-94 (10 μM) treatment for 12 hours.

MCF-7 cells displayed significantly more AP-1 ($p \leq 0.001$) and less NF-κB ($p \leq 0.0001$) transcriptional activity compared to MCF-7 C2 cells, which had less AP-1 and more NF-κB (Fig. 10a and b). Neither MCF-7 nor MCF-7 C2 cells displayed any significant change in AP-1 transcriptional activity following inhibitor treatment. However, in MCF-7 C2 cells, U0126 evoked a significant ($p \leq 0.01$) ~1.5 fold decrease in NF-κB transcriptional activity, while BB-94 treatment had no statistical effect (Fig. 10b). Both untreated MDA-MB-231 and 231-PDX cells showed a similar pattern of AP-1 and NF-κB transcriptional activity to MCF-7 C2 cells, that of low AP-1 and high NF-κB transcriptional activity. Moreover, treatment of MDA-MB-231 cells with U0126 caused a significant ($p \leq 0.05$) ~1.95 fold decrease in NF-κB transcriptional activity, a decrease also observed in the 231-PDX cell line (Fig. 10c and d). These results suggest that the levels of phosphorylated ERK1/2 present within each breast cancer cell line heavily influenced NF-κB transcriptional activity and that this is conserved among breast cancer cell lines.

3.6 Only MDA-MB-231 cells treated with MERK1/2 inhibitor exhibited both reduced migratory and invasive potential

The migratory potential of MDA-MB-231 cells was examined through treatment with DMSO (0.1%), U0126 (10 μM), BB-94 (10 μM), or Furin Inhibitor I (20 μM) during

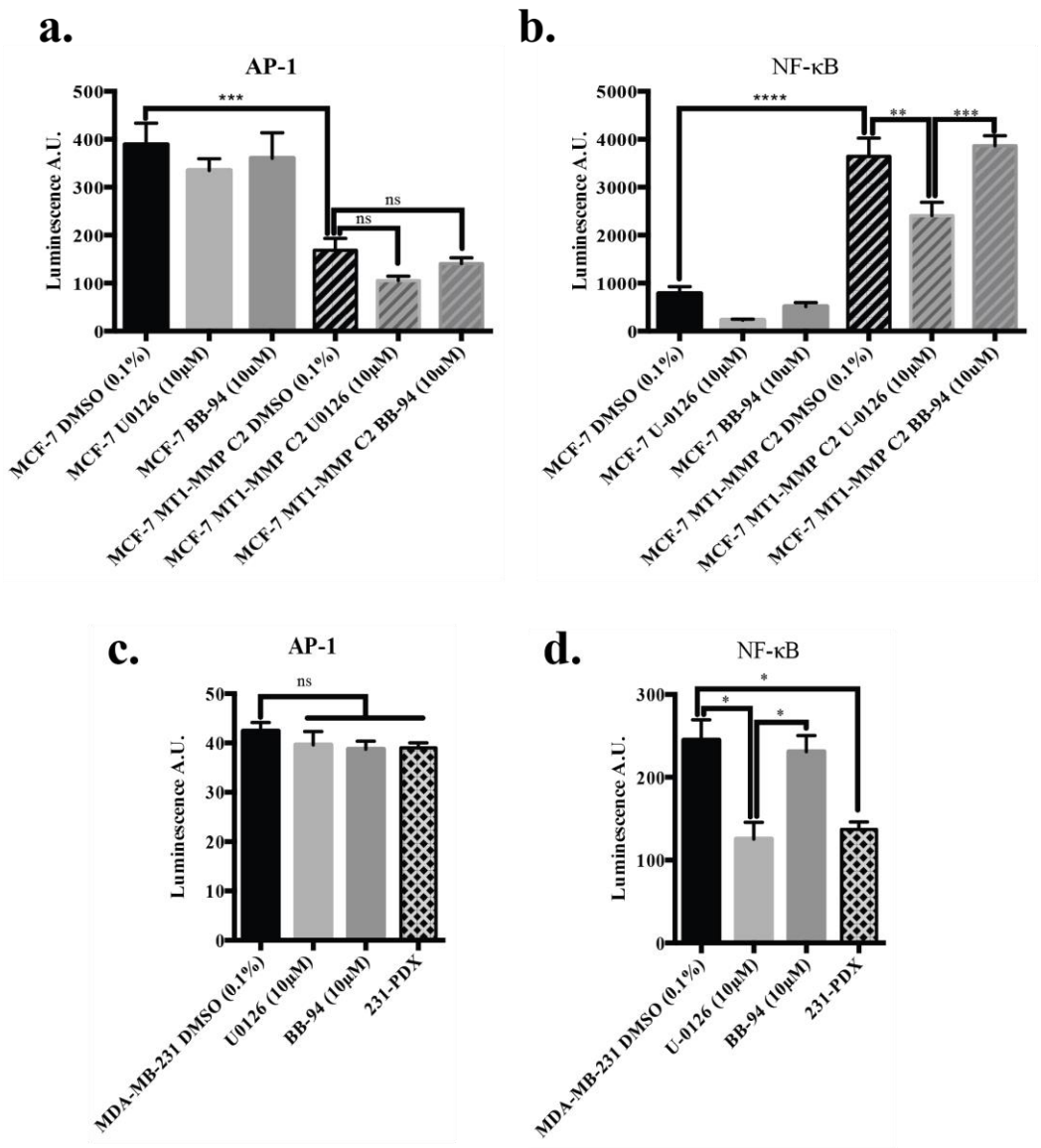
a.
AP-1
Luminescence A.U.
500
400
300
200
100
0
***
ns
ns
MCF-7 DMSO (0.1%)
MCF-7 U0126 (10μM)
MCF-7 BB-94 (10uM)
MCF-7 MT1-MMP C2 DMSO (0.1%)
MCF-7 MT1-MMP C2 U0126 (10μM)
MCF-7 MT1-MMP C2 BB-94 (10uM)
b.
NF-κB
Luminescence A.U.
5000
4000
3000
2000
1000
0
****
**
***
MCF-7 DMSO (0.1%)
MCF-7 U-0126 (10μM)
MCF-7 BB-94 (10uM)
MCF-7 MT1-MMP C2 DMSO (0.1%)
MCF-7 MT1-MMP C2 U-0126 (10μM)
MCF-7 MT1-MMP C2 BB-94 (10uM)
c.
AP-1
Luminescence A.U.
50
40
30
20
10
0
ns
MDA-MB-231 DMSO (0.1%)
U0126 (10μM)
BB-94 (10μM)
231-PDX
d.
NF-κB
Luminescence A.U.
300
200
100
0
*
*
*
MDA-MB-231 DMSO (0.1%)
U-0126 (10μM)
BB-94 (10μM)
231-PDX

Figure 10. Inhibition of ERK1/2 phosphorylation affects transcription of NF-κB more strongly than inhibition of MT1-MMP catalytic site activity in breast cancer cells.

(a, b) MCF-7 breast cancer cells and MCF-7 MT1-MMP C2 cells were seeded at a density of $3.0x10^4$/mL and transfected with mammalian 3xAP-1 or 3xNF-κB luciferase reporter plasmids. After 24 hours of transfection, cells were treated with DMSO (0.1%), U0126 (10 μM), or BB-94 (10 μM) for 12 hours. Bioluminescent signal resulted from the oxidation of D-Luciferin. Luciferase activities in triplicate samples were measured. Values represent mean ± SEM from three independent transfection experiments. MCF-7 cells contained more AP-1 and less NF-κB transcriptional activity compared to MCF-7 C2 cells, One-way ANOVA followed by Tukey's post hoc test; ****, $p \leq 0.0001$,***, $p \leq 0.001$, **, $p \leq 0.01$. **(c, d)** MDA-MB-231 breast cancer cells treated with either DMSO (0.1%), U0126 (10 μM), or BB-94 (10 μM), and MDA-MB-231 cells stably expressing alpha1-Antitrypsin Portland (*α1-PDX*), 231-PDX, were seeded at a density of $3.0x10^4$/mL and transfected with mammalian 3xAP-1 or 3xNF-kB luciferase reporter plasmids. After 24 hours of transfection, cells were treated with DMSO (0.1%), U0126 (10 μM), or BB-94 (10 μM) for 12 hours. Bioluminescent signal resulted from the oxidation of D-Luciferin. Luciferase activities in triplicate samples were measured. Values represent mean ± SEM from three independent transfection experiments. MDA-MB-231 cells contained less AP-1 and more NF-κB transcriptional activity, whereby treatment of MDA-MB-231 cells caused a significant decrease in NF-κB transcriptional activity, One-way ANOVA followed by Tukey's post hoc test; *, $p \leq 0.05$.

a scratch wound closure assay over a 24-hour period, where images were taken at 2, 6, 12, and 24 hours (Fig. 11a). Only MDA-MB-231 cells treated with U0126 were significantly ($p \leq 0.01$) less efficient at wound closure, showing ~12% decrease and were therefore less migratory, compared to DMSO (0.1%) treated cells at 12 hours post wound generation (Fig. 11b). The impact of MEK1/2 inhibition, MMP site inhibition, and alteration of MT1-MMP activation, on migratory and invasive potential in MDA-MB-231 cells were also investigated using transwell assays. MDA-MB-231 cells were treated with DMSO (0.1%), U0126 (10 μM), or BB-94 (10 μM), and 231-PDX cells, where migration was observed through uncoated transwell insert, or invasion through a Matrigel-coated transwell insert, for 24 and 48 hours respectively. MDA-MB-231 cells treated with the MEK1/2 inhibitor U0126 were significantly ($p \leq 0.01$) by 25% less efficient at migration through the transwell pores, while the pan-MMP catalytic site inhibitor BB-94 did not affect the migratory ability of these cells ($p > 0.05$). It is not surprising that inhibition of MMP catalytic site activity did not affect MDA-MB-231 migratory potential, as there was no physical barrier present to be degraded. 231-PDX cells were significantly ($p \leq 0.01$) 19% less migratory compared to MDA-MB-231 parental cells. (Fig. 11c).

When Matrigel was present and invasion required, MDA-MB-231 cells treated with U0126 were significantly ($p \leq 0.0001$) 90% less efficient at invading through the barrier, as were BB-94 treated cells that were significantly ($p \leq 0.0001$) 62% less efficient compared to DMSO (0.1%) treated MDA-MB-231 cells. 231-PDX cells were also significantly ($p \leq 0.5$) 10% less invasive compared to MDA-MB-231 parental cells. These results demonstrated the overall importance of phospho-ERK1/2 signalling in influencing cell movements, as impeding this signalling pathway affected both migratory and invasive potential of MDA-MB-231 cells, a well-classified invasive breast cancer cell type (Fig. 11c).

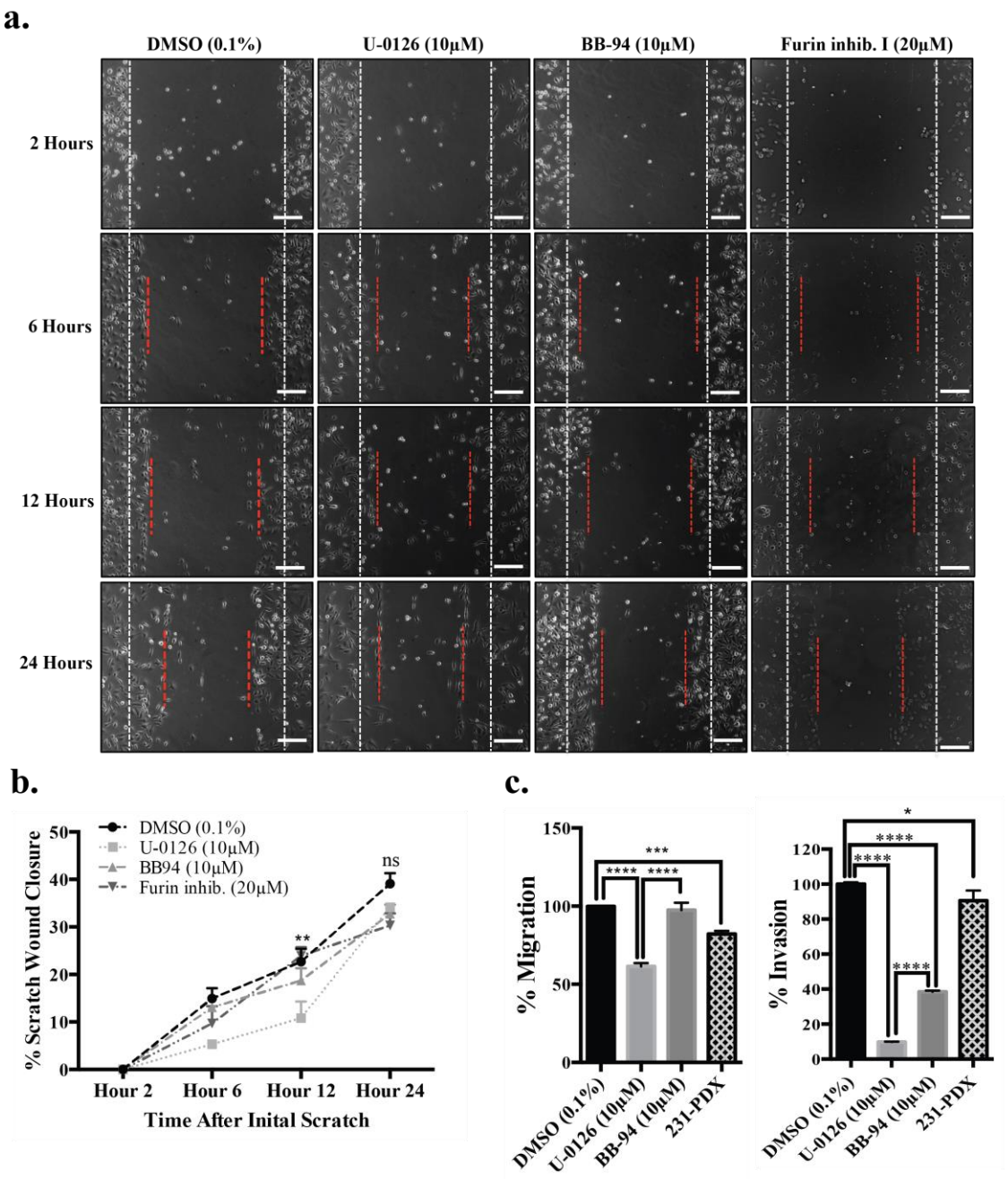
a.
DMSO (0.1%)
U-0126 (10µM)
BB-94 (10µM)
Furin inhib. I (20µM)
2 Hours
6 Hours
12 Hours
24 Hours
b.
DMSO (0.1%)
U-0126 (10µM)
BB94 (10µM)
Furin inhib. (20µM)
% Scratch Wound Closure
ns
**
Hour 2
Hour 6
Hour 12
Hour 24
Time After Inital Scratch
c.
% Migration
***
****
****
DMSO (0.1%)
U-0126 (10µM)
BB-94 (10µM)
231-PDX
% Invasion
*
****
****
****
DMSO (0.1%)
U-0126 (10µM)
BB-94 (10µM)
231-PDX

Figure 11. Inhibition of ERK1/2 phosphorylation is more influential on cell migration and invasion than inhibition of MMP enzymatic activity or MT1-MMP activation.

(a) MDA-MB-231 breast cancer cells were seeded at a density of $2.5x10^5$/mL, treated with either DMSO (0.1%), U0126 (10 μM), BB-94 (10 μM), or Furin Inhibitor I (20 μM), and allowed to form a monolayer for 24 hours. A scratch was made in the monolayer and the closure of this scratch was monitored at time points of 2, 6, 12, and 24 hours after the initial scratch. White dotted lines indicate the initial scratch size; red dotted lines indicate the scratch size at the respective times point. **(b)** Scratch closure was quantified by dividing the width of the scratch at the respective day by the initial scratch size and then expressing it as mean percentage ± SEM, as analyzed by one-way ANOVA followed by Tukey's post hoc test; **, $p \leq 0.01$, ns, $p > 0.05$. Scale bars = 100 μm. U0126 treatment was successful at decreasing migration up until 12 hours post wound generation. **(c)** Twenty thousand MDA-MB-231 cells treated with either DMSO (0.1%), U0126 (10 μM), or BB-94 (10 μM), or 231-PDX cells, were seeded onto a transwell insert (migration), or an insert coated with 20% Matrigel (invasion), and incubated for 24 (migration) and 48 hours (invasion) respectively. Number of migrated/invaded cells were normalized to DMSO (0.1%) treated MDA-MB-231 cells and expressed as a mean percentage ± SEM. One-way ANOVA followed by Tukey's post hoc test; ****, $p \leq 0.0001$, **, $p \leq 0.01$, *, $p \leq 0.05$. Both migration and invasion of MDA-MB-231 cells was significantly decreased following U0126 treatment. BB-94 treatment however, only affected invasion resulting in a significant decrease in invasive potential of MDA-MB-231 breast cancer cells. 231-PDX cells also less migratory and less invasive compared to MDA-MB-231 cells.

3.7 MDA-MB-231 cells with decreased ERK1/2 phosphorylation, inhibited MMP catalytic activity, or altered MT1-MMP activation all exhibited morphological changes in 3D cell culture

In order to determine the effects of the inhibitors used on cell morphology, MDA-MB-231 and 231-PDX cells were embedded in 50% Matrigel and treated with DMSO (0.1%), U0126 (10 μM), or BB-94 (10 μM). By Day 5, morphological differences among the treatments were apparent (Fig 12a). MDA-MB-231 cells treated with U0126 (10 μM) and BB-94 (10 μM) were significantly ($p \leq 0.0001$) less protrusive (~ 2- 3 protrusions per colony) than MDA-MB-231 parental cells (~9 per colony) or 231-PDX cells (~6 per colony). Alternatively, MDA-MB-231 cells treated with U0126 and BB-94, and 231-PDX cells all had significantly ($p \leq 0.01$) more disseminations per colony compared to MDA-MB-231 cells treated with DMSO (Fig. 12b). These results indicated that treatment altering ERK1/2 phosphorylation, MT1-MMP activity, or MT1-MMP activation caused changes within these cells to divide and move rather than remain stationary and invade. Control MDA-MB-231 cells treated with DMSO displayed a meshwork phenotype of cells resulting from a combination of round clumped and elongated cells. Inhibition of ERK1/2 phosphorylation achieved by U0126 treatment abolished the ability of MDA-MB-231 cells to from elongated processes and resulted in small round single cells with very concentrated F-actin. Inhibition of MMP catalytic activity through treatment with BB-94 resulted in large distinct aggregations of round cells, however some BB-94 treated MDA-MB-231 cells were still able to elongate in a manner similar to the morphology of control cells. Lastly, 231-PDX cells exhibited large round clumps of cells that lacked long elongated cell morphology (Fig 12c). The morphological changes observed in each treatment and cell line were supported by quantitative analysis of protrusions and disseminations per cell colony.

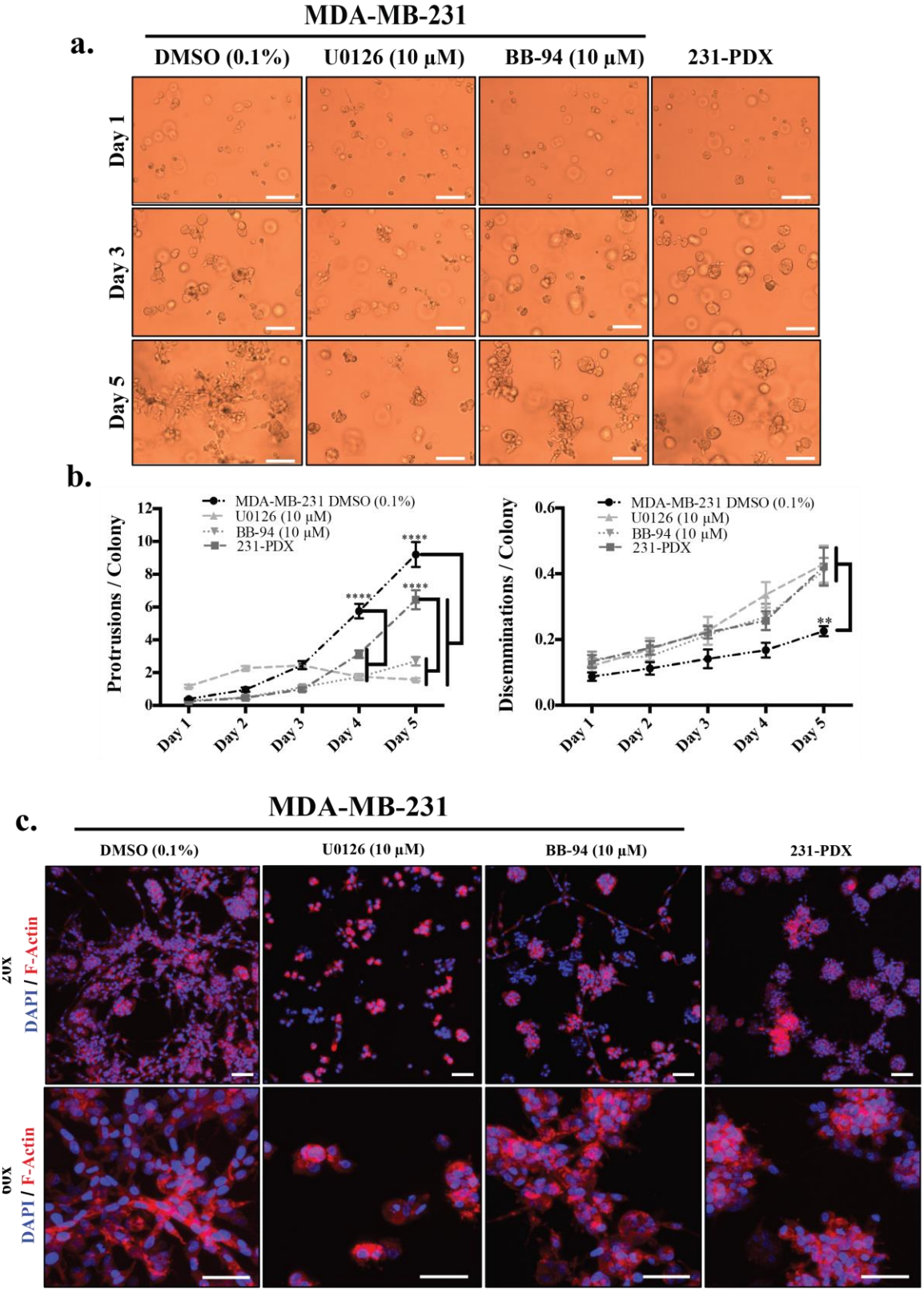
a.
MDA-MB-231
DMSO (0.1%)
U0126 (10 µM)
BB-94 (10 µM)
231-PDX
Day 1
Day 3
Day 5
b.
MDA-MB-231 DMSO (0.1%)
U0126 (10 µM)
BB-94 (10 µM)
231-PDX
Protrusions / Colony
Disemminations / Colony
Day 1
Day 2
Day 3
Day 4
Day 5
****
**
c.
MDA-MB-231
DMSO (0.1%)
U0126 (10 µM)
BB-94 (10 µM)
231-PDX
DAPI / F-Actin
40X
60X

Figure 12. Interfering with MT1-MMP activation, MT1-MMP catalytic activity, and MAPK signalling affects 3D morphology of MDA-MB-231 breast cancer cells.

(a) MDA-MB-231 breast cancer cells treated with DMSO (0.1%), U0126 (10 μM), or BB-94 (10 μM), and MDA-MB-231 cells stably expressing *alpha1-Antitrypsin Portland*, 231-PDX, were embedded in 50% Matrigel and incubated in medium containing 10% FBS with the respective inhibitor treatment. Images were taken every day for 5 days using DIC microscopy at 10x (50 μm z-stacks, 2 μm slices). Shown is a representative focal panel field of view of each cell line with respective treatment at day 1, 3, and 5. Scale bars = 100 μm. **(b)** Five z-stacks per cell line/treatment were acquired and disseminations and protrusions were blindly counted and expressed as a mean normalized to the colony number per z-stack ± SEM. MDA-MB-231 breast cancer cells treated with DMSO (0.1%) exhibited the highest number of protrusions per colony but lowest number of disseminations per colony, while MDA-MB-231 cells treated with U0126 (10 μM) exhibited the lowest number of protrusions per colony, but the highest number of disseminations per colony, as analyzed two-way ANOVA followed by Tukey's post hoc test; ****, $p \leq 0.0001$, **, $p \leq 0.01$. **(c)** MDA-MB-231 cells treated with DMSO (0.1%), U0126 (10 μM), or BB-94 (10 μM), and MDA-MB-231 cells stably expressing *alpha1-Antitrypsin Portland*, 231-PDX, were embedded in 50% Matrigel, incubated in medium containing 10% FBS with the respective inhibitor treatment for 5 days and processed for immunocytochemistry to examine nuclei and F-actin distribution. Samples were imaged using confocal microscopy at 20x and 60x and are displayed as a 3D volume overlay showing DAPI (blue) and Alexa Fluor 633 phalloidin (red) channels, where all treatments are morphologically different from one another. Scale bars = 100 μm. All experiments were repeated in triplicate with comparable results.

3.8 Changes in MT1-MMP activation, ERK1/2 phosphorylation, and *MMP-2* and *MMP*-9 mRNA levels *in vitro* contributed to *in vivo* tumour growth

To assess the role of level of MT1-MMP activation, MMP activity, and ERK1/2 phosphorylation in tumourigenicity, artificial Matrigel tumours composed of ZsMDA-MB-231 and Zs231-PDX cells were injected into a wound in the CAM vasculature of a nine-day-old chicken embryo and incubated for eight days. ZsMDA-MB-231 Matrigel tumours were subjected to DMSO (0.1%), U0126 (10 μM), or BB-94 (10 μM) every 48 hours. Following incubation, vascularization of the tumour site was observed. ZsMDA-MB-231 Matrigel tumours treated with DMSO (0.1%) had the highest incidences of vascularization (19/21) and complete wound closure (13/16 closed) at the injection site. Conversely, ZsMDA-MB-231 tumours treated with U-0126 had the least incidences of vascularization (3/14) and incomplete wound closure (1/12 closed), while BB-94 treated ZsMDA-MB-231 tumours displayed reduced incidences of vascularization (5/12) and decreased wound closure (2/10 closed). Zs231-PDX tumours exhibited intermediate vascularization (9/13) and variable wound closure (3/8 closed) (Figure. 13a-c).

Excision and cross sectioning of ZsMDA-MB-231 control Matrigel tumours revealed vascularization not only on the surface of the tumor, but also throughout (Figure. 13d). Internal vascularization of ZsMDA-MB-231 control tumours indicates the possibility that other Matrigel tumors with surface vascularization contain additional vasculature running throughout the inside of the tumors (Data to be published in Cepeda et al., 2016).

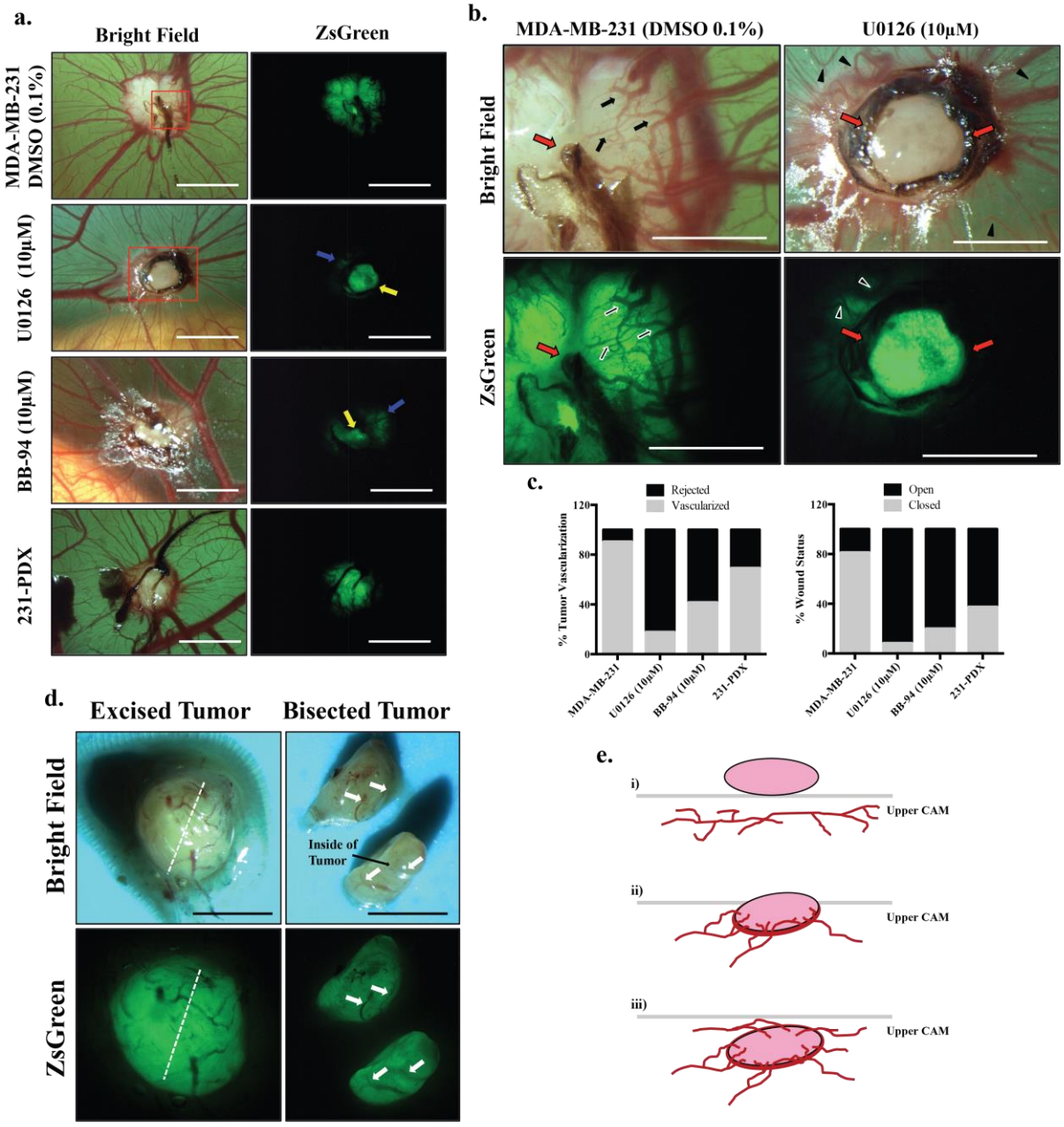
a.
Bright Field
ZsGreen
MDA-MB-231 DMSO (0.1%)
U0126 (10μM)
BB-94 (10μM)
231-PDX
b.
MDA-MB-231 (DMSO 0.1%)
U0126 (10μM)
Bright Field
ZsGreen
c.
Rejected
Vascularized
% Tumor Vascularization
120
80
40
0
MDA-MB-231
U0126 (10μM)
BB-94 (10μM)
231-PDX
Open
Closed
% Wound Status
d.
Excised Tumor
Bisected Tumor
Bright Field
ZsGreen
Inside of Tumor
e.
i)
Upper CAM
ii)
Upper CAM
iii)
Upper CAM

Figure 13. MDA-MB-231 breast cancer cells treated with U0126 showed fewer incidences of vascularization and wound closure within avian CAM.

ZsGreen-tagged MDA-MB-231 (ZsMDA-MB-231 and ZsGreen-tagged 231-PDX (Zs231-PDX) cell lines were combined with Matrigel and injected into a wound made in the vasculature of the CAM of a nine-day-old chicken embryo. Embryos were incubated for eight days, the introduced cells were treated with either DMSO (0.1%), U0126 (10 μM), or BB-94 (10 μM), every 48 hours directly onto the tumour injection site. Nine days post wound generation; bright field and fluorescence stereomicroscopy were used to examine the tumour site, where vascularization of the tumour was assessed by identifying novel capillaries around the tumours growing within the CAM. Wound closure was assessed based on growth and closure of scar tissue via the resultant lack of tumour present above the CAM and regression of originally wounded vessels. **(a)** Representative bright field and fluorescence microscopy images of complete and partial submersion of tumours beneath the CAM at day nine post wound generation. Complete submersion of tumours beneath CAM with ZsMDA-MB-231 (top panel) and Zs231-PDX cells (bottom panel). Partial submersion of tumour treated with U0126 (10 μM) and BB-94 (10 μM). Blue arrows indicate submerged tumours, yellow arrows represent tumours that remained above the CAM. Scale bars = 2 mm. **(b)** Enlarged bright field and fluorescence stereomicroscopy images of areas denoted by red boxed outline in (a) of ZsMDA-MB-231 cells treated with DMSO (0.1%) and U0126 (10 μM) to show vascularization and wound closure. Left panels (top and bottom), show high levels of vascularization surrounding DMSO (0.1%) treated tumours (black arrows), and the most incidence of complete wound closure (black outline, red arrow). Vascularization in ZsGreen cells is visualized as darkened areas of contrast against green fluorescence (white outline, black arrow), right panels (top and bottom). Inhibitor (U0126, 10μM) treated tumours displayed a vascularization that looped away from the tumour (black arrow heads) accompanied by incomplete wound closure delineated by scabbed borders (black outline, red arrows).

Scale bar = 1mm. **(c)** Multiple chicken embryos (N ≥ 12) were wounded, injected, and had tumour sites assessed for vascularization and completeness of wound closure. ZsMDA-MB-231 cells treated with DMSO (0.1%) had the highest number of incidences of vascularization and complete wound closure. ZsMDA-MB-231 Matrigel tumours treated with U0126 (10 μM) showed the least incidences of tumour vascularization and incomplete wound closure, while BB-94 (10 μM) treated tumours exhibited intermediate incidences of tumour vascularization and incomplete wound closure. Zs231-PDX Matrigel tumours displayed intermediate incidences of tumour vascularization and variable wound closure. A chi-squared test of independence was performed to examine the relationship between cell line / treatment and vascularization. The relationship between these variables was significant X^2 (4, *N*= 59) = 19.76; ***,p <0.001. A chi-squared test of independence was performed to examine the relationship between cell line / treatment and wound closure. The relationship between these variables was significant X^2 (4, *N*= 46) = 17.83; ***,p <0.001. **(d)** A tumour from MDA-MB 231 cells expressing ZsGreen was excised from a chicken embryo 8 days post-implantation and imaged using brightfield and fluorescence microscopy. Vessels within the tumour (white arrows) can be seen by the presence of blood (dark colour) and absence of fluorescent signal (ZsGreen), which indicate that these vessels originate from the chicken embryo. Excision of the tumour revealed vascularization present on the surface of the tumour, and cutting the tumour in cross section showed vascularization throughout the center (white arrows). The image of the upper half of the tumour is maintained in original position, while the lower half of the sectioned tumour is rotated 90° to reveal internal vessels. Scale bars = 2 mm**. (e)** Schematic illustration representing the relative positions of the tumours within the cam CAM, and vasculature. Shown are cross-sections perpendicular to the images shown in **(a).** i) Un-invaded, un-vascularized tumours remain sitting on top of the CAM, representative of incidences of tumour rejection. ii) Vascularized tumours that retain an open wound were seen in ZsMDA-MB-231 cells treated with inhibitors and Zs231-PDX cells. iii) Vascularized tumours with complete CAM wound closure and vascularization, occurred with ZsMDA-MB-231 DMSO (0.1%) and Zs231-PDX tumours.

Chapter 4

4 Discussion

This work aimed to examine the effects of MT1-MMP proteolytic and non-proteolytic functions on the invasive ability of cells, by manipulating MT1-MMP activation (chemically and genetically), catalytic activity (chemically), and ERK1/2 phosphorylation (chemically). This study used MCF-7 breast cancer cells, which are deficient in MT1-MMP and phospho-ERK1/2, as well as other cell lines, which have increased *MT1-MMP* levels (MCF-7 MT1-MMP C2), high levels of active MT1-MMP and phospho-ERK1/2 (MDA-MB-231 cells), and cells that have altered levels of active MT1-MMP and phospho-ERK 1/2 (231 PDX cells). These cells all were subjected to inhibitors targeting ERK1/2 phosphorylation (U-0126), MMP catalytic activity (BB-94), and furin convertase activity (Furin inhibitor I). I hypothesized that inhibiting ERK1/2 phosphorylation, MMP catalytic activity, or furin convertase activity, would alter the expression of key ECM remodeling proteins, the gelatinases (MMP-2 and MMP-9) and subsequently alter breast cancer cell invasion. My results indicate that inhibiting MT1-MMP activation or activity, or ERK1/2 phosphorylation, results in an inverse expressional relationship between MMP-2 and MMP-9 and reduced cell invasion. Moreover, a possible pathway influencing breast cancer cell invasion can be proposed: Active MT1-MMP is required to initiate the MAPK signalling pathway, resulting in ERK1/2 phosphorylation, and subsequent transcriptional activity of NF-κB to influence *MMP-9* transcription. This model will be discussed below by examining the overall effects (changes in transcription, protein levels, and cell motility) of inhibiting ERK1/2 phosphorylation, MMP catalytic activity, or MT1-MMP activation in individual sections.

4.1 Inhibiting ERK1/2 phosphorylation inversely effects gelatinase expression, reduces total MT1-MMP active protein levels, and decreases migratory and invasive potential of breast cancer cells

Proper phospho-ERK1/2 signalling is essential in many cellular processes including migration, proliferation, and apoptosis (Fujioka et al., 2006). As discussed below,

treatment of MCF-7, MCF-7 C2, and MDA-MB-231 cells with MEK1/2 kinase inhibitor (U-0126) decreases phospho-ERK1/2 and alters *MT1-MMP*, *MMP-2*, and *MMP-9* mRNA levels (Fig. 2 and 3). Total MT1-MMP protein is decreased (Fig. 4a and b), as well as migration and invasion in 2D and 3D space are reduced (Fig. 11, 12, 13).

4.1.1 Decreasing ERK1/2 phosphorylation increased *MMP-2* mRNA levels, but decreased *MMP-9* mRNA levels in MCF-7 MT1-MMP C2 and MDA-MB-231 breast cancer cells

The binding of TIMP-2 to the hemopexin domain of MT1-MMP initiates the MAPK pathway by an uncharacterized mechanism to result in the phosphorylation and successive activation of ERK1/2 — this activation being a non-proteolytic function of MT1-MMP. Sequentially, phospho-ERK1/2 is translocated to the nucleus of the cell to influence transcription factors, including AP-1, which is known to regulate the transcription of a broad number of MMPs, and NF-κB, which regulates only specific MMPs, namely MT1-MMP and MMP-9 (Overall, and López-Otín 2002).

Inhibiting ERK1/2 phosphorylation in both MCF-7 C2 and MDA-MB-231 cells resulted in increased *MMP-2* and decreased *MMP-9* mRNA levels (Fig. 2b and 3c), indicating that the mechanism between phospho-ERK1/2 and gelatinase expression is conserved between breast cancer cell lines. Additionally, as decreasing phospho-ERK1/2 decreased *MMP-9* mRNA levels, but increased *MMP-2* mRNA levels, it can be surmised that phospho-ERK1/2 acts directly upon transcription factors to positively influence *MMP-9* expression, and negatively affect *MMP-2* expression. Both MMP-2 and MMP-9 are considered potent ECM remodelers as they share the target substrate collagen IV, an abundant component of basement membranes. Active degradation of basement membrane substrate is needed in many critical developmental events such as epithelial to mesenchymal transitions, and is also needed for cancer cell invasion and for metastasis to occur (Hotary et al., 2006).

The MMP transcriptional regulatory mechanisms are complex. Most MMPs are not expressed in adult cells under quiescent conditions, but their transcription can be induced

in tumour or stromal cells by various signals, such as cytokines, growth factors and oncogene products. Additionally, the signal-transduction pathways that mediate the activity of MMP transcriptional activators are also diverse. NF-κB is known to interact with phospho-ERK1/2 and is well known for its importance in regulation of *MMP-9* expression (Overall, and López-Otín 2002). Here, inhibition of phospho-ERK1/2 in MCF-7 C2 and MDA-MB-231 cells resulted in decreased NF-κB transcriptional activity, indicating further support for a mechanism of phospho-ERK1/2 regulation of MMP-9 (Fig. 10b and d). A similar study performed by Lee et al., (2013) in bladder cancer cells, also suggests a relationship among phospho-ERK1/2, NF-κB, and *MMP-9* expression. Lee et al., (2013) demonstrated in bladder cancer cells that upon chemical inhibition of phospho-ERK1/2, NF-κB transcriptional activity and *MMP-9* expression was decreased. To confirm regulation of MMP-9, NF-κB transcriptional activity was also chemically inhibited and resulted in decreased *MMP-9* expression in bladder cancer cells. To further support the relationship among phospho-ERK1/2, NF-κB, and *MMP-9* mRNA levels as presented here (Fig. 2, 3 and 10), assays should be performed in MCF-7, MCF-7 C2, and MDA-MB-231 cells with an NF-κB inhibitor to observe changes that occur in ERK1/2 phosphorylation, as well as *MMP-2* and *MMP-9* mRNA levels. When these cells are treated with the NF-κB inhibitor, it is proposed that ERK1/2 phosphorylation will remain basal, *MMP-9* mRNA levels will be decreased, and *MMP-2* mRNA levels will be unaffected as the promoter region of MMP-2 does not contain a NF-κB binding domain (Overall, and López-Otín 2002). However, when cells are treated with inhibitors for both ERK1/2 phosphorylation and NF-κB, a decrease in phospho-ERK1/2 and *MMP-9* expression are predicted, whereas *MMP-2* mRNA levels remains increased. The regulation of *MMP-2* expression through phospho-ERK1/2 is more complex than that just described for *MMP-9*. AP-2 has been shown in various other cell types to be critically responsible for *MMP-2* expression (Fig. 1) (Overall and López-Otín, 2002). The MAPK/ERK pathway is known to interact with the PI3K/AKT pathway, as Ras also activates PI3K resulting in the activation of AKT, with AP-2 a downstream target of AKT. To investigate this proposed interaction, AKT phosphorylation and AP-2 transcriptional activity should be targeted to observe changes in *MMP-2* expression (Moulick et al., 2013).

Inhibition of ERK1/2 phosphorylation additionally decreased *MT1-MMP* mRNA levels in MDA-MB-231 cells (Fig. 3c) and decreased total MT1-MMP protein in MCF-7 C2 cells (Fig. 4a), indicating that the mechanism regulating phospho-ERK1/2 and *MT1-MMP* is conserved between breast cancer cell lines. Transcriptional regulation of MT1-MMP may occur in similar fashion to that of MMP-9 —through phospho-ERK1/2's influence on NF-κB transcriptional activity, as the MT1-MMP promoter also contains an NF-κB binding domain (Overall and López-Otín 2002). Interestingly, only MCF-7 C2 cells exhibited decreased total MT1-MMP, specifically less active MT1-MMP protein, despite both cell lines having decreased *MT1-MMP* RNA levels. MDA-MB-231 MT1-MMP protein levels remained unaffected, indicating differential post transcriptional or post translational regulation of MT1-MMP transcript in this more invasive breast cancer cell line.

Collectively, decreased *MMP-9* and *MT1-MMP* mRNA levels following inhibition of ERK1/2 phosphorylation observed in this study is consistent with other studies. This relationship is well documented and occurs in many different cell lines such as rhabdomyosarcoma, fibrosarcoma, bladder carcinoma, colon adenocarcinoma, and prostate carcinoma (Tanimura et al., 2003). However, my observation of increased *MMP-2* mRNA levels following decreased phospho-ERK1/2, is novel as previously *MMP-2* and -*9* mRNA levels are always altered in the same direction, while in this study, levels are always inverse.

4.1.2 Decreased migratory and invasive potential is observed with decreased phospho-ERK1/2 *in vitro*, *ex vivo*, and *in vivo* in MDA-MB-231 breast cancer cells

Phospho-ERK1/2 influences the migratory and invasive potential of cells through activation of a multitude of genes whose products control cytoskeletal arrangements, presence or absence of cell surface receptors, ECM degradation, and the release of cytokines and growth factors. Consequently, inhibition of ERK1/2 phosphorylation in invasive MDA-MB-231 cells resulted in decreased migration (Fig. 11) and invasion in diverse assays investigating cell motility (Fig. 11c, 12, and 13). This study further

supports the necessity of proper phospho-ERK1/2 signalling in order to achieve cell migration and invasion (Meloche, and Pouysségur, 2007).

Invasive capabilities were examined using a transwell invasion assay and 3D cell culture, both of which showed decreased invasive potential following treatment with the MEK1/2 kinase inhibitor, U0126. Acquisition of an invasive phenotype requires modulation of cell-ECM interactions through cytoskeletal organization, proteolysis of the extracellular matrix, and migration (Friedl and Wolf, 2003).

Upon inhibition of ERK1/2 phosphorylation in 3D cell culture, the morphology of MDA-MB-231 breast cancer cells changes to become round, with a minimally protrusive phenotype, as fluorescence microscopy revealed a condensed and aggregated F-actin cytoskeletal network, contrasting that which forms in untreated cells (Fig. 12c). Previous studies have found that the filamentous F-actin regulatory protein, cortactin, plays an important role in tumour cell movement and invasion through organization of plasma membrane protrusions. Cortactin is positively regulated through phosphorylation by phospho-ERK1/2, to promote APR2/3-mediated actin networks (Kelley et al., 2011). The reduction of protrusions and associated condensed actin phenotype observed in 3D cell culture following treatment with U0126 could be attributed to deficiency in cytoskeletal organization, such as cortactin stabilization.

For reduced invasion, in addition to deficiencies in cytoskeletal arrangement, degradation of ECM substrates is also thought to be compromised. Breast cancer cells in which ERK1/2 phosphorylation was inhibited also exhibited changes in mRNA and altered protein levels of MT1-MMP, MMP-2, and MMP-9. Specifically, cells with decreased phospho-ERK1/2 consequently have decreased active MT1-MMP (Fig. 4b and c) and pro-MMP-9 protein, but elevated levels of pro-MMP-2 protein (Fig. 3a). With a resultant lack of active MT1-MMP present on the cell surface, MT1-MMP-medicated pro-MMP-2 activation would also be reduced consequently reducing the activation of pro-MMP-9. Therefore cells with decreased phospho-ERK1/2 also have minimal ability to degrade ECM constituents as evidenced by reduced invasive potential in the Matrigel coated transwell invasion assay (Fig. 11c).

MT1-MMP is essential for forming filipodia and lamellipodia in migration and invadapodia during invasion. The formation of invadapodia requires actin polymerization to form a membrane protrusion, followed by MT1-MMP shuttled to the distal end (Artym, 2006). While the basal machinery of invadapodia still functions in the absence of MT1-MMP, the resulting structures are non-functional and do not degrade ECM substrates (Buccione et al., 2009; Itoh et al., 2006). Thereby, the minimal protrusions that did form following U0126 treatment, in MDA-MB-231 cells, most likely lacked MT1-MMP protein at the distal end, and also had reduced secretory vesicle transportation of gelatinase proteins to the cell surface that resulted from altered MT1-MMP expression and expected activation deficiency.

To better understand the mechanisms involved in invasion, migration was investigated using scratch wound closure and transwell mediated assays, both of which demonstrated decreased migration when ERK1/2 phosphorylation was inhibited (Fig. 11). U0126 treated MDA-MB-231 cells showed decreased scratch wound closure up until 12 hours post wound generation, after which distance migrated is equivalent to that of untreated cells at 24 hours. These changes could be a result of depleted inhibitor over time, or by increased cell number over time. During cell proliferation, rapid and persistent nuclear transfer of phosphorylated ERK1/2 during the entire G0 to G1 period of the cell cycle is crucial to ensure rapid cell growth and cell abundance (Mebratu and Tesfaigzi, 2009). As such, in the presence of U0126, proliferation of these cells is minimal, as they cannot transition out of G0, and thus if they do not enter the cell cycle, they can be more prone to cell migration. Therefore, comparable migratory ability between untreated and U0126 treated MDA-MB-231 cells at 24 hours can be attributed to the decreased effect of inhibitor over time as apposed to cell proliferation. Consistent with the scratch assay, cells treated with U0126 and induced to migrate through a porous transwell barrier, also exhibited decreased migration. The transwell assay was performed over a 24-hour span, where only cells capable of cytoskeletal rearrangement pass through the barrier. Additional to cortactin stabilization, previous studies also indicate that phospho-ERK1/2 activates cell motility machinery by enhancing myosin light-chain kinase (MLCK) activity leading to increased MLC phosphorylation and enhanced cell migration (Reddy

et al., 2003). Decreasing phospho-ERK1/2 would lead to the reduction of MLCK activity to result in decreased migration.

Through targeting the MT1-MMP non-proteolytic function, ERK1/2 phosphorylation, both cytoskeletal organization and ECM proteolysis, which are necessary for invasion, have been considerably impaired. These observations are also of importance when assessing tumour vascularization and wound closure data observed in the CAM of chicken embryos. A wound was generated into the CAM vasculature whereby an artificial tumour consisting of Matrigel and MDA-MB-231 cells was injected. Treatment with U0126 resulted in the least number of incidences of tumor vascularization and incomplete wound closure compared to control MDA-MB-231 cells. As previously discussed, inhibition of phospho-ERK1/2 impairs migratory and invasive potential of cells to then prevent movement of cells. Additionally, growth factors critical to angiogenesis such as VEGF family members, can be sequestered within the ECM, and are cleaved by MMP-9 to stimulate proliferation and migration of endothelial cells (Bergers et al., 2000; Yu and Stamenkovic, 2000). Here MDA-MB-231 cells treated with U0126 expressed very little *MMP-9* mRNA resulting in negligible levels of active MMP-9; reduction of this gelatinase is one possible explanation for lack of tumour vascularization in the chick CAM model. Phospho-ERK1/2 signalling itself is also involved in numerous angiogenic processes such as endothelial cell division, influencing selective degradation of basement membrane structures, endothelial cell migration and the formation of tubular structures (Hoeben et al., 2004). Likewise, this can also affect vascularization of the tumour, as well as impairing growth of surrounding vessels. Moreover, the chicken tumor vascularization assay is a holistic *in vivo* assay, making exploring inhibitor effects solely on tumour cell invasion and vascularization difficult, as phospho-ERK1/2 inhibition is expected to be influencing cells not only within, but surrounding the tumour. Decreased vascularization and wound closure of U0126 treated MDA-MB-231 tumours in the chick CAM is most likely a combination resulting from inhibitory effects on both the cells within the tumour and nearby endothelial cells within the CAM.

Exploring the effects of ERK1/2 phosphorylation through inhibition has revealed its

importance in diverse cellular processes involving MT1-MMP and gelatinase MMPs levels, cell migration and invasion, to ultimately modulate tumour vascularization and wound closure in an *in vivo* model. The usefulness of broad spectrum targeting of phospho-ERK1/2 through MEK1/2 kinase inhibition in breast cancer cells is mitigated by the many roles phospho-ERK1/2 plays in diverse cellular processes, including cancer progression. In order to further explore the cellular consequences of ERK1/2 inhibition in an MT1-MMP specific context, the hemopexin domain of MT1-MMP should be targeted to prevent the binding of TIMP-2 to decrease activation of the MAPK pathway and precisely investigate the downstream role of this ligand-receptor interaction.

4.2 Inhibiting MMP catalytic activity increases total MT1-MMP active protein levels, inversely effects gelatinase expression, and decreases invasive potential of breast cancer cells

MMPs have been well documented to degrade all constituents of the ECM, influencing availability of growth factors, growth factor receptors, chemokines, and cell adhesion molecules, in order to elicit cell behaviours such as migration and invasion.

As will be discussed below, treatment of MCF-7, MCF-7 C2, and MDA-MB-231 cells with a pan-MMP catalytic activity inhibitor batimastat (BB-94) subsequently alters *MT1-MMP*, *MMP-2* and *MMP-9* mRNA levels, increases total MT1-MMP protein (predominately active MT1-MMP) (Fig. 4 and 5), as well as decrease invasive potential in 2D and 3D space (Fig. 11, 12, 13).

4.2.1 Inhibition of MMP activity by BB-94 addition decreased *MMP-2* mRNA levels, but increased *MMP-9* mRNA levels in MCF-7 MT1-MMP C2 and MDA-MB-231 breast cancer cells

Pan-inhibition of MMP catalytic activity in both MCF-7 C2 and MDA-MB-231 cells resulted in increased *MT1-MMP* expression, perhaps as a compensatory mechanism as active MT1-MMP protein levels were increased. Furthermore, BB-94 treatment of MCF-7 C2 resulted in increased levels of ERK1/2 phosphorylation as shown by western blot

(Fig. 4a and b). Additionally, BB94 treated MCF-7 C2 and MDA-MB-231 cells exhibited decreased *MMP-2*, but increased *MMP-9* mRNA levels (Fig. 4d and 5c), indicating that the mechanism of gelatinase expression, as it is proposed to be regulated by the activity state of MT1-MMP, is conserved between breast cancer cell lines. When the catalytic domain of MT1-MMP is inhibited, all proteolytic functions are decreased, including pro-MMP-2 activation mediated by TIMP-2. Nonetheless, the hemopexin domain of MT1-MMP is still available for TIMP-2 binding. In this situation increased phospho-ERK1/2 levels seen following MMP catalytic site inhibition can be attributed to availability of the MT1-MMP hemopexin domain to still bind to TIMP-2 and initiate MAPK activation. Indeed, TIMP-2 mutants incapable of binding the MT1-MMP catalytic site are still able to induce the MAPK pathway (D'Alessio et al., 2008; Sounni et al., 2010). Thus, despite MMP catalytic inhibition, MAPK activation can still occur, whereby activity of phospho-ERK1/2 could be influencing the increased expression of *MT1-MMP* in these two cell lines, perhaps as a compensatory mechanism for catalytic inhibition.

Increased *MT1-MMP* mRNA is not a result of transcriptional activity of transcription factors AP-1 or NF-κB (Fig. 10), as their activity was not altered in the presence of MMP catalytic site inhibition. MT1-MMP transcriptional control is unique compared to other MMP family members due to differences in its promoter sequence. Lohi et al., (2000) identified a GC-rich region within the promoter region of MT1-MMP as the putative binding sequence for the Sp1 transcription factor in multiple cell lines (Sroka et al., 2007). Phospho-ERK1/2 directly phosphorylates Sp1 to increase Sp1 transcriptional activity specifying this transcription factor as a possible target for increased *MT1-MMP* mRNA levels. Changes in Sp1 transcriptional activity should be investigated following BB-94 treatment in order to confirm involvement of this transcription factor. Ultimately the increase in *MT1-MMP* mRNA levels following catalytic site inhibition resulted in increased total MT1-MMP protein, with the greatest increase seen with active MT1-MMP levels in MCF-7 C2 cells (Fig. 4b and c). More active MT1-MMP present on the cell surface, whether catalytically inhibited by BB-94 or not, would still have the ability to activate phospho-ERK1/2 signalling, and therefore influence MT1-MMP expression in a proposed positive loop. However, MDA-MB-231 MT1-MMP protein levels were not altered following treatment with BB-94, suggesting that the more invasive cells, unlike

the MCF-7 cells, regulate MT1-MMP differently both post transcriptionally and post translationally.

In cells treated with BB-94, increased levels of active MT1-MMP resulted in increased ERK1/2 phosphorylation and increased mRNA levels of both *MT1-MMP* and *MMP-9*. These observations further support my hypothesis that a signalling pathway exists that co-regulates these proteins. However, in cells treated with BB-94, transcriptional activity of AP-1 and NF-κB remained unchanged by the application of the inhibitor (Fig. 10). As *MMP-9* mRNA levels increased, changes in expression of these transcription factors is hypothesized to increase. Promotion of MMP-9 transcription is controlled by many other transcription factors such as KRE, TIE, and RCE (Fig. 1) (Overall and López-Otín, 2002). Any of these regulating proteins can be turned on or repressed by phospho-ERK1/2, and disrupt endogenous transcription factor stoichiometry to be influencing the increased expression of *MMP-9* in cells treated with BB-94. Others have reported that the influence of phospho-ERK1/2 on *MMP-2* expression is complex, where crosstalk between the PI3K/AKT pathway has been proposed (Moulick et al., 2013).

In a proteolysis dependent pathway, a cell is proposed to be able to detect the cleavage ability of proteins on its cell surface. That being said, catalytically active MT1-MMP is necessary to activate pro-MMP-2. With a lack of ability by MT1-MMP to activate MMP-2, a cell may have feedback mechanisms whereby the expression of MMP-2 is reduced, and MMP-9, which can be activated independently of MT1-MMP, would not be regulated by the same mechanism.

4.2.2 Inhibition of MMP cleavage activity does not affect migration, but does decrease invasive potential of MDA-MB-231 breast cancer cells

MT1-MMP localization is well characterized as it is found at the leading edge of cells during migration, and in membrane protrusions called invadapodia during invasion (Artym, 2006). MDA-MB-231 breast cancer cells are highly invasive yet upon treatment with the pan-MMP catalytic site inhibitor BB-94, invasion is drastically reduced as demonstrated by decreased invasion through a Matrigel coated transwell barrier (Fig.

11c), a less protrusive phenotype in 3D cell culture (Fig. 12), and decreased vascularization and wound closure in the avian embryo CAM assay (Fig. 13). Intriguingly, the migratory ability of these cells is not impaired. MDA-MB-231 BB-94 treated cells do not exhibit changes in the active forms of the MT1-MMP protein, nor ERK1/2 phosphorylation, therefore supporting unchanged migratory ability, and the changes observed during invasion can be attributed to proteolysis alone.

A number of observations have been made regarding MT1-MMP activity influencing the migration of cells in a manner not dependent on proteolytic activity. These include amino acid sequences in the catalytic domain that do not impact enzymatic activity (Woskowicz et al., 2013), and interactions of ECM substrates with the hemopexin domain of MT1-MMP to initiate MAPK signalling (Zarrabi et al., 2011). In further support of these non-catalysis dependent migration-promoting characteristics of MT1-MMP, migratory abilities of MDA-MB-231 cells were not impaired when treated with BB94. Treating these cells did not impact migration to close a wound in the scratch wound closure assay (Fig. 11a and b), nor did it impact migration though a porous barrier in the transwell migration assay (Fig. 11c). As migration alone does not require degradation of ECM constituents, and relies more on cytoskeletal rearrangements, the changes observed in *MMP-2* and *MMP-9* mRNA levels are assumed not to impact this cell motility event.

Invasion on the other hand, was considerably impacted by inhibition of MMP catalytic activity, as all MT-MMPs present on the cell surface and all soluble MMPs secreted by MDA-MB-231 cells would have inhibited enzymatic activity. This is evident based on decreased transwell invasion (Fig. 11c) and a noticeably less protrusive phenotype in 3D culture (Fig. 12). As BB-94 treated MDA-MB-231 cells do not have changes in MT1-MMP protein levels or ERK1/2 phosphorylation, which are involved in invadapodia and cytoskeletal stabilization respectively, I postulated that the decreased protrusiveness of cells is attributed to MMP catalytic inhibition. Phenotypically, cells with MMP catalytic site impairment were much more aggregated compared to the elongated phenotype of control MDA-MB-231 cells. BB-94 treated cells appear to have gone from an elongated mesenchymal morphology, seen in untreated MDA-MB-231, to a more amoeboid ellipsoid shape. This transition is often seen when MMPs or serine proteases are

inhibited. Cells adapt to altered catalytic abilities by using a protease-independent amoeboid method of movement involving weak interactions with surrounding matrix in order to passively move through existent spaces within the ECM (Fiedl and Wolf, 2003).

BB-94 impaired invasion was apparent in CAM vascularization of artificial Matrigel tumours. These tumours showed decreased vascularization and inhibited wound closure following consistent application of BB-94 inhibitor (Fig. 13). In clinical application, BB-94 has been shown to convert ascite tumours into avascular tumours in mice with cervical carcinoma xenografts (Davies et al., 1993, Lu et al., 2011). In these conditions, BB-94 did not affect cell proliferation or migration, but did inhibit endothelial cell sprouting and morphogenesis, preventing the formation of complex networks and tubule-like structures. This suggests BB-94 may inhibit both early and late stages of angiogenesis. As the CAM tumour vascularization assay involves a whole functioning organism, it is uncertain to attest the reduction in tumour vascularization to inhibition of MMP catalytic ability of MDA-MB-231 cells within the tumour or to surrounding endothelial cells within the avian embryo CAM.

Investigating the implications of pan-MMP inhibition in invasive MDA-MB-231 breast cancer cells has demonstrated a compensatory effect of increased *MT1-MMP* and *MMP-9* expression when MMP catalytic activity is inhibited. However, increased expression of *MT1-MMP* and *MMP-9* is ineffective in rescuing invasive potential in 2D and 3D space, as well as *in vivo* tumour vascularization.

4.3 *MT1-MMP* overexpression in MDA-MB-231 breast cancer cells altered pro- and active forms of MT1-MMP and inversely affects gelatinase expression

Instead of chemically altering pro- and active MT1-MMP levels in MDA-MB-231 breast cancer cells, *MT1-MMP* overexpression cell lines were generated from these parental cells to further increase total MT1-MMP protein present within cells. Compared to parental MDA-MB-231cells, MDA-MB-231 C2 and C3 cell lines both have moderate amounts of pro- and predominately active MT1-MMP (Fig. 9a). Additionally in these cells *MMP-2* and *MMP-9* mRNA levels are altered, where both cell lines have decreased

MMP-2 and increased *MMP-9* mRNA and protein levels (Fig. 9b and c). This was also seen with MCF-7 C2 and MDA-MB-231 cells treated with BB-94 (Fig. 4d and 5c), where overall MT1-MMP protein increase consisted of predominately active MT1-MMP (MCF-7 C2 cells), with similar increased *MMP-9* mRNA and decreased *MMP-2* mRNA levels as a result (MCF-7 C2 and MDA-MB-231 cells).

MDA-MB-231 C1 cells displayed both excessive pro- and active forms of MT1-MMP. Together with this *MT1-MMP* overexpression, *MMP-2* mRNA levels are increased and *MMP-9* mRNA levels are decreased. This cell line in particular demonstrates that there are optimal levels of active MT1-MMP needed to influence *MMP-9* expression. Whereby MMP-9 expression could be decreased by the amount of pro-MT1-MMP present or through repression or activation of cell signalling pathways, such as MAPK and PI3K/AKT respectively. Most importantly, the genetic modification of *MT1-MMP* overexpression in MDA-MB-231 cell lines supports the continually observed inverse relationship of expression of the two gelatinases, and the contribution active MT1-MMP plays in cell signalling to influence *MMP-9* expression.

4.4 Inhibiting furin convertase activity alters MT1-MMP activation, inversely effects gelatinase expression, and alters cell migratory and invasive potential

In this section, I will examine the role of inhibition of MT1-MMP activation on MMP expression as well migration and invasive potential of breast cancer cells. Treatment of MCF-7, MCF-7 C2, and MDA-MB-231 cells with furin convertase inhibitor, Furin Inhibitor I, decreased *MMP-9* mRNA levels and increased *MMP-2* mRNA levels (Fig. 6c and 7c). Only MCF-7 C2 cells showed decreased *MT1-MMP* mRNA and active MT1-MMP protein levels, when treated with Furin Inhibitor I (Fig. 6a and b). As treatment of MDA-MB-231 cells with the furin inhibitor did not alter MT1-MMP protein forms, a stable MDA-MB-231 line (231-PDX) was created. 231-PDX cells overexpress *α1-PDX*, a small peptide that elicits the same effect as Furin Inhibitor I, to bind and block the active site of furin. These 231-PDX cells where furin activity is lower, exhibited increased *MT1-MMP* mRNA levels, and consequently, more of both pro-MT1-MMP and active MT1-MMP (Fig. 8). Additionally, 231-PDX cells have more phospho-ERK1/2 and

more *MMP-9* mRNA in agreement with the proposed model of phospho-ERK1/2 directly influencing *MMP-9* expression.

4.4.1 Chemical inhibition of furin decreased levels of active MT1-MMP, phospho-ERK1/2, and *MMP-9* mRNA, but increased *MMP-2* mRNA, and did not change cell migratory ability

Active MT1-MMP present on the cell surface is dictated by intercellular activation within the Golgi and trans-Golgi network through a protein convertase called furin (Seidah et al., 2008). Inhibition of furin in MCF-7 C2 and MDA-MB-231 breast cancer cell lines resulted in decreased phospho-ERK1/2, decreased *MMP-9* mRNA levels, and increased *MMP-2* mRNA levels. The consistency between the two cell lines regarding decreased phospho-ERK1/2 signalling, and inverse expression of the gelatinase MMPs demonstrates a conserved mechanism for influencing *MMP-2/-9* expression.

MCF-7 C2 cells exhibited a dose dependent decrease in active MT1-MMP and phospho-ERK1/2 levels following treatment with Furin Inhibitor I (Fig. 6a and b), while MDA-MB-231 cells showed decreased *MT1-MMP* mRNA and ERK1/2 phosphorylation levels, but unaltered MT1-MMP protein forms (Fig. 7). Additionally, both cell lines when treated with Furin Inhibitor I, demonstrated the inverse mRNA level relationship seen with the two gelatinases, where *MMP-9* mRNA levels were decreased and *MMP-2* mRNA levels were increased at 20 μM treatment. The results from furin inhibited MCF-7 C2 cells, which showed decreased active MT1-MMP, phospho-ERK1/2 and *MMP-9* mRNA levels, further supports the hypothesis that active MT1-MMP is necessary for MAPK pathway activation, and phospho-ERK1/2 acts directly to influence *MMP-9* expression. Regulation of *MMP-2* expression is not directly regulated by phospho-ERK1/2, but attributed to crosstalk between MAPK and other pathways. Furthermore, the dose-dependent treatment of MCF-7 C2 cells with Furin Inhibitor I, highlights the importance of a proper stoichiometric relationship between the levels of active MT1-MMP and MMP-2. Cells treated with 5 μM and 10 μM of the inhibitor have relatively more active MT1-MMP and less MMP-2 mRNA, while cells treated with 20 μM of the inhibitor have less active MT1-MMP and more MMP-2 mRNA. It is interesting that in a

situation where there is less active MT1-MMP, which is needed to active pro-MMP-2, that there is upregulation of the expression of *MMP-2*. In this case, I predicted that decreased activation of pro-MMP-2 on the cell surface is resulting in a feedback mechanism to increase *MMP-2* transcription.

In terms of cell motility, the migratory ability of MDA-MB-231 cells treated with Furin Inhibitor I observed via a scratch wound closure assay, was not impaired (Fig. 11a and b). MT1-MMP is known to be found in the leading edge of a migrating cells (Friedl and Wolf, 2003), and as MT1-MMP protein levels were unaffected in Furin inhibitor I treated MDA-MB-231 cells, it is unsurprising that treated cells retained migratory efficiency. Although phospho-ERK1/2 levels are decreased (Fig. 7a and b) in treated MDA-MB-231 cells, migration is not (Fig. 11a and b), and it poses the question of the proportional amount of phospho-ERK1/2 needed to stabilize actin-associated structures and promote cell motility.

4.4.2 Overexpression of *α1-PDX* increased active MT1-MMP, phospho-ERK1/2, *MMP-9* mRNA levels, but decreased *MMP-2* mRNA in MDA-MB-231 cells

As chemical inhibition was ineffective in changing MT1-MMP activation in MDA-MB-231 breast cancer cells, the stable cell line 231-PDX was created overexpressing *α1-PDX*, a small peptide that inhibits the convertase activity of furin (Thomas, 2002). 231-PDX cells have more total MT1-MMP protein, both pro and active forms, compared to MDA-MB-231 cells (Fig. 8b and c). Additionally, these cells have increased phospho-ERK1/2 and elevated *MT1-MMP* mRNA levels (Fig. 8c and d). 231-PDX cells also exhibited an inverse expressional relationship between MMP-2 and MMP-9, decrease and increase respectively (Fig. 8d).

Although it was expected that overexpression of *α1-PDX* and resultant furin inhibition would cause less active MT1-MMP, the presence of more pro- and active MT1-MMP was a surprising result. However, increased levels of active MT1-MMP are still consistent with my overall hypothesis, as 231-PDX cells also had elevated ERK1/2 phosphorylation and increased *MMP-9* mRNA. However, altering MT1-MMP activation

in MDA-MB-231 cells did not induce changes in levels of transcription factors AP-1 and NF-κB (Fig. 10c and d), therefore other transcription factors which are regulated by phospho-ERK1/2 and are MMP-9 specific, such as RCE, TIE, or KRE, or MT1-MMP specific, Sp-1, should be assessed in 231-PDX cells (Overall and López-Otín 2002).

Increased active MT1-MMP levels following expression of *α1-PDX* has been noted in other cancerous cell lines as well, including squamous cell carcinoma, epidermoid carcinoma cells, and pharyngeal carcinoma cells (Bassi et al., 2001). Additionally, CHO cells co-transfected to secrete a soluble form of MT1-MMP and *α1-PDX*, displayed an increase in total MT1-MMP protein with predominately active MT1-MMP (Coppola et al., 2008). MT1-MMP has been found to be activated through furin-independent mechanisms primarily by other active MMPs (Rozanov et al., 2001; Sato et al., 1999). For example there is evidence that MT1-MMP may undergo a two-step activation process, including autocatalysis (Strongin, 2010). If furin-dependent mechanisms of activation are being inhibited by *α1-PDX* peptides, it is possible that feedback occurs to transcriptionally upregulate MT1-MMP expression, and additional pro-MT1-MMP proteins are being translated and activated by a furin-independent manner to result in increased active MT1-MMP present within 231-PDX cells.

4.4.3 Overexpression of *α1-PDX* in MDA-MB-231 cells exhibit decreased migration and invasive potential

231-PDX cells are the only experimental cell in this study that exhibited high increased levels of active MT1-MMP protein and *MMP-9* mRNA, accompanied by moderately increased ERK1/2 phosphorylation, all features that could increase cell migration and invasion. Nonetheless, 231-PDX cells exhibited decreased transwell migration, decreased transwell invasion (Fig. 11c), decreased protrusions in 3D cell culture (Fig. 12b), and decreased vascularization and wound closure in an avian embryo CAM wound assay (Fig. 13).

In 3D cell culture, 231-PDX cells have a very round morphology, with fewer protrusions than MDA-MB-231 cells, and lack the meschenymal-like elongated cell phenotype. 231-PDX cells are morphologically most like MDA-MB-231 C2 cells —circular and round,

with decreased protrusions (Cepeda et al., 2016). Furthermore, MDA-MB-231 C2 cells have increased total *MT1-MMP* mRNA compared to MDA-MB-231 parental cells and high active MT1-MMP protein, increased *MMP-9* mRNA but decreased *MMP-2* mRNA (Fig. 9), all similar features of 231-PDX cells. Through analysis of both MCF-7 and MDA-MB-231 MT1-MMP overexpression cell lines, Cepeda et al (2016) found that as levels of MT1-MMP overexpression increased, the migratory and invasive potential of breast cancer cells decreased, and 231-PDX cells fit into this categorization as exemplified by transwell migration and invasion assay. Furin also cleaves a wide variety of substrates in addition to MT1-MMP, such as TGF-β, stromolysin-3, growth factors, and adhesion molecules, which are also important for proper cell motility (Strongin, 2010). Activation of other furin substrates could be altered by the presence of α1-PDX peptides and additionally be contributing factors in decreased cell migration, invasion, and altered cell morphology in 231-PDX cells.

Analysis of vascularization and wound closure of 231-PDX comprised Matrigel tumors in an avian CAM assay revealed intermediate incidences of vascularization and variable wound closure (Fig. 13c). This assay is very general, and it is difficult to assess if lack of vascularization and wound closure is attributed to decreased migratory and invasive potential of 231-PDX cells, altered MMP expression, changes in TGF-β, growth factors, or adhesion molecules, or due to changes in secreted VEGF family members. MDA-MB-231 naturally express high levels of VEGF family members needed to promote development of new vasculature (Di Benedetto et al., 2015) whereby cleavages of VEGF are executed by MMP-9 (Bergers et al., 2000; Yu and Stamenkovic 2000). It is possible that in modulating MT1-MMP protein forms, resultant ERK phosphorylation levels, and *MMP-9* expression, that other aspects needed for cell movement and angiogenesis were altered as well in order to produce this very intermediate characterization of vascularization and wound closure.

Chapter 5

5 Conclusion

MT1-MMP proteolytic and non-proteolytic functions are strongly implicated in the promotion and progression of cancer by promoting cell migration and invasion. As shown here, by disrupting ERK1/2 phosphorylation, MMP catalytic activity, or MT1-MMP activation, the migratory and invasive potential of MDA-MB-231 breast cancer cells is impaired. I initially hypothesized that the levels of phosphorylated ERK1/2 would be proportional to the levels of active MT1-MMP, and be correlated with increased *MMP-2* and *MMP-9* mRNA and increased invasive potential of breast cancer cells.

Inhibition of ERK1/2 phosphorylation caused decreased *MT1-MMP* mRNA and subsequently decreased active MT1-MMP protein levels. This resulted in decreased ERK1/2 phosphorylation and subsequent decreased NF-κB transcriptional activity. However the mRNA levels of the two gelatinases were not affected proportionally to ERK1/2 phosphorylation — an inverse relationship between *MMP-2* (increased mRNA) and *MMP-9* (decreased mRNA) was observed indicating *MMP-9* expression was more directly controlled by phospho-ERK1/2. Cells with reduced active MT1-MMP levels exhibited decreased migratory and invasive potential. Inhibition of MMP catalytic activity by BB-94 caused an increase in phospho-ERK1/2 and successive increased *MT1-MMP* mRNA and protein levels. Furthermore, following BB-94 treatment phospho-ERK1/2 was increased and gelatinase expression was inversely associated —increased *MMP-9* mRNA and decreased *MMP-2* mRNA, and invasive potential was reduced. The effect inhibition of MT1-MMP activation, by the inhibition of furin, was dependent on mode of inhibition. Chemical alteration of furin convertase activity caused decrease active MT1-MMP, decreased phospho-ERK1/2, decreased *MMP-9* mRNA levels, and decreased *MMP-2* mRNA levels. However, counter to my original hypothesis, invasive potential was not increased despite having increased active MT1-MMP protein, phospho-ERK1/2 and *MMP-9* mRNA. Therefore cells that have levels of phospho-ERK1/2, active MT1-MMP, or *MMP-9* mRNA above or below their endogenous levels, invasive

potential is reduced. Additionally, despite the gelatinase MMPs sharing substrate similarity, this study proposes that altering *MMP-2* or *MMP-9* expression and proposed functions do not compensate for one another *in vitro*. As consequential to chemical or genetic alteration of cell specific components, *MMP-2* and *MMP-9* expression was always effected in an inverse manner (Fig. 14).

Through targeting of different proteolytic and non-proteolytic functions of MT1-MMP this study proposes that active MT1-MMP is needed for induction of MAPK signalling causing increased phospho-ERK1/2. Phospho-ERK1/2 then influences MT1-MMP and MMP-9 specific transcription factor NF-κB to ultimately regulate their respective expression. *MMP-2* expression is indirectly regulated through proposed feedback mechanisms and signalling pathway cross talk. This study demonstrates the difficulty of designing direct protein targeting cancer therapeutics, as MMP and cell signalling functions are complexly intertwined.

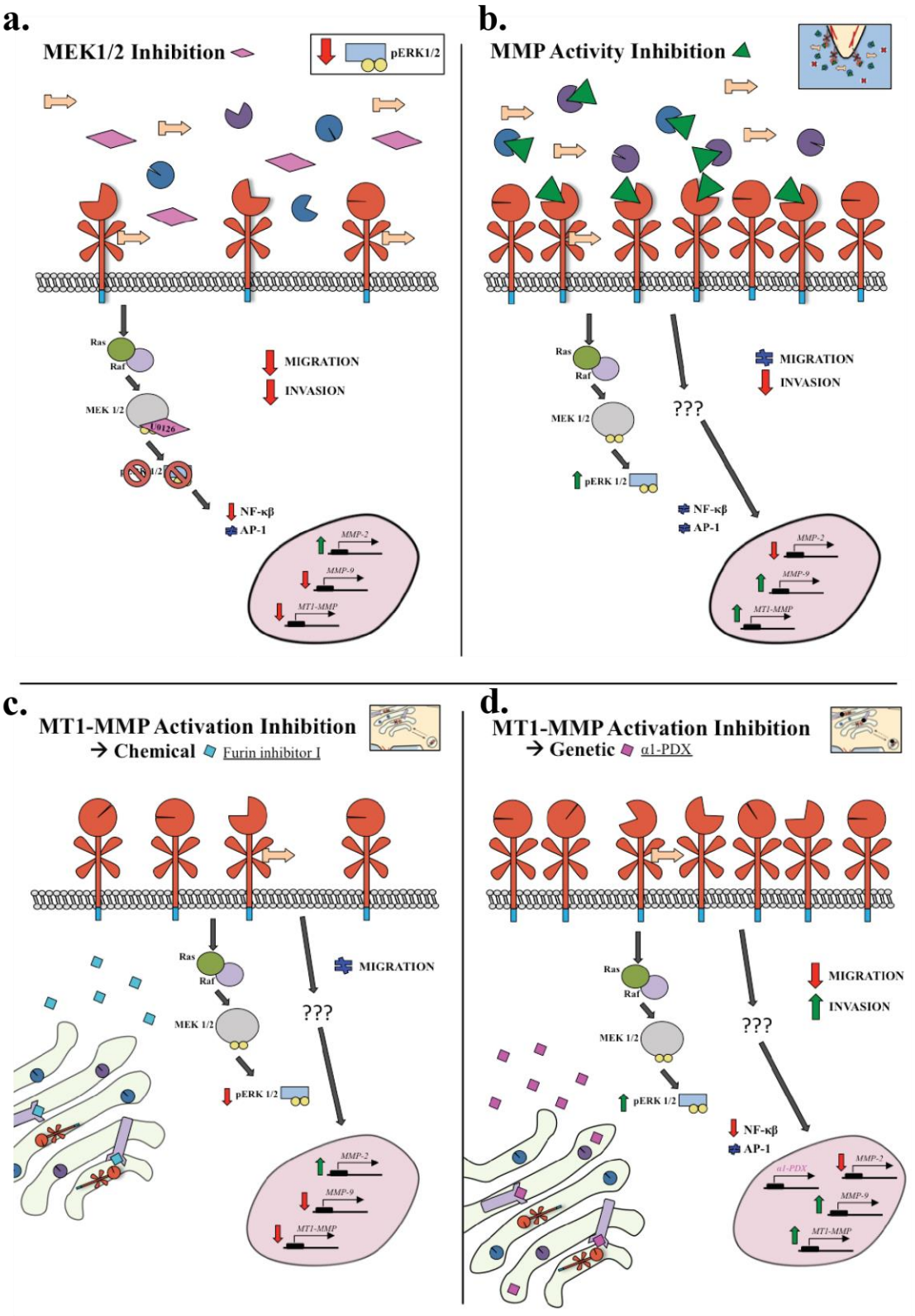
a.
MEK1/2 Inhibition
pERK1/2
Ras
Raf
MEK 1/2
U0126
MIGRATION
INVASION
NF-κβ
AP-1
MMP-2
MMP-9
MT1-MMP
b.
MMP Activity Inhibition
Ras
Raf
MEK 1/2
pERK 1/2
???
MIGRATION
INVASION
NF-κβ
AP-1
MMP-2
MMP-9
MT1-MMP
c.
MT1-MMP Activation Inhibition
→ Chemical
Furin inhibitor I
Ras
Raf
MEK 1/2
pERK 1/2
???
MIGRATION
MMP-2
MMP-9
MT1-MMP
d.
MT1-MMP Activation Inhibition
→ Genetic
α1-PDX
Ras
Raf
MEK 1/2
pERK 1/2
???
MIGRATION
INVASION
NF-κβ
AP-1
α1-PDX
MMP-2
MMP-9
MT1-MMP

Figure 14. Proposed cell models individually outlining cellular outcomes of inhibiting ERK1/2 phosphorylation, MMP catalytic activity, or altering of MT1-MMP activation via changes in MMP transcription and protein levels, ERK1/2 phosphorylation, and cell motility.

(a) Treatment of breast cancer cells with MEK1/2 inhibitor (U0126) resulted in decreased ERK1/2 phosphorylation, decrease in the activity of MT1-MMP and MMP-9 specific transcription factor NF-κB, but no change in AP-1 transcription. Levels of *MMP-2* mRNA were increased, while mRNA levels of *MMP-9* and *MT1-MMP* were decreased. Consequently, there was less overall MT1-MMP (less pro- and active) protein. Moreover, migration and invasive potential was decreased in cells treated with U0126. **(b)** Treatment of breast cancer cells with the pan-MMP inhibitor (BB-94) resulted in decreased MMP catalytic activity. Subsequently, BB-94 treated cells displayed decreased ERK1/2 phosphorylation, but no change in the activity of transcription factors AP-1 and NF-κB. However, MMP mRNA levels were altered. *MMP-2* mRNA was decreased, while *MMP-9* and *MT1-MMP* mRNA was increased As a result, cells treated with BB-94 had more MT1-MMP protein overall, with an increase in both pro- and active forms. Furthermore, inhibition of MMP catalytic activity did not influence migratory potential, but decreased invasive potential. In this BB-94 treatment, it is possible that an alternative pathway influences MMP expression, as more active MT1-MMP did not result in an increase in phospho-ERK1/2, nor was the activity of transcription factors changed. **(c)** Altering MT1-MMP activation by chemical inhibition (Furin inhibitor I) reduced active MT1-MMP protein levels. Decreased levels of active MT1-MMP resulted in decreased phospho-ERK1/2 as well as decreased *MT1-MMP* and *MMP-9* mRNA levels, but increased *MMP-2* RNA levels. Altering MT1-MMP activation did not change the migratory potential of cells. As Furin Inhibitor I elicited a weaker effect on MDA-MB-231 cells than U0126 or BB-94, stable MDA-MB-231 breast cancer cells were generated expressing Alpha1-Antitrypsin Portland, as an alternative approach to block MT1-MMP activation. **(d)** MDA-MB-231 cells stably overexpressing *α1-PDX*, 231-PDX, displayed more pro- and more active MT1-MMP compared to MDA-MB-231 parental cells. This resulted in increased phospho-ERK1/2 but decreased activity of NF-κB and no change in activity of AP-1. However, *MMP-9* and *MT1-MMP* mRNA was increased, and *MMP-2*

mRNA was decreased. Migratory and invasive potential was decreased in 231-PDX cells. Ultimately, the results from each respective treatment propose a pathway in which active MT1-MMP is needed to initiate the MAPK pathway resulting in subsequent ERK1/2 phosphorylation, activation of NF-κB, expression of *MMP-9*.

References

Alblazi, K. M., and Siar, C. H. 2015. Cellular protrusions--lamellipodia, filopodia, invadopodia and podosomes--and their roles in progression of orofacial tumours: current understanding. *Asian Pacific Organization for Cancer Prevention*. 6 (6): 2187-91.

Artym, V. V. 2006. Dynamic Interactions of Cortactin and Membrane Type 1 Matrix Metalloproteinase at Invadopodia: Defining the Stages of Invadopodia Formation and Function. *Cancer Research*. 66 (6): 3034–3043.

Bateman, J. F., Boot-Handform, R. P., and Lamandé, S. R. 2009. Genetic Diseases of Connective Tissues: Cellular and Extracellular Effects of ECM Mutations. *Nature Reviews. Genetics.* 10 (3): 173–83.

Bassi, D. E., De Cicco, R. L., Mahloogi, H., Zucker, S., Thomas, G., Klein-Szanto, A. J. P. 2001. Furin inhibition results in absent or decreased invasiveness and tumorigenicity of human cancer cells. *Proceedings of the National Academy of Sciences*. 98 (18): 10326–31.

Bergers, G., Brekken, R., McMahon, G., Vu, T. H., Itoh, T., Tamaki, K., Tanzawa, K, et al. 2000. Matrix Metalloproteinase-9 Triggers the Angiogenic Switch during Carcinogenesis. *Nature Cell Biology.* 2 (10): 737–44.

Björklund, M., and Koivunen, E. 2005. Gelatinase-Mediated Migration and Invasion of Cancer Cells. *Biochimica et Biophysica Acta - Reviews on Cancer.* 1755 (1): 37–69.

Bourboulia, D., and Stetler-Stevenson, W. G. 2010. Matrix Metalloproteinases (MMPs) and Tissue Inhibitors of Metalloproteinases (TIMPs): Positive and Negative Regulators in Tumour Cell Adhesion. *Seminars in Cancer Biology.* 20 (3): 161–68.

Buccione, R., Caldieri, G., and Ayala, I. 2009. Invadopodia: Specialized tumour cell structures for the focal degradation of the extracellular matrix. *Cancer and Metastasis Reviews*. 28 (1): 137–49.

Butcher, D. T., Alliston, T., and Weaver, V. M. 2009. A tense situation: forcing tumour progression. *Nature Reviews. Cancer.* 9 (2): 108–22.

Cathcart, J., Pulkoski-Gross, A., and Cao, J. 2015. Targeting Matrix Metalloproteinases in Cancer: Bringing New Life to Old Ideas. *Genes and Diseases.* 2 (1). 26–34.

Cepeda, M., Pelling, J., Evered, C., Williams, K., Freedman, Z., Stan, I., Willson, J., Leong, H. S., and Damjanovski, S. 2016. Less is More: Low Expression of MT1-MMP Is Optimal To Promote Migration and Tumourigenesis of Breast Cancer Cells. *BMC Molecular Cancer.* Submitted.

Coppola, J. M., Bhojani, M. S., Ross, B. D., and Rehemtulla, A. 2008. A Small-Molecule Furin Inhibitor Inhibits Cancer Cell Motility. *Neoplasia*. 10 (4): 363–70.

Cvetković, D., Goertzen, C. G.-F., and Bhattacharya, M. (2014). Quantification of Breast Cancer Cell Invasiveness Using a Three-dimensional (3D) Model. *Journal of Visualized Experiments : JoVE*. (88), 1–9.

D'Alessio, S., Ferrari, G., Cinnante, K., Scheerer, W., Galloway, A.C., Roses, D.F., Rozanov, D.V., Remacle, A.G., Oh, E.S., Shiryaev, S.A., Strongin, A.Y., Pintucci, G., and Mignatti, P. 2008. Tissue inhibitor of metalloproteinases-2 binding to membrane- type 1 matrix metalloproteinase induces MAPK activation and cell growth by a non-proteolytic mechanism. *Journal of Biological Chemistry*. 283 (1): 87–99.

Davies, B., Brown , P. D., Crimmin, M. J., and Balkwill, F. R. 1993. A synthetic matrix metalloproteinase inhibitor decreases tumor burden and prolongs survival of mice bearing human ovarian mouse xenografts. Cancer Research. 53 (1): 2087–91.

DeSilva, D. R., Jones, E. A., Favata, M. F., Jaffee, B. D., Magolda, R. L., Trzaskos, J. M., and Scherle, P. A. 1998. Inhibition of Mitogen-Activated Protein Kinase Kinase Blocks T Cell Proliferation but Does Not Induce or Prevent Anergy. *Journal of Immunology.* 160 (9): 4175–81.

De Wever, O., Demetter,P., Mareel, M., and Bracke, M. 2008. Stromal Myofibroblasts Are Drivers of Invasive Cancer Growth. *International Journal of Cancer.* 123 (10): 2229–38.

Di Benedetto, M., Toullec, A., Buteau0Lozano, H., Abdelkarim, M., Vacher, S., Velasco, G., Christofari, M., Pocard, M., Bieche, I., and Perrot-Applant, M. 2015. MDA-MB-231 breast cancer cells overexpressing single VEGF isoforms display distinct colonisation characteristics. *British Journal of Cancer.* 13 (5): 773–85.

Egeblad, M., and Werb., Z. 2002. New Functions for the Matrix Metalloproteinases in Cancer Progression. *Nat Rev Cancer*. 2 (3): 161–74.

Erler, J. T., and Weaver, V. M. 2009. Three-Dimensional Context Regulation of Metastasis. *Clinical and Experimental Metastasis.* 26 (1): 35–49.

Frantz, C., Stewart, K. M., and Weaver, V. M. 2010. The Extracellular Matrix at a Glance. *Journal of Cell Science.* 123: 4195–4200.

Friedl, P., and Wolf, K. 2003. Tumour-cell invasion and migration: diversity and escape mechanisms. *Nature Reviews. Cancer*. *3* (5): 362–74.

Fujioka, A., Terai, K., Itoh, R. E., Aoki, K., Nakamura, T., Kuroda, S., Nishida, E., and Matsuda, M. 2006. Dynamics of the Ras/ERK MAPK Cascade as Monitored by

Fluorescent Probes. *Journal of Biological Chemistry.* 281 (13): 8917–26.

Giannelli, G., Falk-marzillier, J., Schiraldi, O., Stetler-stevenson, W. G., and Quaranta, V. 2016. Induction of Cell Migration by Matrix Metalloprotease-2 Cleavage of Laminin-5. *American Association for the Advancement of Science.* 277 (5323): 225–28.

Gross, Jerome, and Charles M. Lapiere. 1962. Collagenolytic Activity in Amphibian Tissues : A Tissue Culture Assay. Processings of the National Academy of Sciences of the United States of America. 48 (6): 1014-22.

Gum, R., Wang, H., Lengyel, E., Juarez, J., and Boyd, D. 1997. Regulation of 92 kDa Type IV Collagenase Expression by the Jun Aminoterminal Kinase- and the Extracellular Signal-Regulated Kinase-Dependent Signalling Cascades. *Oncogene*. 14 (12): 1481–93.

Hiratsuka, S., Watanabe, A., Aburatani, H., and Maru, Y. 2006. Tumour-Mediated Upregulation of Chemoattractants and Recruitment of Myeloid Cells Predetermines Lung Metastasis. *Nature Cell Biology.* 8 (12): 1369–75.

Hoeben, A., Landuyt, B., Highley, M. S., Wildiers, H., Van Oosterom, A. T., and De Bruijn, E. A. 2004. Vascular Endothelial Growth Factor and Angiogenesis. Pharmacological Reviews. 56 (1): 549 – 80

Holliday, D. L., and Speirs, V. 2001. Choosing the right cell line for breast cancer research. *Breast Cancer Research.* 13(4):215– 221.

Holmbeck, K., Bianco, P., Caterina, J., Yamada, S., Kromer, M., Kuznetsov, S. A., Mankani, M., et al. 1999. MT1-MMP-Deficient Mice Develop Dwarfism, Osteopenia, Arthritis, and Connective Tissue Disease due to Inadequate Collagen Turnover. *Cell*. 99 (1): 81–92.

Hotary, K, Li, X. Y., Allen, E., Stevens, S. L., and Weiss, S. J. 2006. A Cancer Cell Metalloprotease Triad Regulates the Basement Membrane Transmigration Program. *Genes and Development.* 20 (19): 2673–86.

Hynes, R. O., and Naba, A. 2012. Overview of the Matrisome-An Inventory of Extracellular Matrix Constituents and Functions. *Cold Spring Harbor Perspectives in Biology* 4 (1): 1–16.

Itoh, Y., Takamura, A., Ito, N., Maru, Y., Sato, H., Suenaga, N., Aoki, T., and Seiki, M. 2001. Homophilic Complex Formation of MT1-MMP Facilitates proMMP-2 Activation on the Cell Surface and Promotes Tumour Cell Invasion. *EMBO Journal*. 20 (17): 4782–93.

Itoh, Y., Ito, N., Nagase, H., Evans, R. D., Bird, S. A., and Seiki, M. 2006. Cell surface

collagenolysis requires homodimerization of the membrane-bound collagenase MT1-MMP. *Molecular Biology of the Cell*. 17 (12): 5390–9.

Järveläinen, H. 2009. Extracellular Matrix Molecules: Potential Targets in Pharmacotherapy. *Pharmacology Reviews.* 61 (2): 198–223.

Kalluri, R. 2003. Basement Membranes: Structure, Assembly and Role in Tumour Angiogenesis. *Nature Reviews. Cancer.* 3 (3): 422–33.

Kaplan, R. N., Riba, R. D., Zacharoulis, S., Bramley, A. H., Vincent, L., Costa, C., MacDonald, D. D., et al. 2005. VEGFR1-Positive Haematopoietic Bone Marrow Progenitors Initiate the Pre-Metastatic Niche. *Nature.* 438 (7069): 820–27.

Kelley, L. C., Haynes, K. E., Gatesman Ammer, A., Marion, K. H., and Weed, S. C. 2011. Revisiting the ERK/Src cortactin switch. *Communicative and Integrative Biology.* 4 (2): 205-07.

Khasigov, P. Z., Podobed, O. V., Gracheva, T. S., Salbiev, K. D., Grachev, S. V., and Berezov, T. T. 2003. Role of Matrix Metalloproteinases and Their Inhibitors in Tumour Invasion and Metastasis. *Biochemistry. Biokhimiia* 68 (7): 711–17.

Klein, T., and Bischoff. R. 2011. Physiology and Pathophysiology of Matrix Metalloproteases. *Amino Acids.* 41 (2): 271–90.

Koshikawa, N., Giannelli, G., Cirulli, V., Miyazaki, K., and Quaranta, V. 2000. Role of cell surface metalloprotease MT1-MMP in epithelial cell migration over laminin 5. *Journal of Cell Biology*. 148 (3): 615–624.

Lambert, E., Bernard Haye, D., and Petitfrère, E. 2004. TIMPs as Multifacial Proteins. *Critical Reviews in Oncology/Hematology.* 49 (3): 187–98.

Lee, S. J., Cho, S. C., Lee, E. J., Kim, S., Lee, S. B., Lim, J. H., Choi, Y. H., Kim, W. J., and Moon, S. K. 2013. Interleukin-20 Promotes Migration of Bladder Cancer Cells through Extracellular Signal-Regulated Kinase (Erk)-Mediated Mmp-9 Protein Expression Leading to Nuclear Factor (Nf-Kb) Activation by Inducing the up-Regulation of p21waf1 Protein Expression. *Journal of Biological Chemistry.* 288 (8): 5539–52.

Lehti, K., Valtanen, H., Wickström, S., Lohi, J., and Keski-Oja, J. 2000. Regulation of Membrane-Type-1 Matrix Metalloproteinase Activity by Its Cytoplasmic Domain. *Journal of Biological Chemistry.* 275 (20): 1506–13.

Lohi J, Lehti K, Valtanen H, Parks WC, and Keski-Oja J (2000). Strutural analysis and promoter characterization of the human membrane- type matrix metalloproteinase-1 (MT1-MMP) gene. *Gene* 242 (1): 75 – 86.

López-Otín, C., and Matrisian, L. M. 2007. Emerging Roles of Proteases in Tumour Suppression. *Nature Reviews. Cancer* 7 (10): 800–808.

Low, A., Bone, A., Johnson, D., and Dickson, B. 1996. The Matrix Metalloproteinase Inhibitor Batimastat (BB-94) Retards Human Breast Cancer Solid Tumour Growth but not Ascites Formation in Nude Mice. *Clinical Cancer Research*. 2 (1): 1207–15.

Lu, P., Takai, K., Weaver, V. M., and Werb, Z. 2011. Extracellular Matrix Degradation and Remodeling in Development and Disease. *Cold Spring Harb Perspectives Biology*. 3 (12): 1–24.

Marshall, J. (2011). Transwell Invasion Assays. In C. M. Wells and M. Parsons (Eds.), *Cell Migration: Developmental Methods and Protocols* (2nd ed., Vol. 769, pp. 97–110). New York: Humana Press.

Martin, G. R., and Timpl, R. 1987. Laminin and Other Basement Membrane Components. *Annual Review of Cell and Developmental Biology*. 3 (3): 57–85.

Mebratu, Y., and Tesfaigzi, Y. 2009. How ERK1/2 Activation Controls Cell Proliferation and Cell Death Is Subcellular Localization the Answer? *Cell Cycle*. 8 (8): 1168–75.

Meloche, S., and Pouysségur, J. 2007. The ERK1/2 Mitogen-Activated Protein Kinase Pathway as a Master Regulator of the G1- to S-Phase Transition. *Oncogene*. 26 (22): 3227–39.

Mook, O. R. F., Frederiks, W. M., and Van Noorden, C. J. H. 2004. The Role of Gelatinases in Colorectal Cancer Progression and Metastasis. *Biochimica et Biophysica Acta* 1705 (2): 69–89.

Moulick, S., Pal, S., Biswas, J., and Chatterjee, A. 2013. Role of ERK in Modulating MMP 2 and MMP 9 with Respect to Tumour Invasiveness in Human Cancer Cell Line MCF-7 and MDA-MB-231. *Journal of Tumor*. 2 (2): 87-98.

Mouw, J. K., Ou, G., and Weaver, V. M. 2014. Extracellular Matrix Assembly: A Multiscale Deconstruction. *Nature Reviews. Molecular Cell Biology*. 15 (12): 771–85.

Mori, H., Tomari, T., Koshikawa, N., Kajita, M., Itoh, Y., Sato, H., ... Seiki, M. 2002. CD44 directs membrane-type 1 matrix metalloproteinase to lamellipodia by associating with its hemopexin-like domain. *EMBO Journal*. 21 (15): 3949–3959.

Naba, A., Clauser, K. R., Hoersch, S., Liu, H., Carr, S. A., and Hynes, R. O. 2012. The Matrisome: In Silico Definition and In Vivo Characterization by Proteomics of Normal and Tumour Extracellular Matrices. *Molecular and Cellular Proteomics* 11 (4): 1–18.

Nagase, H., Visse, R., and Murphy, G. 2006. Structure and Function of Matrix Metalloproteinases and TIMPs. *Cardiovascular Research.* 69 (3): 562–73.

Overall, C. M., and C. Lopez-Otin. 2002. Strategies for MMP inhibition in cancer: innovations for the post-trial era. *Nature Reviews.* 2 (1): 657-72.

Pahwa, S., Stawikowski, M. J., and Fields, G. B. 2014. Monitoring and Inhibiting MT1-MMP during Cancer Initiation and Progression. *Cancers.* 6 (1): 416–35.

Paszek, M. J., Zahir, N., Johnson, K. R., Lakins, J. N., Rozenberg, G. I., Gefen, A., Reinhart-King, C. A., et al. 2005. Tensional Homeostasis and the Malignant Phenotype. *Cancer Cell.* 8 (3): 241–54.

Paulsson, M. 1992. Basement Membrane Proteins: Structure, Assembly, and Cellular Interactions. *Critical Reviews in Biochemistry and Molecular Biology.* 27 (1-2): 93–127.

Poincloux, R., Lizárraga, F., and Chavrier, P. 2009. Matrix Invasion by Tumour Cells: A Focus on MT1-MMP TRAFficking to Invadopodia. *Journal of Cell Science.* 122 (17): 3015–24.

Reddy, K. B., Nabha, S. M., and Atanaskova, N. 2003. Role of MAP kinase in tumor progression and invasion. *Cancer and Metastasis Reviews.* 22 (1): 395–403.

Roberts, P., and Der, C. 2007. Targeting the RAF-MEK-ERK Mitogen-Activated Protein Kinase Cascade for the Treatment of Cancer. *Oncogene* 26: 3291–3310.

Rozanov, D. V., Deryugina, E. I., Ratnikov, B. I., Monosov, E. Z., Marchenko, G. N., Quigley, J. P., and Strongin, A. Y. (2001). Mutation analysis of membrane type-1 matrix metalloproteinase (MT1-MMP): The role of the cytoplasmic tail Cys574, the active site Glu 240, and furin cleavage motifs in oligomerization, processing, and self-proteolysis of MT1-MMP expressed in breast carcin. *Journal of Biological Chemistry*. 276 (28): 25705–14.

Rozario, T, and DeSimone, D. W. 2010. The Extracellular Matrix in Development and Morphogenesis: A Dynamic View. *Developmental Biology.* 341 (1): 126–40.

Sabeh, F., Li, X. Y., Saunders, T. L., Rowe, R. G., and Weiss, S. J. 2009. Secreted versus Membrane-Anchored Collagenases: Relative Roles in Fibroblast-Dependent Collagenolysis and Invasion. *Journal of Biological Chemistry.* 284 (34): 23001–11.

Sanes, J. R. 2003. The Basement Membrane/basal Lamina of Skeletal Muscle. *Journal of Biological Chemistry.* 278 (15): 12601–4.

Sato, T., Kondo, T., Fujisawa, T., Seiki, M., and Ito, A. (1999). Furin-independent pathway of membrane type 1-matrix metalloproteinase activation in rabbit dermal fibroblasts.

Journal of Biological Chemistry. 274 (52): 37280–84.

Scamuffa, N., Calvo, F., Chrétien, M., Seidah, N. G., and Khatib, A. 2006. Proprotein Convertases: Lessons from Knockouts. *FASEB Journal : Official Publication of the Federation of American Societies for Experimental Biology.* 20 (12): 1954–63.

Schaefer, L., and Schaefer, R. M. 2010. Proteoglycans: From Structural Compounds to Signalling Molecules. *Cell and Tissue Research.* 339 (1): 237–46.

Seidah, N. G., Mayer, G., Zaid, A., Rousselet, E., Nassoury, N., Poirier, S., Essalmani, R., and Prat, A. 2008. The Activation and Physiological Functions of the Proprotein Convertases. *International Journal of Biochemistry and Cell Biology.* 40 (6-7): 1111–25.

Seiki, M. 2003. Membrane-Type 1 Matrix Metalloproteinase: A Key Enzyme for Tumour Invasion. *Cancer Letters.* 194 (1): 1–11.

Sounni, N. E., Rozanov, D. V., Remacle, A. G., Golubkov, V. S., Noel, A., and Strongin, A. Y. 2010. Timp-2 Binding with Cellular MT1-MMP Stimulates Invasion-Promoting MEK/ERK Signalling in Cancer Cells. *International Journal of Cancer*. 126 (5): 1067–78.

Sroka, I. C., Nagle, R. B., and Bowden, G. T. 2007. Membrane-Type 1 Matrix Metalloproteinase Is Regulated by Sp1 through the Differential Activation of AKT, JNK, and ERK Pathways in Human Prostate Tumor Cells. *Neoplasia*. 9 (5): 406–17.

Stöcker, W., and Bode, W. 1995. Structural Features of a Superfamily of Zinc-Endopeptidases: The Metzincins. *Current Opinion in Structural Biology* 5 (3): 383–90.

Sternlicht, M. D., and Werb, Z. 2001. How Matrix Metalloproteinases Regulate Cell Behavior. *Annual Review of Cell and Developmental Biology.* 17 (1): 463–516.

Stetler-Stevenson, W. G. 2008. The Tumour Microenvironment: Regulation by MMP-Independent Effects of Tissue Inhibitor of Metalloproteinases-2. *Cancer and Metastasis Reviews.* 27 (1): 57–66.

Stetler-Stevenson, W. G., and Seo, D. W. 2005. TIMP-2: An Endogenous Inhibitor of Angiogenesis. *Trends in Molecular Medicine.* 11 (3): 97–103.

Strongin, A. Y. 2010. Proteolytic and Non-Proteolytic Roles of Membrane Type-1 Matrix Metalloproteinase in Malignancy. *Biochimica et Biophysica Acta - Molecular Cell Research.* 1803 (1): 133-41.

Takahashi, Y., Kawahara, F., Noguchi, M., Miwa, K., Sato, H., Seiki, M., Inoue, H., Tanabe, T., and Yoshimoto, T. Y. 1999. Activation of Matrix Metalloproteinase-2 in

Human Breast Cancer Cells Overexpressing Cyclooxygenase-1 or -2. *FEBS Letters.* 460 (1): 145–48.

Tanimura, S., Asato, K., Fujishiro, S., and Kohno, M. 2003. Specific blockade of the ERK pathway inhibits the invasiveness of tumor cells: down-regulation of matrix metalloproteinase-3/-9/-14 and CD44. *Biochemical and Biophysical Research Communications.* 304 (1): 801-07.

Thomas, G. 2002. Furin at the Cutting Edge: From Protein Traffic to Embryogenesis and Disease. *Nature Reviews. Molecular Cell Biology.* 3 (10): 753–66.

Torricelli, A. M., Singh, V., Santhiago, M. R., and Wilson, S. E. 2013. The Corneal Epithelial Basement Membrane: Structure, Function, and Disease. *Investigative Ophthalmology and Visual Science.* 54 (9): 6390–6400.

Toth, M., Sohail, A., and Fridman, R. 2001. Assessment of Gelatinases (MMP-2 and MMP-9) by Gelatin Zymography. *Methods in Molecular Medicine*. 878 (1): 121–35.

Toth, M., I. Chvyrkova, M.M. Bernardo, S. Hernandez-Barrantes, and Fridman, R. 2003. Pro-MMP-9 activation by the MT1-MMP/MMP-2 axis and MMP-3: role of TIMP-2 and plasma membranes. *Biochemical and Biophysical Research Communications*. 308 (1): 386-395.

Ueda, J., Kajita, M., Suenaga, N., Fujii, K., and Seiki, M. 2003. Sequence-specific silencing of MT1-MMP expression suppresses tumour cell migration and invasion: importance of MT1-MMP as a therapeutic target for invasive tumours. *Oncogen.*, 22 (54): 8716–22.

Uekita, T., Itoh, Y., Yana, I., Ohno, H., and Seiki, M. 2001. Cytoplasmic Tail-Dependent Internalization of Membrane-Type 1 Matrix Metalloproteinase Is Important for Its Invasion-Promoting Activity. *Journal of Cell Biology.* 155 (7): 1345–56.

Visse, R., and Nagase, H. 2003. Matrix Metalloproteinases and Tissue Inhibitors of Metalloproteinases: Structure, Function, and Biochemistry. *Circulation Research.* 92 (8): 827–39.

Woskowicz, A. M., Weaver, S. A., Shitomi, Y., Ito, N., and Itoh, Y. 2013. MT-LOOP-dependent localization of membrane type I matrix metalloproteinase (MT1-MMP) to the cell adhesion complexes promotes cancer cell invasion. *The Journal of Biological Chemistry*. 288 (49): 35126–37.

Yu, Q, and Stamenkovic, I. 2000. Cell Surface-Localized Matrix Mealloproteinase-9 Proteolytically Activates TGF-Beta and Promotes Tumour Invasion and Angiogenesis. *Genes and Development.* 14: 163–76.

Zarrabi, K., Dufour, A., Li, J., Kuscu, C., Pulkoski-Gross, A., Zhi, J., ... Cao, J. 2011. Inhibition of Matrix Metalloproteinase 14 (MMP-14)-mediated cancer cell

migration. *Journal of Biological Chemistry*. 286 (38): 33167–77.

Zhen, G., and Cao, X. 2014. Targeting TGF-B Signalling in Subchondral Bone and Articular Cartilage Homeostasis. *Trends in Pharmacological Sciences.* 35 (5): 227–36.

Curriculum Vitae

Name: Caitlin Evered

Post-secondary Education and Degrees:

The University of Western Ontario
London, Ontario, Canada
2014-2016 M.Sc.

The University of Western Ontario
London, Ontario, Canada
2010-2014 B.Sc. Honour's Specialization in Biology

Honours and Awards

Gillis and Jenny Driesman Graduate Scholarship, 2016
Ontario Graduate Scholarship, 2015-2016
Western Graduate Research Scholarship, 2014-2016
Clement Yung Memorial Award, 2013-2014
Dean's Honour Role, 2011-2014
The Western Scholarship of Distinction, 2010

Related Work Experience

Teaching Assistant, Scientific Methods 2290F/G
The University of Western Ontario
Winter 2015, Summer 2015

Teaching Assistant, Developmental Biology 3338A
The University of Western Ontario
Fall 2014, Fall 2015

Undergraduate Research Student, Bio 4999E
The University of Western Ontario
Damjanovski Laboratory
2013-2014

Publications:

Cepeda, M., Pelling, J., **Evered, C.,** Williams, K., Freedman, Z., Stan, I., Willson, J., Leong, H. S., and Damjanovski, S. 2016. Less is More: Low Expression of MT1-MMP Is Optimal To Promote Migration and Tumourigenesis of Breast Cancer Cells. *BMC Molecular Cancer,* Submitted.